THE EFFECT OF STRONTIUM-CONTAINING SILICON-DOPED HYDROXYAPATITE CERAMICS ON BONE DEFECT HEALING

A THESIS SUBMITTED TO
THE GRADUATE SCHOOL OF NATURAL AND APPLIED SCIENCES
OF
MIDDLE EAST TECHNICAL UNIVERSITY

BY

GÖZDE KERMAN

IN PARTIAL FULFILLMENT OF THE REQUIREMENTS
FOR
THE DEGREE OF DOCTOR OF PHILOSOPHY
IN
BIOTECHNOLOGY

JANUARY 2011

Approval of the thesis:

THE EFFECT OF STRONTIUM-CONTAINING SILICON-DOPED HYDROXYAPATITE CERAMICS ON BONE DEFECT HEALING

submitted by **GÖZDE KERMAN** in partial fulfillment of the requirements for the degree of **Doctor of Philosophy in Department of Biotechnology, Middle East Technical University** by,

Prof. Dr. Canan Özgen _____
Dean, Graduate School of **Natural and Applied Sciences**

Prof. Dr. İnci Eroğlu _____
Head of Department, **Biotechnology**

Prof. Dr. Feza Korkusuz _____
Supervisor, **Physical Education and Sports Dept., METU**

Prof. Dr. Mürvet Volkan _____
Co-Supervisor, **Chemistry Dept., METU**

Examining Committee Members:

Prof. Dr. Muharrem Timuçin _____
Metallurgical and Materials Engineering Dept., METU

Prof. Dr. Feza Korkusuz _____
Physical Education and Sports Dept., METU

Prof. Dr. Petek Korkusuz _____
Histology and Embryology Dept., Hacettepe University

Assoc. Prof. Dr. Ayşen Tezcaner _____
Engineering Sciences Dept., METU

Assoc. Prof. Dr. Caner Durucan _____
Metallurgical and Materials Engineering Dept., METU

Date: 24.01.2011

I hereby declare that all information in this document has been obtained and presented in accordance with academic rules and ethical conduct. I also declare that, as required by these rules and conduct, I have fully cited and referenced all material and results that are not original to this work.

Name, Last name: Gözde Kerman

Signature:

ABSTRACT

THE EFFECT OF STRONTIUM-CONTAINING SILICON-DOPED HYDROXYAPATITE CERAMICS ON BONE DEFECT HEALING

Kerman, Gözde
Ph.D., Department of Biotechnology
Supervisor : Prof. Dr. Feza Korkusuz
Co-Supervisor: Prof. Dr. Mürvet Volkan

January 2011, 137 pages

Hydroxyapatite (HA) based bioceramics have been developed to treat bone defects for the last 30 years. Doping HA with elements is a common approach to increase mechanical strength, biocompatibility and osteointegrity. Bone morphogenetic protein (BMP)-containing bioceramic composites enhance osteointegrity and induce bone formation. Strontium (Sr) is currently used to treat osteoporosis clinically as this element inhibits bone resorption and stimulates bone formation.

In this study, HA was doped with silicon (Si), Sr, BMP-2 and evaluated in cortical bone defect healing. Ceramics were produced and tested mechanically after characterization. Sr release from ceramics was assessed. Ceramics were further evaluated in *in vitro* and *in vivo* conditions.

X-ray diffraction analysis results of HA were in line with the literature and Sr-Si-HA ceramics showed similar intensities with HA. Ceramics had 36.9 to 41.6% porosity. Compression strength of Sr1000-Si-HA ceramics was 117.5 MPa which was more than that of the other groups. Consistent Sr

release was observed in the Sr1000-Si-HA and the Sr250-Si-HA groups. Sr1000-Si-HA and Sr250-Si-HA ceramics showed higher cellular proliferation rates than the other groups *in vitro*. BMP addition increased alkaline phosphatase activities and DNA amounts. BMP-Sr-Si-HA group presented higher (0.304±0.02 g/cm^2) bone mineral density values than the other groups 4 weeks after implantation however differences between groups were not significant *in vivo*. Sr-Si-HA and BMP-Sr-Si-HA composites stimulated new bone formation at cortical bone defects of tibia according to micro computerized-tomography and histological results. Findings of this study promote future research on Sr containing bioceramics in treatment of orthopedic problems.

Keywords: Hydroxyapatite, Defect healing, Strontium, BMP-2

ÖZ

KEMİKTE DEFEKT İYİLEŞMESİNE STRONSİYUM İÇEREN SİLİSYUM-HİDROKSİAPATİT SERAMİKLERİNİN ETKİSİ

Kerman, Gözde
Doktora, Biyoteknoloji bölümü
Tez Yöneticisi : Prof. Dr. Feza Korkusuz
Ortak Tez Yöneticisi: Prof. Dr. Mürvet Volkan

Ocak 2011, 137 sayfa

Hidroksiapatit(HA) temelli seramikler kemikte defekt tedavisi için son 30 yıldan beri geliştirilmektedir. HA kırılgan bir yapıda olduğu için, mekanik direncinin, biyouyumluluğunun arttırılması ve kemikle bütünleşmesini sağlamak için çeşitli elementlerle desteklenmeye çalışılmaktadır. Kemik morfogenetik protein(BMP) içeren kompozitler, implantın kemikle bütünleşmesini ve yeni kemik oluşumu arttırır. Stronsiyum(Sr) kemik rejenerasyonunu teşvik edip, kemik rezorpsiyonunu önlediği için osteoporoz tedavisinde kullanılmaktadır.

Bu çalışmada Silisyum(Si) ve Sr ile desteklenmiş HA seramikleri, BMP-2 ile takviye edilerek kortikal kemikte defekt tedavisi açısından değerlendirilmiştir. Seramikler karakterizasyon testlerinin ardından mekanik açıdan test edilmiştir. Seramiklerden Sr salımı da incelenmiştir. Ayrıca, biyoseramikler, hücre kültürü ve *in vivo* koşullarda değerlendirilmiştir.

HA'nın X ray-difraksiyon testi sonuçları diğer araştırmaların sonuçlarına uyum göstermiştir ve Sr-Si-HA seramiklerinin intensity değerleri HA ile

benzerlik göstermektedir. Seramiklerin gözenekliliklerinin % 36.9-41.6 oranında olduğu tespit edilmiştir. Sr(1000ppm)-Si-HA seramiklerinin kompresyon direnci 117.51 MPa olarak ölçülmüştür ve bu değer karşılaştırılan diğer seramikler gruplarınınkinden daha yüksektir. Sr(1000ppm)-Si-HA ve Sr(250ppm)-Si-HA gruplarında istikrarlı Sr salımı gözlenmiştir. Hücre kültür sonuçlarına göre, Sr(1000ppm)-Si-HA ve Sr(250ppm)-Si-HA seramiklerinin hücresel proliferasyon etkisi diğer gruplardan daha fazla ölçülmüştür. Seramiklere BMP ilavesi ile hücre kültür ortamında alkalen fosfataz (ALP) aktivitesinde ve DNA miktarında artış gözlenmiştir. *In vivo* deney sonuçlarına göre, implantasyondan 4 hafta sonra, BMP-Sr-Si-HA grubunda diğer gruplara göre daha yüksek kemik mineral yoğunluğu 0.304±0.02 g/cm^2 olarak gözlenmiştir. Ancak grupların BMD değerleri arasındaki farklılıklar istatistiksel olarak anlamlı çıkmamıştır. Buna rağmen mikro bilgisayarlı-tomografi analiz ve histolojik incelemelere göre, BMP-Sr-Si-HA ve Sr-Si-HA seramikleri, tibiadaki kortikal defekt alanlarında yeni kemik oluşumunu diğer gruplara oranla daha çok arttırmıştır. Bu çalışmanın sonuçları ortopedik problemlerin tedavisinde Sr içeren biyoseramiklerin araştırmalarını teşvik etmektedir.

Anahtar Kelimeler: Hidroksiapatit, Defekt iyileşmesi, Stronsiyum, BMP-2

Dedicated to my parents,

ACKNOWLEDGEMENTS

I would like to give my special thanks to Prof. Dr. Feza Korkusuz for his guidance, support and valuable suggestions for my thesis studies.

I also acknowledge Prof. Dr. Petek Korkusuz for her useful suggestions, interest for improving this thesis and giving me permission to study in her lab.

I would like to express my special thanks to Prof. Dr. Hasan Uludağ for his guidance, mentoring, attention, patience and also providing me opportunity to work in his lab.

I would like to extend my thanks to Prof. Dr. Muharrem Timuçin for his suggestions and guidance for this thesis study. And also I acknowledge Assoc. Prof. Dr. Nurşen Koç for her suggestions and patience to my questions about Metallurgical and Materials Engineering.

I wish to express my sincere thanks to Prof. Dr. Murvet Volkan for her suggestions, advices and the extra time she has spent for this thesis.

I acknowledge Cezary Kucharski for his support, guidance at cell culture studies. I would like to thank to Asist. Prof. Dr. Ilkan Tatar for his help and support for micro CT measurements. I wish to express my thanks to Sedat Acar for all his support and goodwill during long hours we worked hard together.

I would like to thank to Murat Kaya, Rumeysa Gürbüz, Eda Öztürk and also to send my thanks to my friends, Nesrine Zakaryia, Vanessa Incani and Ross Fitzsimmons for their help, friendship and support for my thesis study.

I would like to express my sincere thanks to my parents, for their continuous support, help, encouragement, interest, suggestions, thoughtfulness, time and effort they have spent for me.

TABLE OF CONTENTS

ABSTRACT.....iv
ÖZ.....vi
ACKNOWLEDGEMENTS.....ix
TABLE OF CONTENTS.....x
LIST OF TABLES.....xiii
LIST OF FIGURES.....xiv
LIST OF ABBREVIATIONS.....xvii
CHAPTERS
1. INTRODUCTION.....1
1.1. Structure and Function of Bone.....1
1.2. Bone Metabolism.....4
1.3. Osteoporosis.....5
1.3.1. Mechanism of Osteoporosis.....5
1.3.2. Economic Importance of Osteoporosis in the World.....6
1.3.3. Postmenopausal Osteoporosis.....7
1.4. Bone Mineral Density (BMD) 9
1.5. Biomaterials.....10
1.5.1. Mineral Scaffolds.....11
1.5.2. Bioceramics.....12
1.6. Bone Morphogenetic Proteins (BMP) 13
1.7. Strontium.....14
1.8. Research Questions.....14
1.9. Hypothesis.....14
1.10. Literature Review and Rational.....15
1.10.1. Osteoporosis Models in Rats.....15
1.10.2. Trials with HA Ceramics.....16

1.10.3 Trials Related to Defect Healing in Rats.....19
1.10.4. Trials with BMP-2 for Bone Formation.....20
1.10.5. Trials with Sr Substituted Bioceramics.....22
1.11. Originality.....26
1.12. Aims of The Study.....27
2. MATERIALS and METHODS 30
2.1. Design.....30
2.2. Development of The Ceramic Systems.....31
2.2.1. Preparation of The Ceramic Systems.....31
2.2.2. Material Properties.....33
2.2.2.1. X-Ray Diffraction(XRD) Analysis.....33
2.2.2.2. Porosity Test.....35
2.2.2.3. Compression Test.....37
2.2.2.4. Scanning Electron Microscopy.....38
2.3. Sr Release Test.....38
2.4. *In Vitro* Experiments.....40
2.4.1. Tests and Microscope Observation for *In Vitro* Experiments.....42
2.4.1.1. MTT Test.....42
2.4.1.2. ALP Test.....43
2.4.1.3. DNA Test.....43
2.4.1.4. SEM Observation.....45
2.5. *In Vivo* Experiments.....45
2.5.1. Ovariectomy Operation.....46
2.5.2. Defect Formation.....49
2.5.3. After Defect Formation.....49
2.5.4. Tests and Measurements for *In Vivo* Experiments.....50
2.5.4.1. Micro CT 50
2.5.4.2. Histology and Histomorphometry 51
2.6. Statistics.....54
3. RESULTS 56

3.1. Ceramic Properties.....56
3.1.1. Compression Test.....56
3.2. Sr Release Test.....57
3.3. *In Vitro* Tests.....59
3.3.1. Proliferation Test by MTT.....59
3.3.2. ALP tests.....65
3.3.3. DNA tests.....67
3.3.4. ALP/DNA Ratio.....71
3.3.5. SEM Images.....74
3.4. *In Vivo* Tests.....74
3.4.1. Radiology.....74
3.4.1.1. Periosteal Reaction Results.....74
3.4.1.2. Bone Union Results.....75
3.4.1.3. Remodeling Results.....76
3.4.1.4. Implant Integration Results.....77
3.4.1.5. Overall Radiological Scores.....78
3.4.2. DXA Results.....79
3.4.2.1. DXA Results of First Stage Experiments.....79
3.4.2.2. DXA Results of Second Stage Experiments.....79
3.4.3. Micro CT.....81
3.4.4. Histology and Histomorphometry.....82
4. DISCUSSION.....87
5. CONCLUSION.....100
REFERENCES.....102
APPENDIX - ETHICAL COMMITTEE APPROVAL.....134
CURRICULUM VITAE.....135

LIST OF TABLES

TABLES

Table 2.1. Material weights for the preparation of the ceramics……32

Table 2.2. Bulk density (g/cm^3) of ceramics used in this study……..36

Table 2.3. Histological scoring system for tissue response……54

Table 3.1. Compressive strength (MPa) (Ave±SD (Range: Min-Max)) of ceramics assessed in this study……56

Table 3.2. Sr amount (mg) released from the ceramics into 20 mg distilled water……58

Table 3.3. Bone mineral density (g/cm^2) of the Si-HA implanted and defect created tibia Ave±SD (Range: Min-Max)……..80

Table 3.4. Bone mineral density (g/cm^2) of the bioceramic implanted tibia Ave±SD (Range: Min-Max) ……80

Table 3.5. BMD results of the femur to assess OVX and time related changes……..80

Table 3.6. BMD results of the vertebra to assess OVX and time related changes..……80

Table 3.7. Results of histomorphometrical analysis. (defcbt/nbt: ratio of cortical bone thickness at defect area to normal cortical bone thickness, ntb/defarea: ratio of the new trabecular bone area in the defect/total defect area) ……..83

LIST OF FIGURES

FIGURES

Figure 1.1. Schematic diagram of bone.....2
Figure 1.2. Trabecular thinning related to age.....8
Figure 1.3. The groups that were tested in all experiments and their evaluations by radiology, dual energy X-ray absorptiometry, micro-tomography and histology.....29
Figure 2.1. Ceramics that were used in all experiments.....33
Figure 2.2. XRD graphs of HA, Si-HA, Sr250-Si-HA, Sr500-Si-HA, Sr1000-Si-HA ceramics.....34
Figure 2.3. Porosity percentages of the ceramics assessed in this study.....36
Figure 2.4. Schimadzu mechanical testing machine.....37
Figure 2.5. SEM images (a,b, c, d) of Si-HA, Sr250-Si-HA, Sr500-Si-HA, Sr1000-Si-HA ceramics.....38
Figure 2.6. LEEMAN-ICP-OES spectrometry and software.....39
Figure 2.7. Spectrophotometer and the software during measurement.....43
Figure 2.8. Preparation of standard curve samples for the DNA assay.....44
Figure 2.9. Fluroskan Ascent Microplate Fluorometer and Ascent software.....44
Figure 2.10. XP images of rats.....47
Figure 2.11. DXA machine and appearance of results during measurement.....48
Figure 2.12. The uterus and ligation of the ovaries.....48
Figure 2.13. Formation of cortical cavity and filling with bioceramics.....49
Figure 2.14. Micro CT measurement.....51
Figure 2.15. Samples in DeCastro solution.....51

Figure 2.16. Semi-enclosed Benchtop Tissue Processor and Modular Tissue Embedding Center.....51
Figure 2.17. Samples had been embedded with paraffin.....52
Figure 2.18. Sliding microtome that was utilized for taking sections from samples (Samples were collected by microscope slides). 52
Figure 3.1. Compressive strength (MPa) of ceramics assessed in this study.....57
Figure 3.2. Sr release (mg/kg) from ceramics that were incubated in distilled water for 3 and 14 days (n=1 in all groups).....58
Figure 3.3. MTT calibration revealed increasing number of cells.....59
Figure 3.4. MTT assay results (a.u.) of cells that were applied to the ceramics.....60
Figure 3.5. MTT assay results (a.u.) of cells that were incubated with BMP-containing ceramics.....61
Figure 3.6. Photos of ceramics in wells before MTT test at day 1.....62
Figure 3.7. Photos of ceramics in wells before MTT test at day 6.....63
Figure 3.8. Ceramics in wells before the MTT test on day 12.....64
Figure 3.9. ALP assay results (a.u.) of ceramics.....65
Figure 3.10. ALP assay results (a.u.) of BMP containing ceramics.....66
Figure 3.11. Standard curve of the DNA assay.....68
Figure 3.12. DNA assay results (µg/tablet) of the ceramics.....69
Figure 3.13. DNA assay results (µg/tablet) of BMP containing ceramics.....70
Figure 3.14. ALP/DNA ratio of cells (a.u./µg) that were incubated with the ceramics.....72
Figure 3.15. ALP/DNA ratio (a.u./µg) of cells that were incubated with BMP-containing ceramics.....73
Figure 3.16. SEM pictures of the cells that were incubated with the HA, the Sr250-Si-HA and the Sr500-Si-HA ceramics.....74
Figure 3.17. Periosteal reaction results of tibiae (control: defect only; control 2: normal bone) of the groups 75

Figure 3.18. Bone union scores of the tibiae (control: defect only; control 2: normal bone) of the groups 76
Figure 3.19. Remodeling results of tibiae (control: defect only; control 2: normal bone) of the groups 77
Figure 3.20. Implant integration results of tibiae (control: defect only; control 2: normal bone) of the groups 78
Figure 3.21. Overall radiological scores of the tibiae (control: defect only; control 2: normal bone) of the groups. 78
Figure 3.22. Micro CT images of the cortical defect into ceramic implanted group (a, b) and normal bones (c, d).....81
Figure 3.23. Percent bone volume results of samples that were ceramic implanted.....81
Figure 3.24. A to B (HE stained) and C to D (MT stained) show long term (31week) implanted Si-HA ceramics. I: Implant, HE: Hematoxylin & Eosin, MT: Masson's Trichrome.....82
Figure 3.25. Endochondral (in D) and intramembranous (A-C, E-J) ossification steps are noted within the defect site of implant applied and control groups. I: Implant, NB: New bone, CB: Cortical bone, BM: Bone marrow, Ca: Cartilage, HE: Hematoxylin Eosin, MT: Masson's Trichrome.....85
Figure 3.26. The defect area is nearly totally ossified in all groups. I: Implant, NB: New bone, CB: Cortical bone, BM: Bone marrow, HE: Hematoxylin Eosin, MT: Masson's Trichrome.....86
Figure 4.1. Ca release (mg/kg) from ceramics that were incubated in distilled water for 3 and 14 days (n=2 in all groups).....91

LIST OF ABBREVIATIONS

ALP	Alkaline Phosphatase Activity
BMU	Basic Multicellular Unit
bFGF	Basic Fibroblast Growth Factor
β-TCP	beta-Tricalcium Phosphate
BMD	Bone Mineral Density
BMP	Bone Morphogenetic Protein
BSU	Bone Structural Unit
d_{bulk}	Bulk density
Ca	Calcium
CaP	Calcium Phosphate
CaSR	Calcium Sensing Receptor
DNA	Deoxyribonucleicacid
DMSO	Dimethylsulfoxide
DXA	Dual X-Ray Absorptiometry
GAG	Glycosaminoglycans
HBSS	Hanks' Balanced Salt Solution
HE	Hematoxylin & Eosin
HA	Hydroxyapatite
ICBM	Inactive Collagen Bone Matrix
JCPDS	Joint Committee on Powder Diffraction and Standards
M-CSF	Macrophage Colony Stimulating Factors
Mg	Magnesium
MT	Masson's Trichrome
MSC	Mesenchymal Stem Cells
Micro CT	Micro Computerized Tomography
OB	Osteoblast

Oc	Osteoclast
OVX	Ovariectomy
PTH	Parathyroid hormone
P	Phosphor
PEG	Polyethylene glycol
PLGA	Poly(lacticacid-co-glycolic acid)
PCR	Polymerase Chain Reaction
RANK	Receptor Activator of Nuclear factor κ β
RANKL	Receptor Activation of Nuclear Factor κ β -Ligand
ROI	Regions Of Interest
SEM	Scanning Electron Microscope
Si	Silicon
Si-HA	Silicon doped Hydroxyapatite
Sr	Strontium
Sr-HA/PEEK	Sr-containing hydroxyapatite/polyetheretherketone
d_{th}	Theoretical density
3D	Three dimensional
tcps	Tissue culture polystyrene
TGF-β	Tissue Growth Factor-beta
Ti	Titanium
VEGF	Vascular Endothelial Growth Factor
XRD	X-Ray Diffraction
XP	X-Ray picture

CHAPTER 1

INTRODUCTION

1.1. Structure and Function of Bone:

Bone protects internal organs such as the brain, the spinal cord and the lungs and plays a crucial role in hematopoiesis (Kwan et al., 2008). Its functions furthermore include movement and storage of minerals.

Bone is a regenerating tissue whose properties change according to the mechanical requirements of the environment (Bronner et al., 1999). Two types of bone exist at the macrostructure level, viz. cortical (compact) and cancellous (trabecular). Long bones (i.e. humerus, femur, tibia) have a cortical frame at the exterior and a trabecular constitution on the interior (Rho et al., 1998). What differentiates these two types of bone is their porosity and density properties (Carter et al. (1977), Gibson LJ (1985)). Cortical bone is dense and has regular microscopic channels; 80 % of the skeletal mass of the human is cortical bone. Trabecular bone, on the other hand, has a microstructure composed of irregular convolutions of lamellae (Enlow DH, 1963, 1968) and constitutes 20% of the human bone mass (Frost HM (1995), Jee WSS (1999)). The periosteum, the outer fibrous membrane of bones, includes blood vessels and nerve endings. The endosteum, the internal surface, is in contact with marrow, blood vessels, osteoblasts and osteoclasts (Brandi ML, 2009). Haversian canal encompasses blood vessels. Volkmann's canal which carries arteries does interconnections between Haversian canals and periosteum.

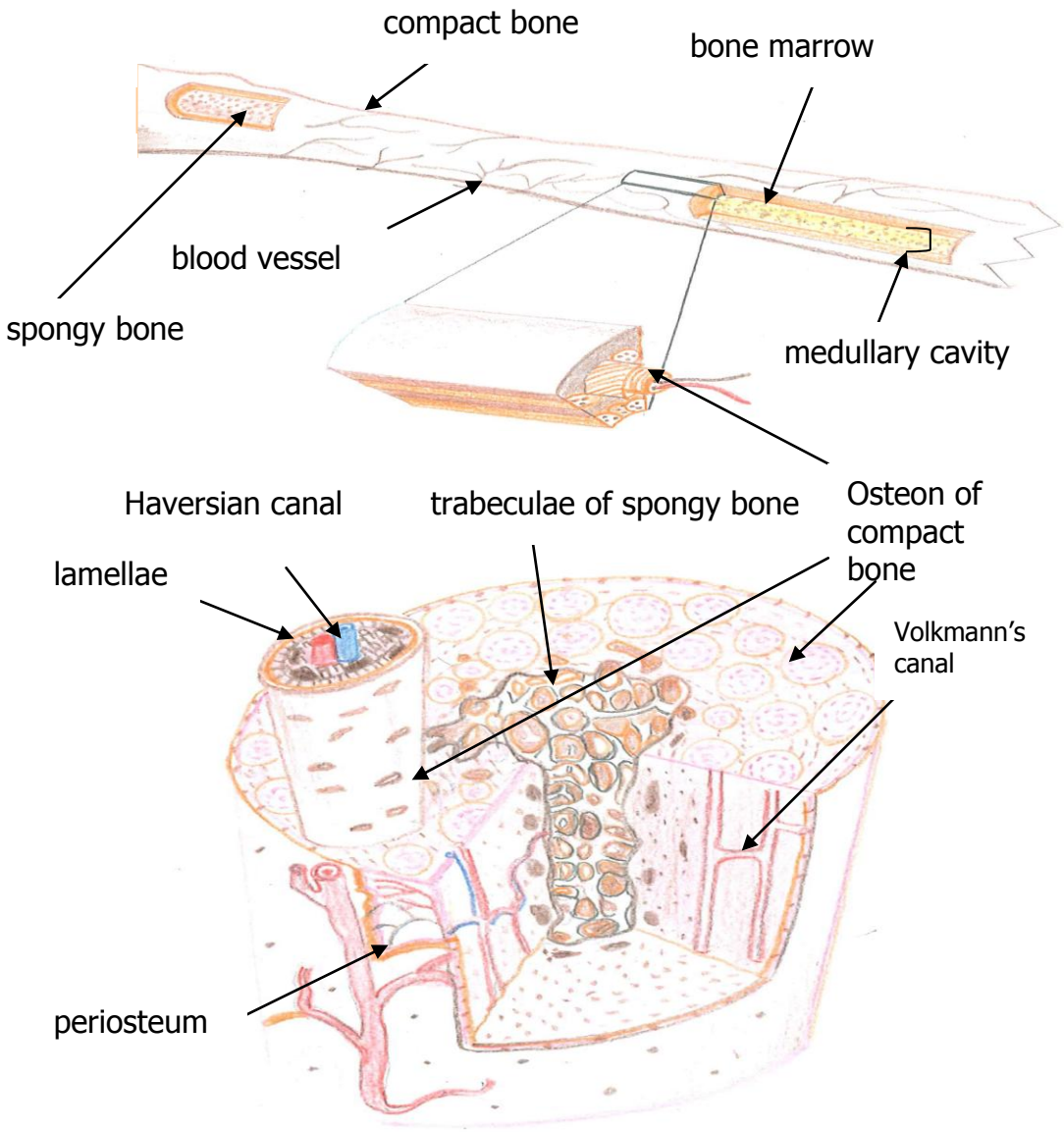

Figure 1.1. Schematic diagram of the bone.

Bone is composed of cells, mineralized extracellular matrix and organic extracellular matrix. Cells are mainly 3 types: osteoblasts (OB), osteocytes and osteoclasts (Oc). OBs, acquired from mesenchymal stem cells (MSC), have a role in depositing calcified matrix and release crucial growth factors for osteogenesis and are also known to organize calcium (Ca) and phosphate to support hydroxyapatite (HA) formation (Manolagas SC, 2000). The Ca sensing receptor (CaSR) is expressed in the proliferation or bone formation

phases of OBs in cultures (Chattopadhyay et al., 2004). When bone formation is complete, OBs are surrounded by a new bone matrix and differentiate into osteocytes. Osteocytes are mechanosensitive cells (Klein-Nulend et al., 1995) remaining within their lacunae deep within the mineralized matrix and are mostly interconnected by their cellular processes. Oc(s) are multinucleated cells by differentiation and fusion of mononuclear-monocyte-macrophage lineage precursors after stimulus by receptor activation of nuclear factor κ β-ligands (RANKL) and macrophage colony stimulating factors (M-CSF) (Boyle et al. (2003), Lacey et al. (1998), Yasuda et al. (1998)). Oc(s) participate in bone remodelling by breaking down the components of bone with the action of lysosomal enzymes as well as low local pH, which facilitates mineral dissolution (Javaid et al., 2008). After osteoclastic bone resorption, osteoblastic bone formation physiologically occurs to fill the defect site and/or repair the defect. The new bone that is formed is named as the Bone Structural Unit (BSU; Frost HM, 1964).

Mineralized extracellular matrix is about 65% of the composition of bone and contains HA. The crystalline mineral component has the following apatitic structure:

$(Ca,X)\ (PO_4,\ HPO_4,CO_3)(OH,Y)_2)$ (Le Geros et al., 2002). X denominates a cation (Mg, Na or Sr ions that can substitute for Ca ions) and Y designates an anion (Cl^- or F^- that can substitute for hydroxyl group (Kim et al. (2003), LeGeros RZ (2002)).

Approximately 35% of bone's composition is organic extracellular matrix that includes collagen I (as much as 90% by weight) and non-collagenous proteins (osteocalcin, osteopontin, etc). Type I collagen permits bone to absorb energy through plastic deformation without the incidence of bone fracture. Collagen I is also involved in bone mineralization (Caetano-Lopes et al. (2007), Seeman et al. (2006a)). Glycosaminoglycans (GAGs) are proteoglycans that are also found in the bone matrix and have a role in regulation of the mineralization process, i.e., they can inhibit or initiate a

mineralization event under the appropriate conditions (Skerry et al. (1990), Rees et al. (2001)).

Ca, phosphor (P), vitamin D are crucial factors in maintaining a healthy bone mass. Different replacements are found in bone mineral as elements such as Al, Ba, Cu, Cl, F, Fe, Mg, K, Na, Si, Sr, Zn (Driessens et al. (1990), Elliot JC (1994)) and have roles in the biological activity of bone mineral and Ca-P based biomaterials.

1.2. Bone Metabolism:

Formation and resorption of bone at a given site is called Bone Remodelling (Frost HM, 1990). Bone remodelling attempts to alternate aged or damaged bone with new bone to avoid the occurrence of fatigue fractures. Oc(s) remove bone, followed by the deposition of new bone by the OBs (Manolagas SC, 2000). Remodelling usually occurs in the trabecular structure. Oc(s) resorb an amount of bone and OBs replenish the resorption cavity. This process is called the "Basic Multicellular Unit" (BMU) (Gerhard et al., 2009). BMU is a combination that includes Oc(s) in front, OBs at the back, and capillary veins in the centre, together with nerve supply and connective tissue that facilitates the modelling (Parfitt AM, 1994). In healthy people, 3-4 million BMUs are formed per year.

Cortical loss of bone is not that significant before the age of 50, but 40% of trabecular loss can occur before that age (Seeman E, 2008). The vertebral body is wider in males than in females and is stronger in young males than females because of size differences (Seeman E, 1998). Also, the total body bone mineral content of new born babies was observed to be lower in winter births than in summer infants because of maternal vitamin D deficiency (Namgung et al., 1992).

1.3. Osteoporosis:

According to the US National Osteoporosis Foundation, osteoporosis is a condition characterized by low bone mass and the structural deterioration of bone tissue. In 1820, Jean C.F.M. Lobstein coined the term osteoporosis to indicate porous bone (Grob GN, 2010). Increased fragility can be seen most characteristically at the hip, wrist, ribs and spine (Hegge et al., 2009). Vertebral fractures are the most usual osteoporotic fractures found in men and women (O'Neill et al. (1996), Naves-Diaz et al. (2000)). Men run a lifetime risk for osteoporotic fractures of 15%, compared with 40% in women (Vanderschueren et al., 2008).

Accelerated bone loss is higher in women than men and arises due to decreased levels of estrogen (Mullender et al., 2005) because the balance between OBs and Oc(s) is controlled by estrogens (ESHRE Capri Workshop Group, 2010). The estrogen effect occurs as a result of nuclear ligand activated receptors, i.e. estrogen receptor –α and –β, that are expressed in bone and cartilage (ESHRE Capri Workshop Group (2010), Venken et al. (2008), Tanko et al. (2008)).

1.3.1. Mechanism of Osteoporosis:

Normal healthy bone has a honeycomb structure while osteoporotic bone has larger holes and spaces in the honeycomb, when inspected at the microscopic level. The morphological properties of osteoporosis are thinning and decrease in the number of the trabeculae (Cummings et al. (2002), Seeman E (2002), Delmas PD (2002)). The reduction in the strength and quality of bone may result in fracture, pain and disability related with osteoporosis (Cooper C, 1997).

In osteoporosis, the lifespan of Oc(s) is extended while the lifespan of OBs is shortened. Therefore, Oc causes resorption and trabecular perforation in the cavities (Manolagas SC, 2000). Bone loss can happen in

two different phases, namely slow or accelerated. In the slow phase, OBs fail to replenish Oc constructed resorption cavities (Riggs et al. (1981, 1986), Parfitt AM (1988)), which results in the gradual thinning of trabeculae (Riggs et al. (1986), Parfitt et al. (1983)). In the accelerated version of bone loss, i.e. postmenopausal bone loss, Oc(s) cause resorption cavities of increased depth, which leads to trabecular perforation.

Receptor activator of nuclear factor κ β (RANK) along with RANKL has a significant role in Oc proliferation and differentiation (Hofbauer et al., 2000). RANKL's binding with and activation of Oc(s) enhance bone resorption (Boyle et al., 2003).

When the outer load applied to bone surpasses its strength, fracture takes place. The ability of a bone to withstand fracture is related to bone mass, bone macro- and micro-architecture, and the internal properties of the materials that constitute bone (Bouxsein et al., 2005).

1.3.2. Economic Importance of Osteoporosis in the World:

Osteoporosis related fractures are a major health problem affecting a growing number of humans worldwide. In Turkey, as reported by the Turkish Statistical Institute in 2008, 16.1% of people older than 15 years of age had muscle and skeleton problems at their waists, and 13.8% of people older than 15 years of age have rheumatic joint diseases (such as rheumatoid arthritis) (Turkey, Health Interview Survey, 2008).

In 2000, the number worldwide of clinically patented fractures in women was 5.5 million and the peak age for the occurrence of fracture was 75-79 (Johnell et al., 2005). Lifetime endangerment of osteoporotic fractures was 40-50% in women and 13-22% in men (Johnell et al., 2005).

European medical aid costs for osteoporosis were € 31.7 billion in 2000 and are estimated to reach € 76.7 billion in 2050 (Kanis et al., 2005). According to 2006 reports, 1.2 million women had osteoporosis in the UK

(Dennison et al., 2006). One third of people aged above 65 fall every year, with 300.000 fracture cases annually in the UK alone (Martin FC, 2009).

Osteoporosis seriously affects the health of an individual as well as the economy of the country. In 2005, USA osteoporosis related fractures cost 19 billion US$ and are predicted to be 25.3 billion US$ by 2025 according to the National Osteoporosis Foundation. More than 3 million osteoporosis related fractures a year are expected in the United States by 2025, with a yearly cost of 25 million $ (Burge et al., 2007). The rate of hip fractures is 2 to 3 times higher in women than in men in the USA. Patients with difficulty in moving, experience psychological difficulties and are prone to depression, and other undesired consequences.

7753 participant, 50 years of age and older, were investigated for a study as part of an osteoporosis report in Canada (Ioannidis et al., 2009). The participants with hip or vertebral fractures had a higher risk of mortality than others.

1.3.3. Postmenopausal Osteoporosis:

Menopause, aging, inherited factors, low Ca intake and absorption, lack of exercise, excessive alcohol consumption along with smoking are the basic factors that contribute to osteoporosis (Prabha Shankar, 2002).

Postmenopausal osteoporosis is caused by deficiency of estrogen after the cessation of ovulation and results in bone loss and negative balance in bone remodelling (Turner et al., 1994). Women have a faster loss of bone mass during the first 5-10 year after menopause due to the decrease in estrogen (Lindsay R, 1988). Estrogen deficiency causes deprivation of trabecular bone in vertebral bone and the epiphyseal segments of long bone (Westerlind et al., 1997). Estrogen deficiency causes rapid bone resorption and low BMD by stimulating osteoclastic activity (Riggs BL, 1991). Studies with MSC from pre- and postmenopausal women showed that postmenopausal women had a low growth rate of MSC and that the MSC

ability to differentiate along osteogenic lineage was lacking (Rodriguez et al., 1999). In addition, reduced parathyroid hormone (PTH) secretion and increased bone loss results in decreased Ca absorption (Riggs BL, 1991).

Three different phases related to changes in bone mass can occur in life; two of them occur in both sexes, whilst the other is associated only with women (Mazess RB (1982), Parfitt AM (1988)). In the first phase, bone growth and an increase in bone mass can be seen. Linear growth reflects the mineralization of endochondral growth, whereas radial growth is related to rate of periosteal apposition, which exceeds the rate of endosteal resorption. At the age of 20, when the growth plate is closed, radial growth continues until 30 to 35 years of age. The slowing of bone mass starts at around 40 years of age (Riggs et al. (1981,1986), Mazess RB (1982)). The third phase applicable to women is related to the accelerated postmenopausal bone loss because of a lack of estrogen (Riggs et al. (1986), Mazess RB (1982), Lindsay et al. (1980), Genant et al. (1982)).

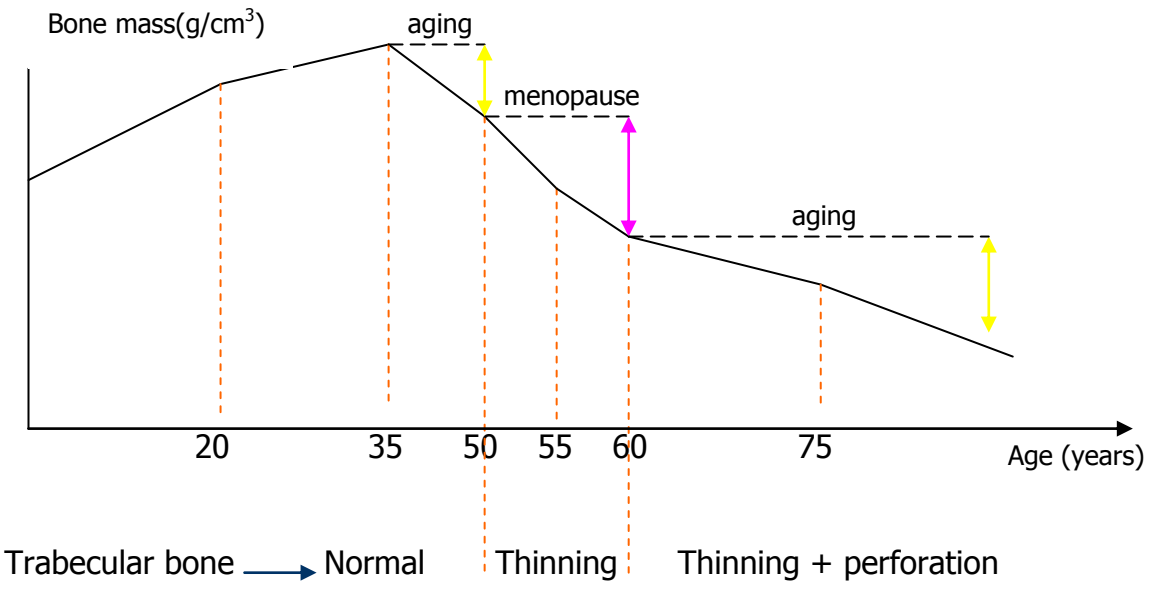

Figure 1.2. Trabecular thinning related to age.

Postmenopausal osteoporosis can affect women 15-20 years after menopause. Trabecular bone loss in this disease results in fractures especially of vertebrae, and the distal forearm and distal ankle. Although osteoporosis is often considered to be a condition of postmenopausal women, 30% of hip fractures occur in men in the USA according to Hegge et al. (Hegge et al., 2009). Rib fractures are often found to be non-spine fractures in men and can be related to osteoporosis (Barrett-Connor et al., 2010). The preponderance of osteoporosis in men was expected to increase by 50% by 2012 (Looker et al., 1997).

1.4. Bone Mineral Density (BMD):

Approximately 90% of bone mass is accumulated by the age of puberty (Duan et al., 2003). BMD increases through childhood and adolescence. Children and teenagers form new bone faster, and young people continue to make more bone than they lose. After menopause, women's bone density can drop by 20% or more (National Osteoporosis Foundation, US).

Informing people about the importance of osteoporosis is crucial. Levy et al. tested whether chart reminders or/and patient education can affect BMD testing among women who are 65 years old. According to the results of that study, the educated group of patients had more BMD testing than chart reminders or regular care (Levy et al., 2009). In developed countries, the elderly population is increasing, so osteoporosis prevention has become a crucial socioeconomic priority.

In 1988, Dual x-ray absorptiometry (DXA) instrumentation was developed to determine the bone mineral density (BMD) of an individual in order to gauge the likeliness that they would get osteoporosis (Sanson G, 2003). DXA uses dual energy transmission scanning to generate photons from an X-ray tube (Wahner et al., 1988) and, by measuring BMD, has

become one of the most standard means of diagnosing osteoporotic bone fracture (Hansen et al., 1990).

The T score in DXA (the mean bone mass of a normal young adult reference population) indicates how much bone density is above/below normal and has been used for diagnosing osteoporosis. When the T score is –1.0 or higher, the BMD status of a person is accepted as normal. If the T score is less than –1.0 but higher than –2.5, the status is called osteopenia. When the T score is –2.5 or less, the status is referred to as osteoporosis, according to World Health Organization (Lewiecki EM, 2009).

The Z score (the mean BMD of a person of the same age) is used to equate bone density to what is normal in someone at the same age and body size. A Z score <-2.0 is normal according to the International Society for Chemical Densitometry (ISCD). An older person might have a normal Z score but can be at risk, so using a Z score to measure BMD is not recommended (National Osteoporosis Foundation).

According to Lewiecki, for diagnosis, fracture risk assessment, monitoring during therapy, ionizing radiation and cost, DXA is the best choice when compared with quantitative ultrasonography and quantitative computed tomography (Lewiecki EM, 2009).

BMD measurement is the current standard in osteoporosis. Osteoporosis research teams have taken BMD measurements as a parameter into their study charts (Yoshimura et al. (2010), Hearn et al. (2010)).

1.5. Biomaterials:

Designing and treatment of biodegradable porous three-dimensional structure is called a scaffold (Hutmacher DW, 2000). These scaffolds can become constructive support for cells for tissue regeneration (Lee et al., 2007). Biomaterials can be used to augment bone tissue in the case of osteoporosis, or other needs, for bone regeneration. The release of pharmacological substances over estimated times, with a suitable release

rate from adequately sized and geometrically shaped biomaterials is important in bone regeneration (Krajewski et al., 2000).

The material should be osteoinductive, biocompatible, osteoconductive, and biodegradable if necessary in order to select a biomaterial for bone implantation. Osteoinductive materials induce uncommitted cells (as MSC) to change phenotypically to osteoprogenitor and chondroprogenitor cells. Cellular proliferation qualifies osteogenesis and cellular differentiation characterizes osteoinduction. Osteoconductivity is the ability of the biomaterial to sustain the attachment of cells, new cell migration and angiogenesis into the graft. Biocompatibility means *in vivo* activity of implants without resulting local and/or systemic responses. The necessary properties of the scaffold include adequate porosity, pore interconnection and permeability for the cells to adhere onto and migrate through the scaffold (Evans et al., 2007). Appropriate bulk biomechanical properties are also needed to support mechanical loads and maintain a space with the right porosity (Sanz-Herrera et al., 2009). Application of scaffolds those are geometrically close to bone as alternatives to allografts or autografts is recommended for the treatment of bone defects. Tissue implant interface is critical in dictating the response to biomaterials (Kwan et al., 2007). Osteointegration of biomaterial is related to the properties of biomaterial and regenerative capability, and the characteristics of the host bone (Mori et al., 1997). Cells are dispersed to their contact area after attachment to the implant. Then, migration of the cells and the release of cytokines and extracellular matrix elements start. Cellular attachments to implants are regulated by integrin mediated signal transduction (Gronowicz et al., 1996).

1.5.1. Mineral Scaffolds:

Calcium phosphate (CaP) ceramics, plaster of Paris, bioactive glass can be examples of this group. Ceramics mimic the inorganic composition of

bone with good integration and have high fracture strength (Temenoff et al., 2000).

Ceramics that are used for bone repair can be classified into 3 types (Kamitakahara et al., 2008):

Bioinert ceramics: These ceramics form a thin non-adherent fibrous layer at the interface between ceramic and bone. Alumina and zirconia are examples of this group that were used in the head of hip joints because of good mechanical strength and the ability to last for a long time.

Bioactive ceramics: These ceramics are osteoconductive. Examples are bioglass, sintered HA ceramics, glass ceramics and wollastonite ceramics.

Bioresorbable ceramics: These ceramics can be degraded with time and replaced by natural bone. Tricalcium phosphate (TCP) and calcite ($CaCO_3$) are typical examples.

Cell attachment and proliferation are mostly related with the chemical and physical properties of the surface of a scaffold. Porosity and interconnectivity are important properties of ceramics advised by researchers (Matsumoto et al., 2009). Porous ceramics can be viewed as comprised of individual cells.

1.5.2. Bioceramics:

Ceramics that are used for the treatment of the human body are called bioceramics. Bioceramics can be of bulk form (named implant) used as filler for injured parts or coating materials (Hench et al., 1993). CaP ceramics such as HA and β-TCP have been applied in bone surgery because of the similarity of their chemical composition to the mineral phase of the bone (Le Geros et al., 1993).

95% of the inorganic part of bone is HA and this material can be found synthetically. The gradual dissolution of CaP crystals (HA) results in Ca and phosphate release into biological fluid that is located in ceramic

macrocrystals and causes precipitation (Jallot et al., 2000). This precipitation results in the association of bone apatite-like crystals with organic proteins (Daculsi G, 1998).

High porosity is recommended for HA in bone treatment because interconnected pores as a framework for bone growth and good blood-nutritional supply by vascular canal organization prevents implant loosening (Bajpai et al., 2010).

Si (silicon) is found at 100 ppm in bone tissue (Schwarz K, 1973). A significant increase in the effect of Si on BMD in the region was observed when added to the diet of men and postmenopausal women (Jugdaohsingh et al., 2004).

1.6. Bone Morphogenetic Proteins (BMP):

BMPs are dimeric molecules with a single interchain disulfide bond (Reddi AH, 1997). Protein adhesion to minerals is related to the structural properties of proteins. Members of BMPs show good interaction with mineralized matrices (Stayton et al., 2003). BMPs are cytokines that have been identified by their role as stimulating endochondral bone formation (Hogan BL, 1996) because of their osteoinductive property (Kenley et al., 1993). BMP has role in intramembranous and endochondral ossification as chemotaxis and mitosis of mesenchymal cells, osteogenic/chondrogenic differentiation (Reddi AH, 2001).

The most studied growth factors are BMP-2, -4, -5, -6 and -7 (Salata et al., 2002) in the Tissue growth factor (TGF)-β family (Reddi AH (2001), Schmitt et al. (1999)). Growth factors enhance bone healing significantly and stimulate the proliferation and differentiation capacities of MSC (Egermann et al., 2005). According to studies, BMP-2 caused the differentiation of MSC into cells by expressing osteoblastic phenotype (Wozney et al., 1998) and stimulated vascular endothelial growth factor (VEGF) secretion, which causes ectopic bone healing with angiogenesis (Deckers et al., 2002).

1.7. Strontium:

Strontium (Sr) was discovered in 1790 as one of the alkaline earth metals. Sr is a trace element that can be found in calcenous rocks, ocean water (Rosenthal et al. (1970,1972), Schroeder et al. (1972)).

Sr is a trace element in the human body. The amount of Sr is 0.01 – 0.008%, especially in bones and teeth (Aoki et al., 1991), and 98% of total body Sr content is found in the skeleton (Skoryna SC, 1984). Sr is mostly integrated by ionic exchange on bone crystal surfaces (Marie et al., 2001). Most of the dietary Sr is absorbed from jejenum (Marcus et al., 1962).

Sr is close to Ca chemically and physically, so can replace Ca in HA easily (Curzon et al., 1983). Sr can accumulate, especially in trabecular parts of bone (Dahl et al., 2001). The amount of Sr in the skeleton is 3.5% of the Ca molar content (Pors Nielsen S, 2004).

1.8. Research Questions:

The first research question of this study is whether adding Sr into silicon doped hydroxyapatite (Si-HA) ceramics will improve compression strength. The second research question is whether Sr-Si-HA bioceramics will release Sr in time. The third research question is whether Sr-Si-HA ceramics are biocompatible with rat bone marrow stem cells in *in vitro* conditions. The fourth research question is whether Sr-Si-HA ceramics promote bone defect healing when implanted into rat tibia. The final research question is whether adding BMP-2 into the Sr-Si-HA ceramics will improve *in vitro* and *in vivo* biocompatibility.

1.9. Hypothesis:

We assumed that (a) adding Sr into Si-HA will improve the compression strengths of the ceramics, (b) a release of Sr from Sr-Si-HA

ceramics can be observed in time, (c) Sr-Si-HA ceramics are biocompatible with rat bone marrow stromal cells, (d) Sr-Si-HA ceramics improve bone defect healing in rats and (e) adding BMP-2 into HA based ceramics enhances *in vitro* and *in vivo* biocompatibility.

1.10. Literature Review and Rational:

1.10. 1. Osteoporosis Models in Rats:

Rats are relatively cheap, easy growing and have similar skeletal properties to humans (Turner et al., 1987, 1988, 2001).

There are different ways to induce osteoporosis in rats. Glucocorticoid usage is one of them. Glucocorticoid administration resulted in increased bone resorption, decreased bone formation and caused pathological fractures (Dempster DW (1989), Van Staa et al. (2000), Angeli et al. (2006), Hulley et al. (1998), Manolagas SC (2000), Canalis et al. (2002)).

A second means of osteoporosis formation is the application of Heparin to rats. Buriana observed a low decrease in alkaline phosphatase (ALP) activity as a result of heparin (Buruiana et al., 1958). Thompson observed low collagen production by bones by applying Dopaheparin to rats for 8 weeks (Thompson Jr et al., 1973).

Cadmium is a kind of contaminant that damages the kidneys and skeletal system (Chalkley et al. (1998), Satarug et al. (2003), World Health Organisation (WHO-1992), Aoshima et al. (2003), Brzoska et al. (2003), Kawamura et al. (1978), Nordberg et al. (2002), Ohta et al. (2000)). Cadmium affected the mineral phase of bones (Choi et al. (2003), Ogoshi et al. (1989, 1992), Uriu et al. (2000)) in rats. Also, Brzoska applied cadmium to rats for 24 months and observed a reduction in mineral content and abnormalities at trabecules, with a decrease in load bearing abilities (Brzoska et al., 2004a, 2004b).

Alcohol usage is another factor that can induce osteoporosis. Ethanol application resulted in hypocalcemia in rats (Peng et al., 1972, 1974) and also decrease in trabecular bone volume (Saville et al. (1965), Baron et al. (1980)). Turner observed a reduction in tibial bone formation caused by ethanol (Turner et al., 1987).

The separation of gluteal muscle partly or totally from bone resulted in a reduction in trabecular bone mass and thickness (Beery-Lipperman et al., 2005).

Ovariectomy (OVX) in rodents caused a loss of trabecular bone, i.e. an artificial menopause (Ammann et al. (1993), Bagi et al. (1994), Chow et al. (1992), Liu et al. (1990)). Bilateral OVX can be the best choice for postmenopausal osteoporosis development and leads to systemic osteoporosis. According to studies, the bone mineralization level became slower during fracture healing of ovariectomized rats (Xu et al., 2002). Bagi and Çömelekoğlu observed a decrease at femur BMD and femoral cortical thickness (Bagi et al. (1997), Çömelekoğlu et al. (2007)) after OVX. Ovariectomized rats had lower fracture healing rates than controls and callus formation was deprived in those rats (Walsh et al., 1997). Also, OVX with low Ca diet application resulted wrecked late repair at femur in rats (Kubo et al., 1999).

There are several ways for osteoporosis formation. One of the main aims of this study was whether the bioceramic systems can be used for bone healing in postmenopausal women in the future. Ovariectomized rats are mostly used as osteopenic models that imitate the development of estrogen deficiency induced osteopenia in humans (Black et al., 1994). OVX had been preferred for induction of osteoporosis for this purpose.

1.10.2. Trials with HA Ceramics:

Bonding to tissue and anti-corrosion properties of biomedical implants are important properties. An ideal orthopedic implant must be biocompatible,

not allergenic and/or toxic, not affected by sterilization and resistant to high temperatures (Köse N, 2010). Bioactive ceramics are known to improve OB growth and differentiation (Marra et al. (1999), Ambrosio et al. (2001)).

The similarity of HA to the inorganic part of bone and its role in the prevention of Ca resorption was observed firstly in the 1960s in *in vitro* and *in vivo* (Fleisch et al., 1969) experiments. HA is a candidate for hard tissue replacements as stainless steel and ceramic based HA caused good fixation, mostly with no fibrous tissue encapsulation (Bobba R 2006a, 2006b). HA bonds to bone, causing interfering layers, because of its biocompatibility, observed in rats at 4 and 8 weeks (Fujita et al., 2003).

The solubility of porous ceramic bodies in physiological fluids and the chemical and physical contact of porous layers with living tissues are crucial factors for biocompatibility (Krajewski et al., 2000). HA has low biodegradability. Chemical bonding occurs when bone tissue and the HA implant are in contact. Due to its characteristics HA is included in the "bioactive ceramics" group (Zhong et al., 2002). Bioactive ceramics such as sintered calcium HA result in a bioactive response in which tissue ingrowth can occur if the material is porous (Hench et al., 1993). One of the most important considerations in the preparation of porous ceramic preparations is avoiding the possible weakening of scaffolds.

Yokoyama et al. applied HA cylinders to parietal bone and then observed apatite surface formation. Also, bone marrow cells loaded on CaP ceramics were implanted into critical sized defects in rat femurs and complete bone union via accelerated bone healing was seen (Ohgushi et al., 1989).

Researchers prefer HA coating in biomedical implants. Zhou applied HA coating onto hydrogels and grew a cell culture. Higher cell numbers were seen in HA coated hydrogel groups during a 5-day study period (Zhou et al., 2009). Sanz Herrera et al. tested dioxide Zirconium Sponceram® carriers mechanically. When they added HA to Sponceram® carriers, the Youngs Moduli (*E*) and compression stress increased more significantly than the non HA-coated implants (Sanz Herrera et al., 2008, 2009). In addition, HA

supported with polyethylene was applied to a cell culture and an increase in cell numbers was observed (Bonfield et al., 2002a).

Growth factors have been added into HA scaffolds in order to enhance healing in orthopedic studies. Andreshak applied basic fibroblast growth factor (bFGF)-impregnated Gelfoam and coralline HA to defects that had been constituted by Kerrison rongeur in the tibia of rats. An increase in cartilage volume by bFGF was seen but the healing was not accelerated in the first few days. Although angiogenic effect by bFGF was observed after 2 weeks, the histological appearance of the treated defect was similar to that of the control groups at 4 weeks. Furthermore, according to bending tests, treated groups were weaker than the controls (Andreshak et al., 1997).

According to Carlisle, Si is essential, especially in the early stage of bone calcification, and has a role in the localization of active growth areas (osteoid) in rat bones (Carlisle EM, 1970,1981). The application of a combination of Si with HA (Si-HA) onto a cell culture caused prevention of inflammation and led to an increase of bone formation (Bonfield et al., 2002). Patel applied Si-HA and HA ceramics to laboratory animals and observed more bone ingrowth and a higher bone mineral apposition rate in the Si-HA implanted groups (Patel et al., 2002). In another study, Silica-CaP nanocomposite scaffolds were evaluated by mechanical and cell culture tests (Gupta et al., 2007). After intense mechanical tests, Polymerase Chain Reaction (PCR) study had been done in *in vitro* conditions. Although the superior effect of scaffold had been observed in cell culture conditions, the scaffolds were not tested in *in vivo* conditions.

The ceramics of this study had HA basement. Sr, Si and BMP-2 were integrated for enhancing mechanical and biological properties of ceramics. There were several studies with especially polymer or metal-reinforced ceramic systems for improving properties. One of the purposes of this thesis was researching bioceramics, which did not contain any supportive biomaterial as metal. The main difference of HA based ceramics of this study from other researches about HA systems, was evaluating them in terms of 3

different subject: with mechanical, *in vitro* and *in vivo* tests. Mechanically strong and biocompatible bioceramics were aimed to be generated in this study.

1.10.3 Trials Related to Defect Healing in Rats:

Different kinds of materials have been applied to defects in numerous orthopaedic studies. Logically, Ca based materials were the preferred ones.

3 types of bone grafts containing different concentrations of Ca–Sr–zinc–silicate glass were evaluated by *in vitro* and *in vivo* tests with rats (Boyd et al., 2009). The grafts were applied to fibroblast cells in culture conditions. Then the grafts were implanted to the femoral defects of healthy and ovariectomized rats, which were caused by dental bur. An alternative bioglass based material Novabone® was used for comparison. The grafts performed well with new bone formation areas in the healthy rats and diminished implant response in the osteoporotic rats. All three grafts caused higher cell viability than the alternative material; Novabone. The grafts that contained higher levels of Sr than others resulted in more bone development.

Develioğlu applied HA based Unilab Surgibone® to calvarial defects of rats that had been formed by trephine (Develioğlu et al., 2005). The material did not reveal significant osteoconductive properties according to histological results. In addition, no foreign body infection was detected at the experiment sites. The grafts were accepted as biocompatible, but more research is needed to investigate their resorption properties.

Kochi applied highly porous HA-containing resins to defects in rats and evaluated using micro focus computerized tomography (Kochi et al., 2009). An increase in bone volume caused by HA was observed.

Mardas investigated the effect of HA-synthetic cell binding peptide on calvarial defects in rats (Mardas et al., 2008). Limited bone formation was detected in the treated defects and the differences between the treatment and control groups were not significant.

CaP bone cement modified with chondroitin sulphate was applied to tibial defects in rats, formed by using a drill (Schneiders et al., 2008). The chondroitin sulphate supported material had more compressive strength than the non-supported material. Bone contact with new bone formation was observed at day 28 in the treatment groups due to the chondroitin sulphate.

Mostly Ca based biomaterials had been tried for defect healing studies. The materials were evaluated by mechanical tests or *in vitro* tests before application and tissue tests after implantation. All three type of assessment were done in this thesis study. Because Ca based materials showed discrepancies between different researches. The results of *in vitro* tests were waited to support the results of *in vivo* tests in this study. Also mechanical test results were shown for bioceramic systems to become an alternative treatment way in the future.

1.10.4. Trials with BMP-2 for Bone Formation:

Bone morphogenetic protein (BMP) triggers bone formation in animal studies and was preferred in bone regeneration studies (Reddi AH (1994,1997), Schmitt et al. (1999)).

Numerous studies have shown the beneficial effect of BMP-2's role in bone formation *in vivo* (Wozney et al. (1988), Wang et al. (1990), Volek-Smith et al. (1996)) and *in vitro* (Katagiri et al. (1990), Chen et al. (1991), Theis et al. (1992), Rosen et al. (1994), Chaudhari et al. (1997), Yamaguchi et al. (1995,1996), Wang et al. (1993), Hay et al. (1999)). Bone morphogenetic proteins were isolated from bovine bone extracts and their stimulation effects on bone formation subcutaneously were observed in rats (Urist MR, 1965). Since BMP-2 can stimulate osteogenic differentiation of MSC (Wang et al., 1990), gene therapy with BMP-2 is an alternative in osteoporosis treatment. Recombinant human BMP-2 (rhBMP-2) caused cartilage and bone formation, applied through implantation, in rats (Wozney et al. (1988), Wang et al. (1990)). BMP-2 and -7 absorbed into collagen sponge, was applied to repair

tibial fracture in spinal fusion treatment (White et al. (2007), Jones et al. (2006), Garrison et al. (2007)). BMP-2 can also affect the absorption properties of HA scaffolds; BMP-2 integrated functionally graded apatite (fg-HA) resulted in the accelerated bioabsorption of materials (Murata et al., 2007).

BMP-2 has been combined with various materials in studies on bone formation. Poly lactic acid-co-glycolic acid (PLGA) microspheres were tried out as carriers for BMP-2 and resulted in an increase in ALP activity in a 70 day period in *in vitro* and *in vivo* studies (Kempen et al., 2008). Biodegradable gelatin hydrogel with BMP-2 has also been tried and the induction of bone formation was observed (Fukunaka et al., 2002).

BMP-2-containing apatite-coated poly D,L-lactide co glycolide/ nanohydroxyapatite (PLGA/HA) particulates has been tested in *in vivo* conditions (Kim et al., 2008). BMP-2 carrying scaffolds caused more bone formation in the calvarial defect model when compared with fibrin gel containing BMP-2. Mineralization in the healed areas was broader in BMP-2 loaded groups than in BMP-2 deficient groups.

Inactive collagen bone matrix (ICBM-means demineralized bone matrix that was extracted with guanidine or urea to deport non collagenous proteins) has been mixed with different concentrations of rhBMP-2 and applied to calvarial defects in rats (Ron et al., 1992). Significant bone regeneration was observed in ICBM+BMP-2 applied groups.

Hirata investigated the effect of carbonate apatite-collagen sponge (in a porous HA frame ring) scaffolds on cell cultures (Hirata et al., 2007). These scaffolds were also reinforced with BMP-2 and applied to the periosteum cranii of rats. The proliferation of OBs, ALP activity in *in vitro* tests and bone formation in *in vivo* tests was observed.

A combination of MSC, HA and BMP-2 had been tested by implantation into rats (Noshi et al., 2001). Although HA and BMP-HA did not show bone formation, in particular MSC-HA-BMP combination resulted in obvious bone formation at all time points.

The time for BMP application has been evaluated with bovine HA implanted in rats (Warnke et al., 2010). Four weeks after the intramuscular insertion of HA blocks to one side of rats, a second block was again inserted to the other side of rats. rhBMP-2 was injected to both blocks during the second implantation. The delayed application of BMP-2 resulted in slightly lower bone density development.

HA and HA-TCP combination ceramics with the magnetic field have been evaluated for their effects on bone healing in *in vitro* conditions. BMP-2 was then added to those ceramics and implanted subcutaneously for observation in *in vivo* conditions (Wu et al., 2010). Ceramics with the magnetic field showed good biocompatibility as the stimulation of cell proliferation and new bone-like tissue formation was seen by the expression of BMP-2.

BMP-2 was evaluated in many researches by *in vitro* tests and *in vivo* tests. BMP-2 was applied in a biomaterial by intramuscularly or to bone defects. BMP-2 was assessed by adding into polymer, HA or collagen based biomaterials mostly. These studies lead us to use BMP-2 for enhancing properties of ceramics. The bioceramics were also containing different concentrations of Sr in this study. By this approach, the effect of BMP-2 had chance to be evaluated with different concentration of Sr in ceramics by *in vitro* and *in vivo* tests.

1.10.5. Trials with Sr Substituted Bioceramics:

The effect of Sr as an input to osteoid tissue development and the repression of the resorptive system in bones were initially observed by Lehnerdt (Lehnerdt F, 1910).

Sr^{+2} has been used since the 1950's for bone healing (Shorr et al. (1952), McCaslin et al. (1959)). One of the first studies about the Sr effect in osteoporosis involved giving Sr lactate, which caused more Ca storage than only Ca administration (Shorr et al., 1952). Sr^{+2} containing drug S12911 (di-

strontium salt of 3-(3-cyano-4-carboxymethyl-5-carboxy2-thienyl)3-azapentanedioic acid) has been tried for the treatment of osteoporosis (Marie et al., 1993) and normalization of bone mineral content has been detected after S12911 application in ovariectomized rats (Marie et al., 1993).

Commercial drugs that contain Sr ranelate have been used as a preventive treatment for osteoporosis (Meunier et al. (2002,2004), Reginster et al. (2005)). Sr ranelate regulates bone cells' CaSR activity by raising the concentration of Ca in the microenvironment (Pi et al., 2004). CaSR's signal resulted in bone formation by OBs (Tang et al. (2007), Ammann et al. (2004), Canalis et al. (1996), Baron et al. (2002), Takahashi et al. (2003)). Sr ranelate triggered an increase in bone resistance of L4 body, trabecular bone volume, trabecular thickness, cortical thickness (Ammann et al., 2004), BMD level (Roux C, 2008), and a reduction in vertebral fracture after a year (Seeman et al., 2006b). According to Ammann's study, a high dosage Sr ranelate treatment in diet affects the bone tissue of vertebra, but lowering amount of drug intake did not give the same result (Ammann et al., 2004). Sr ranelate has been approved as a drug for osteoporosis treatment by the European Union since 2004. Outside of trials on humans, Sr ranelate also increased bone formation and decreased bone resorption in *in vivo* studies in rats (Marie et al. (1993, 2001), Hott et al. (2003)). Sr ranelate caused cell proliferation and collagen-noncollagen protein synthesis stimulation in rat calvarial OB cultures (Canalis et al., 1996). However, there are some disadvantages of Sr ranelate usage. Side effects of Sr ranelate as nausea, headache or diarrhea can be improved with time (Cole et al., 2008). According to reports of UK General Practice Research Database, other symptoms include memory loss, gastrointestinal disturbance, venous thromboembolism, pulmonary embolism, skin response, drug rash with eosinophilia and systemic symptoms (DRESS) and Stevens-Johnson syndrome (Grosso et al. (2008), Vestergaard et al. (2010)). Dermatitis, eczema (Roux C, 2008) and toxic epidermal necrolysis (Lee et al., 2009) were also seen at patients.

Si and Sr substituted ceramics have been researched before. The studies mostly focussed on material properties and cell culture experiments. Si substitution into HA ceramics caused earlier bone repair than only HA ceramics according to a previous *in vivo* study (Hing et al., 2006). Sr silicate ($SrSiO_3$) has been seen to stimulate HA formation. At day 7, $SrSiO_3$ resulted in hydroxycarbonate apatite formation by soaking simulated body fluid. Also $SrSiO_3$ had a cytocompatible effect, resulting in the proliferation of mouse fibroblast and rabbit bone marrow stromal cells (Zhang et al., 2010). Again, in another study using Ibuprofen, Sr-containing HA was shown to have drug loading and controlled release properties (Zhang et al., 2010).

Sr substituted HA coating on titanium implants was researched in ovariectomized rats by Li et al. (Li et al., 2010). After material characterization, a significant difference in Sr substitution was observed in *in vivo* tests. Osteointegration was evaluated by histomorphometry and micro tomography analysis. The Sr containing HA coated implant had better results than only HA coated implants. Titanium mostly caused good biocompatibility in bone; and a coating with Sr was a meaningful decision for enhancing osteointegration. In the ovariectomized rat model, the effect of ceramics could have been assessed using dual-energy X-ray absorptiometry (DXA), X-ray picture (XP) and *in vitro* studies (such as a proliferation test). The above research has certain similarities with this current thesis, but this study also examines the behavior of Sr substituted HA, without a titanium scaffold, in a cell culture environment.

Sr containing HA cement had been applied to hip replacement model and observed for integration of composite to bone (Ni et al., 2006). An apatite layer had been observed at samples that had Sr-HA cement by spectrometry. Examination of apatite layer histomorphometrically could give more clear results.

Sr substituted β-tricalcium phosphate (β-TCP) had been evaluated for release and cytocompatibility properties (Hamdan Alkhraisat et al., 2008). The material caused same effect as not Sr containing material at human OB

culture condition. Although the release test and cytocompatibility have been assessed, the different concentrations of Sr could be compared and wide *in vitro* tests could be done for observation of effect to OBs. This material could be conducted to *in vivo* studies as osteoporotic models.

Sr-containing hydroxyapatite/polyetheretherketone (Sr-HA/PEEK) composites had been tried for load bearing orthopedic applications (Wong et al., 2009). The mechanical properties of human bone had been studied to be mimicked at that study. Bioactivity of Sr containing scaffold was more according to apatite formation assays. But no difference had been observed at cell culture experiments although Sr has positive effects at OBs according to other researches.

Sr containing HA bone cement had been prepared by Guo (Guo et al., 2005). Compressive strength of ceramics had been evaluated with different concentration of Sr content of samples. Although cytotoxicity test and cell culture experiments have been conducted, the composites had not been tried in *in vivo* experiments.

Sr incorporation into bioactive glass had been resulted with enhancement of metabolic activity of OBs. ALP activity had been observed near decrease at Oc activity (Gentleman et al., 2010). However, Bioglass had not been prefferred for fractures at especially load bearing sites.

Sr-doped CaP scaffolds had been incubated with rat OB sarcoma cells and effect of Sr had been evaluated by MTT and ALP assays (Qiu et al., 2006). Sr containing scaffolds resulted significant cell proliferation rates than that of control. The appearance of cell-scaffold contact had been examined by SEM. Porous scaffold thought to be tried for bone regeneration by researchers. When pore formation could be studied, more bone ingrowth can be resulted in this manner.

Near Sr, other elements had been added to researches about bone. Sr and Magnesium (Mg) addition to β-TCP have been tried (Banerjee et al., 2010). The human OB culture conditions resulted with development at cell proliferation and attachment. Also, the ceramics had been evaluated in *in vivo*

conditions and higher bone formation rate had been observed. Near this, lower concentration of Ca had been detected by urine analysis of rats which had Sr contained β-TCP application.

Sr and zinc had been incorporated into Ca-Si system and had been examined with mechanical, *in vitro* and *in vivo* tests (Zreiqat et al., 2010). Induced attachment with proliferation of human bone derived cells had been observed. Effect of growth factor by addition to scaffold may be investigated in this study.

Also, according to researches, Sr addition to ceramics improved their compression strengths (Guo D (2005), Dagang G (2010), Liu WC (2010)).

Sr had been used as treatment for osteoporosis of humans since many years. The effect of Sr-Si – incorporated biomaterials was evaluated by either *in vivo* or *in vitro* tests. In some researches any significant result was obtained. The difference of this thesis study was assessment of different concentration of Sr-containing ceramics by *in vitro* and *in vivo* tests for finding most adequate ceramic constitutions. Also BMP-2 was applied to Sr-containing ceramics because of researching whether effect of BMP-2 could improve the biological properties. Mechanical properties of the ceramics may support the availability of bioceramics for defect healing in the future.

1.11. Originality:

Encouraging results have been obtained by researchers to treat bone defects in OVX rats. The difference of this study is comparison of different concentrations of Sr substituted Si-HA ceramics with BMP-2 addition by *in vitro* and *in vivo* tests. After characterization of ceramics, compression test was performed for measuring strength of materials. The Sr release from ceramics was observed by a spectrometer. Then different concentrations of Sr integrated BMP-2 added ceramics were evaluated by *in vitro* tests for cell proliferation and biocompatibility. *In vitro* tests were important to observe the effects of BMP-2 and Sr in ceramics with OBs. The moderately better Sr

concentration was then selected and assessed in *in vivo* tests using XP, DEXA and micro tomography.

The tests in this study were all linked. The results of each test were analysed and sample concentrations for application to the next test were decided prior to passing on to the next test. The compression test and Sr release test initially gave data about the ceramics. The *in vitro* experiments were important for obtaining the best concentration of Sr in a rat OB culture environment. The application of the ceramics to defects in an ovariectomized rat model resulted to being able to gauge the biological impact of the ceramics using a histological approach.

This research in this thesis was a multidisciplinary study that provides evidence about the effect of BMP and/or Sr-substituted Si-HA ceramics in *in vitro* and *in vivo* conditions after mechanical tests.

1.12. Aims of The Study:

First aim of the study was investigating mechanical characterization of Si-HA ceramics that have also Sr contents. Secondly, observation of behavior of Sr substituted HA ceramics in distilled water environment by spectrometer were undertaken. And lastly, evaluation of effect of BMP and/or Sr incorporated Si-HA ceramics in cell culture and *in vivo* conditions.

Whether adding Sr into Silicon doped Hydroxyapatite ceramics will improve compression strength?

Sr or BMP addition to Si-HA ceramics were researched with four different approaches as their effect at mechanical, chemical, cellular and histological tests. Evaluation of ceramics was done with compression test near observation them by X-ray diffraction test, scanning electron microscope (SEM) and porosity test.

Whether Sr-Si-HA ceramics will release Sr in time?

Sr containing ceramics were waited in distilled water for in time period and the observation of Sr release behavior of ceramics was done by spectrometry.

Whether Sr-Si-HA ceramics are biocompatible with rat bone marrow stem cells in in vitro conditions? Whether adding BMP-2 into the ceramics will improve in vitro biocompatibility?

BMP-2 and/or Sr-containing ceramics were incubated in cell culture environment resulted with cell proliferation, ALP assays and SEM evaluations.

Whether Sr-Si-HA ceramics promote bone defect healing when implanted into rat tibia? Whether adding BMP-2 into the ceramics will improve in vivo biocompatibility?

Investigation of ceramics was finished with applying ceramics to defect areas in ovariectomized rat models. *In vivo* tests had 2 stages. The procedures of both stages were same. Firstly Si-HA ceramics were applied to rats and the biocompatibility properties of them were observed for a long time (31 weeks after implantation). This period was long but beneficial for observation of behavior of Si-HA ceramics before adding Sr into them. Then, Sr substituted Si-HA ceramics had been applied to other groups for examining the effect of that trace element. Effects of ceramics were examined by DXA, XP, micro CT and histology in *in vivo* studies.

The ability of Sr-containing ceramics to support proliferation of rat OBs and defect healing at tibias of rats was investigated in this study. These researches were done with Sr-containing ceramics for observation of their possibility to be used for healing faster at postmenopausal women against possible osteoporotic fractures in the future.

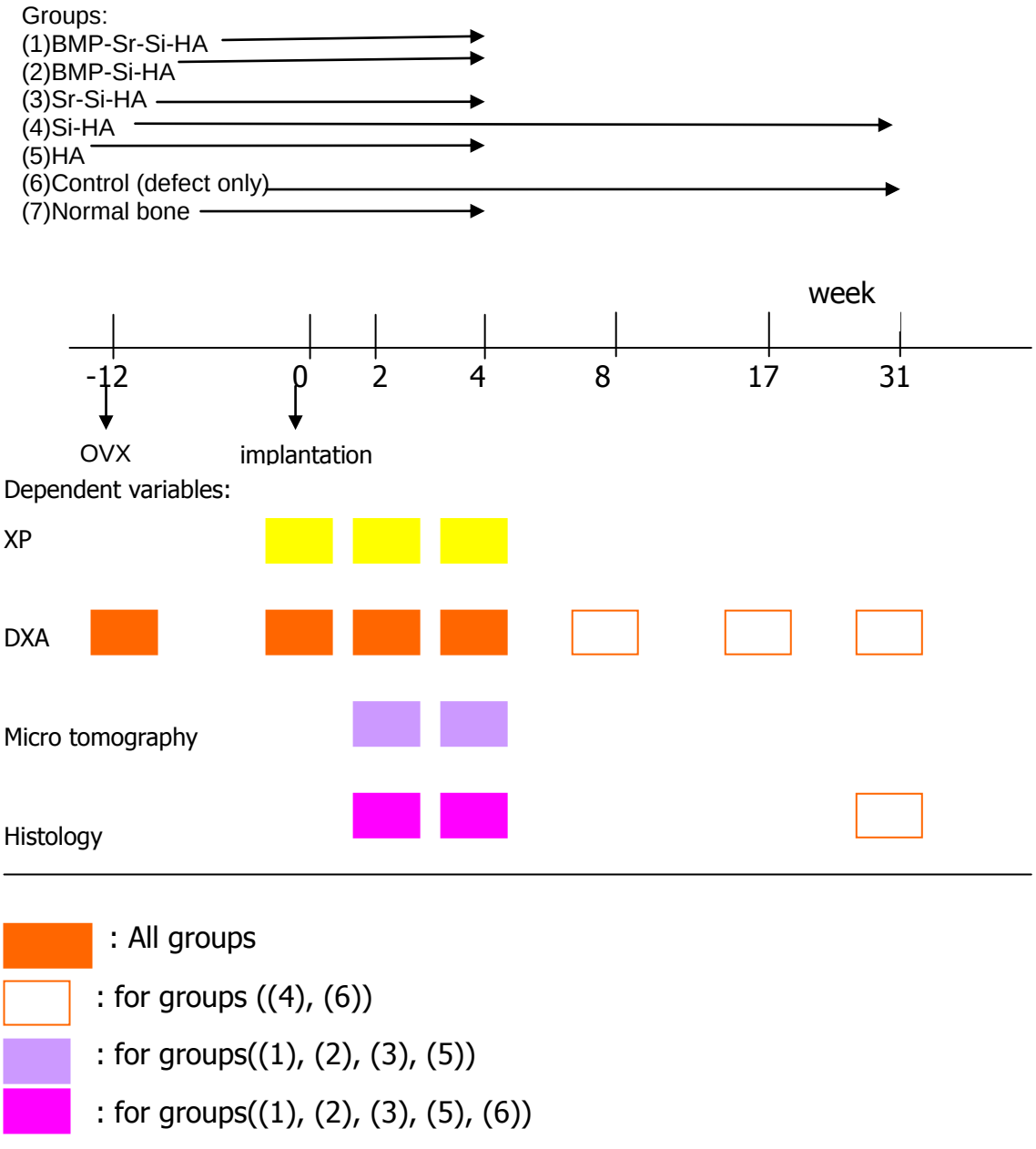

Figure 1.3. The groups that were tested in all experiments and their evaluations by radiology, dual energy X-ray absorptiometry, micro-tomography and histology.

CHAPTER 2

MATERIALS and METHODS

2.1. Design

An interdisciplinary (Materials Engineering, Chemistry, Medicine) multi-center study conducted at Middle East Technical University, Hacettepe University Faculty of Medicine and Alberta University Department of Chemical and Materials Engineering was designed. Departments involved in this study are Metallurgical and Materials Engineering, Chemistry, Chemical and Materials Engineering, Medical Center and Histology and Embryology.

At the first stage of this study, the ceramics were developed and characterized. At the second stage of the study, Sr release was assessed. Compatibility of the bioceramics with cells in culture was evaluated at the third stage of the study and finally the bioceramics were implanted into rat tibia for *in vivo* biocompatibility assessment.

Independent variables of the *in vivo* study were groups (n=4) and time (n=2) and dependent variables were radiology, micro-computer tomography (micro-CT), BMD by DXA and histology scores.

2.2. Development of The Ceramic Systems:

2.2.1. Preparation of The Ceramic Systems:

Ceramics were developed at Middle East Technical University, Department of Metallurgical and Material Engineering Ceramic Laboratory by consultancy of Prof. Muharrem Timuçin.

Molecular formula of calcium HA is $Ca_{10}(PO_4)_6(OH)_2$. HA powder was prepared by precipitation of solid precursors from aqueous solutions which included calcium phosphorus ions (Koç et al., 2004). Suspension of $Ca(OH)_2$ in water with phosphoric acid (H_3PO_4) was prepared to produce the HA powders (Akao et al., 1981). $Ca(OH)_2$ (Merck #102047, Darmstadt, Germany) and orthophosphoric acid (H_3PO_4- Merck #100564, Darmstadt, Germany) diluted in deionized water (0.1M) were used. The amount of materials that were used to prepare ceramics, $Ca(OH)_2$ and H_3PO_4 were adjusted in a manner that a molar ratio of Ca:P=1.67 was maintained in the slurry with this reaction:

$$10Ca(OH)_2 + 6H_3PO_4 \rightarrow Ca_{10}(PO_4)_6(OH)_2 + 18H_2O$$

↓

Hydroxyapatite

$Ca(OH)_2$ powder was first placed into a beaker and deionized water was added. The beaker was placed on a hot plate and contents were mixed for 30 minutes with the magnetic stirrer. The beaker was heated to 85°C. 0.1 M H_3PO_4 solution was added into this mixture through a burette in a drop wise manner. Then the beaker was placed into the oven (90°C) for drying the solution. The obtained powder was pressed into cylindrical tablets under 1250kgf/cm^2 pressure. Pressed tablets were calcinated at 1000°C for 6 hours. Then the tablets were turned to powder form. Few amount of powder form ceramics were brought to XRD test for characterization. After getting XRD results, the procedure was continued. Powder form ceramics were put

into a box containing plastic coated Zirconium balls with ethanol. The box was left to turn for 12 hours onto machine which have rotating columns. Then, the powders were taken out and were put into an agate mortar for blending under ethyl alcohol with 3% polyethylene glycol (PEG). 5 gr ceramic powder was mixed with 2 cc polyethylene glycol and 1 cc ethanol. This mixture was waited 1 day at room temperature for drying. Tablet forms were pressed from dried mixture and sintered at 1200°C in PROTHERM (PLF 15015) sintering furnace for 4 hours. PLF 15015 sintering furnace is capable to reach 1450°C in temperature.

The procedures of Si-HA and Sr-Si-HA powder preparation had been the same as of the HA powder. Si and Sr were added to ceramics at initial part as mixing to $Ca(OH)_2$ containing mixture. The phosphate of HA was partially replaced by Si to produce Si-doped HA. Source of silicon dioxide (SiO_2) was Sigma Aldrich (cat.# S5130).

Sr carbonate was added to ceramics as 250, 500 and 1000ppm amounts. The formula of Sr integrated HA new ceramic was:

$Ca_{10-x}Sr_x(PO_4)_{6-y}(SiO_4)_y(OH)_{2-y.}$

'x' means Sr atoms that were integrated into the ceramic and y designates the SiO_4 content in the ceramic.

Table 2.1. Material weights for the preparation of the ceramics.

Ceramics	$Ca(OH)_2$(gr)	H_3PO_4(cc)	SiO_2(gr)	Sr(cc)
HA	25.8	40.5	-	-
Si-HA	29.6	46,1	0.7	-
Sr250-Si-HA	29.59	47.0	0.2	0.1
Sr500-Si-HA	29.58	47.0	0.2	0.2
Sr1000-Si-HA	29.56	47.0	0.2	0.4

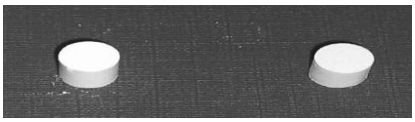

Figure 2.1. Ceramics that were used in all experiments.

2.2.2. Material Properties:

2.2.2.1. X-Ray Diffraction (XRD) Analysis:

X-ray diffraction analysis was carried out as previously described ((Hernandez et al. (2008), Li et al. (2007)). Briefly, the RIGAKU (model:D /max 2200/PC, Tokyo, Japan) instrument was used for material characterization at Middle East Technical University Department of Metallurgical and Material Engineering. The diffractometer had been operated at 40kV and 40mA and powdered samples of ceramics were scanned between 2θ values of 20 and 50°. λ_{value} was 1.542 A°, step size was 0.05° with 3 sec count time in order to determine the crystal structure of each apatite.

XRD result of HA, Si-HA, Sr250-Si-HA, Sr500-Si-HA and Sr1000-Si-HA ceramics are presented in Figure 2.2. The first image in Figure 2.2 presents XRD analysis result of HA. Crystallographic description of HA ceramics was carried out according to the Joint Committee on Powder Diffraction and Standards (JCPDS, HA, 09-0432).

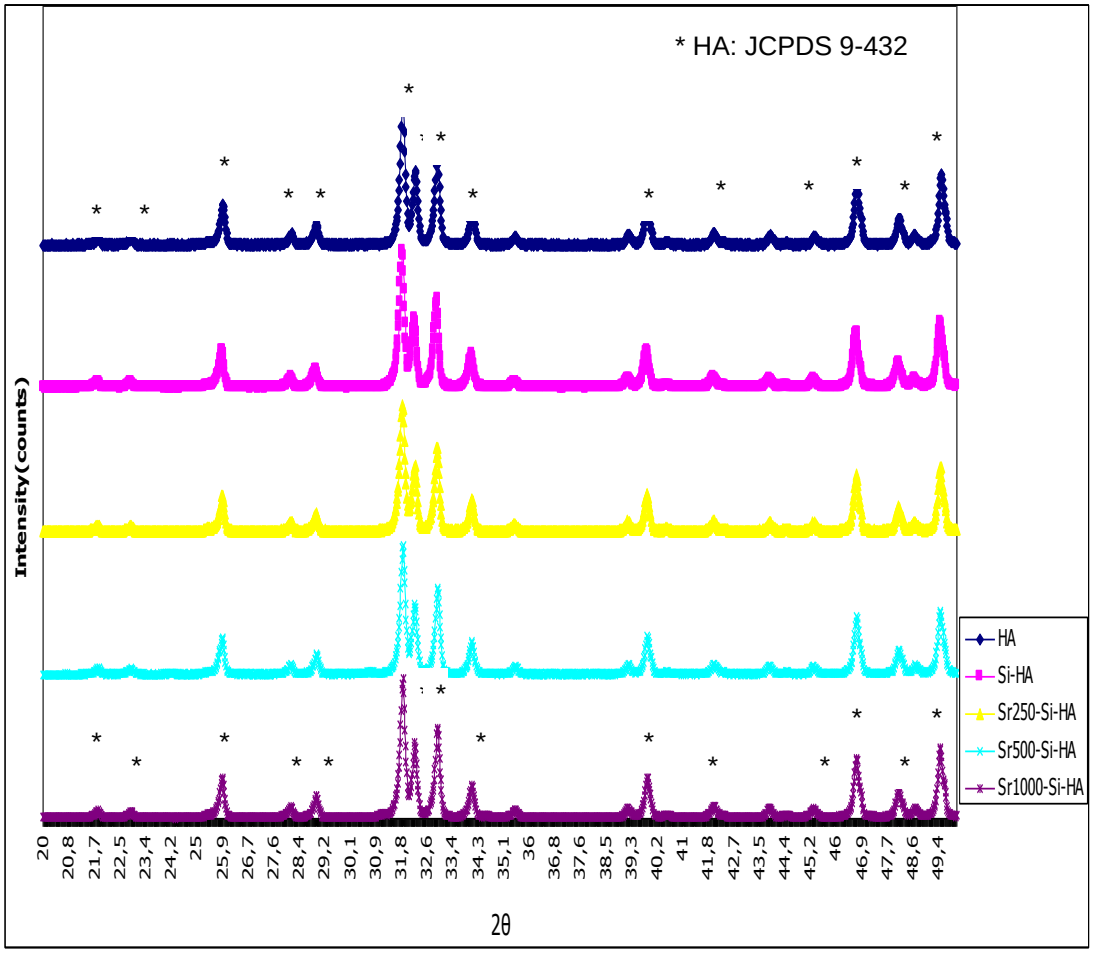

Figure 2.2. XRD graphs of HA, Si-HA, Sr250-Si-HA, Sr500-Si-HA, Sr1000-Si-HA ceramics.

The pattern of the HA sample synthesized in the absence of Sr displays well defined and adequate peaks in agreement with JCPDS, HA, 09-0432. Molar ratio of Ca:P was wanted to be 1.67 in HA ceramic. If more and sharp peaks at around 2θ values of 30°-40° had been seen, the ceramic was named to have CaO or TCP content. If the ceramic have CaO content the molar ratio of Ca:P will be more than 1.67. And if ceramics have TCP content, the Ca:P ratio will be decreased.

2.2.2.2. Porosity Test:

Pore formation in ceramics allows osteoblast penetration and physiological fluid permeation of whole porous apatite scaffold (Landi et al., 2003). Pore formation in the ceramics of this study was important for observation of cell ingrowth into the ceramics in the *in vitro* experiments.

Porosity test in this study can be considered close to Standard Test Method for Water Absorption, Bulk Density, Apparent Porosity, and Apparent Specific Gravity of Fired Whiteware Products (ASTM-C 373-88 (Reapproved 2006)). But xylene had been used in this study instead of water in the protocol and 1 tablet from every ceramic group was included to test. For obtaining porosity firstly, weights of ceramic tablets (W_{dry}) were measured before applying them into xylene. Ceramic tablets were immersed into xylene for 24 h. After 24 h, weight of suspended samples (W_{susp}) was measured. The ceramics were put onto paper towel for wiping out of the xylene from the surface and saturated weights (W_{sat}) were measured.

The results of the test were reached with using the formula given below:

$d_{bulk}=W_{dry}* 0.861 / (W_{sat}-W_{susp})$

d_{bulk}:percentage of ceramic form only

0.861: density of xylene

When d_{bulk} is calculated for every ceramic, another formula had been used for obtaining material percentage and porosity percentage.

d_{bulk} / d_{th}=material%

1-material%=porosity%

d_{th}: is the theoretical density of HA=3.156 g/cm^3

porosity%: percentage of porosity in ceramics

Table 2.2. Bulk density (g/cm^3) of ceramics used in this study.

Material	d_{bulk} (g/cm^3)
HA	1.843
Si-HA	1.914
Sr250-Si-HA	1.99
Sr500-Si-HA	1.89
Sr1000-Si-HA	1.973

The porosity % values of the ceramics are said to be similar (Figure 2.3.). Porosity test had been done with only 1 tablet from every ceramic, so there were no standard deviation results. But the porosity values of all samples can be accepted to be close. The few differences between results might be related to sintering (Bucholz RW, 2002).

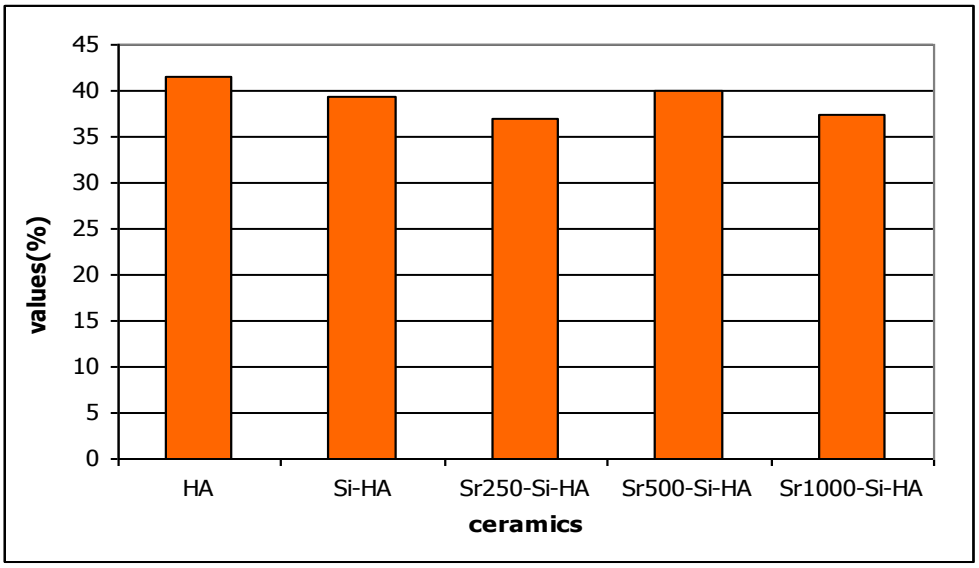

Figure 2.3. Porosity percentages of the ceramics assessed in this study.

2.2.2.3. Compression Test:

The Schimadzu (Schimadzu Corporation, model AGS-J, max 10kN application capacity, Tokyo, Japan) mechanical testing machine and its Trapezium data processing software were used to measure the compression strength of the ceramics.

Figure 2.4. Schimadzu mechanical testing machine.

Cylindrical ceramic tablets (diameter: 9.4-9.8 mm and height:7-7.2 mm in size) were placed in the machine and axial compression load was applied onto the tablets. The load to failure of the tablets was recorded and the strength was calculated. Four ceramic tablets from every ceramic group were included to this test.

$\sigma = F/A$

is the formula that the calculation of the compression strength ”σ” was made. “F” means the load to failure, and “A” is the area of circle, which is the upper part of the cylinder.

2.2.2.4. Scanning Electron Microscopy:

The JSM-6400 scanning electron microscope (JEOL, Tokyo, Japan) equipped with the NORAN System 6 X-Ray microanalysis system was used at the Middle East Technical University, Department of Metallurgical and Material Engineering. SEM examinations were performed on broken surfaces. Tablets were coated with a gold layer by the sputter coating equipment and SEM pictures were obtained.

Sr-Si-HA nanocrystals display more perturbed shapes than Si-HA nanocrystals according to Figure 2.5. The surface of Si-HA sample seemed to be more regular.

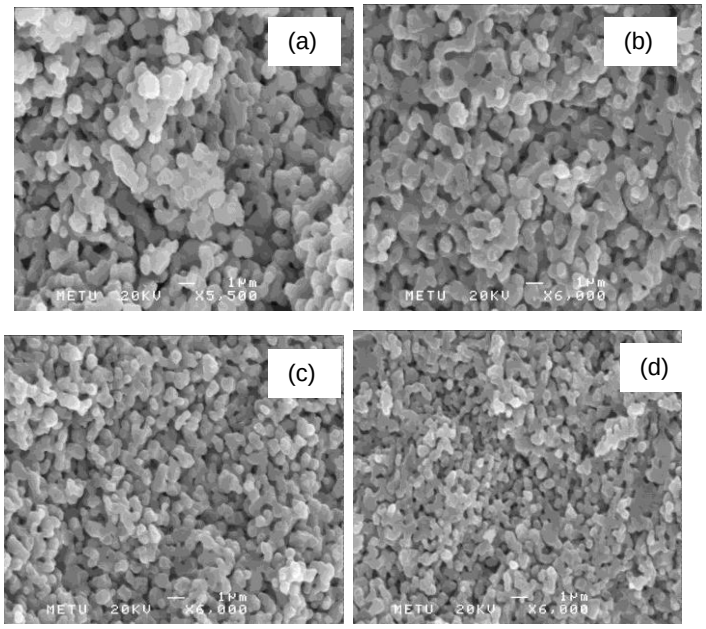

Figure 2.5. SEM images (a, b, c, d) of the Si-HA, the Sr250-Si-HA, the Sr500-Si-HA and the Sr1000-Si-HA ceramics.

2.3. Sr Release Test:

The experiments had two stages. Firstly a ceramic was immersed in an experiment box with 20 ml distilled water and assessed for 3 and 14 days in

room temperature. At the second stage, a ceramic was immersed in 20 ml serum and assessed for 3 and 14 days in 37°C, 5% CO_2 environment.

Ceramics that were incubated in distilled water or serum were:

a) HA

b) Si-HA

c) Sr250-Si-HA

d) Sr500-Si-HA

e) Sr1000-Si-HA

Samples were analysed at 421 nm wavelength using the inductively coupled plasma optical emission spectrometry (Profile Plus ICP-OES, Teledyne Leeman Labs, Hudson, USA) at the Middle East Technical University Department of Chemistry. Software of spectrofotometer is WinICP Database 1,3.

Figure 2.6. LEEMAN-ICP-OES spectrometry and software.

Software has been used for visioning analysis results. A calibration plot in a range of 10 ppm – 0.005 ppm was obtained with Sr (1000 µg/ml, Aldrich, Milwaukee, USA) stock solution. When R^2 value reached 0.99, then all samples were analyzed for their Sr amount. Samples were diluted at 1/3 ratio because of their intense environments.

2.4. *In Vitro* Experiments:

Sr-containing Si-HA ceramics were used in cell cultures for finding the ideal ceramic systems with the ideal Sr ratio after their sterilization in autoclave at 132°C for 45 min. *In vitro* experiments determined cell proliferation by MTT assay, DNA assay, ALP tests and SEM observations.

Cell culture tests and BMP absorption into the ceramics were performed at University of Alberta Department of Chemical and Materials Engineering by the consultancy of Prof. Hasan Uludağ.

6 study groups were established for the cell culture experiments.

i- HA
ii- Si-HA
iii- Sr250-Si-HA
iv- Sr500-Si-HA
v- Sr1000-Si-HA
vi- Control (cell+media)

These groups were tested with and without BMP addition to the environment.

Bone marrow stromal cells were obtained from Sprague Dawley rats. Rats were terminated by CO_2 inhalation and placed in a beaker with 70% ethanol for 10 minutes for surface sterilization. The bone marrow was isolated after the separation of the skin and surrounding soft tissues.

Bones were carefully removed and placed in a 50 ml tube containing sterile Hanks' Balanced Salt Solution (HBSS-Bio Whittaker®, cat. 10-527F). Epiphyses of bones were cut off by using the Littauer bone cutter. The marrow was eluted with the Dulbecco's Modified Eagle Medium (GIBCO®, cat.11995-065) supplemented with 10% heat inactivated fetal bovine serum (FBS: GIBCO®, cat. 26140-079), Penicillin/Streptomycin (GIBCO®, cat.15140-

122) and ascorbic acid (Sigma-Aldrich, cat. A-4544, St. Louis, USA). The same medium had been also used for cells to express osteoblast phenotype.

Cells were centrifuged for 6 minutes at 600 rpm. Supernatant was removed and cells were re-suspended in 10 ml media and plated in T-25 cm^2 flasks (~10 mL culture medium into each). Cells were grown in culture media with 10% FBS.

When cells were grown to ~80% confluence, the medium were vacuumed out from T-25 cm^2 flask; 5 ml of HBSS was added to the flask for cell washing that stayed for 30 s-1min. When HBSS was vacuumed out of the vials, 1ml of Trypsin (Sigma, T4174, St Luis, USA) was applied to the flask for 3 minutes with swirling to dissociate the cells. Cell detachment was observed under the inverted microscope. 5 ml medium was added to the flask and the mixture was collected to a test tube, then centrifuged for 6 minutes at 600 rpm. Supernatant was vacuumed out without touching to cells that were settled at the bottom. Medium had been added to test tube and cell count was conducted using a hemocytometer.

Cells were distributed into 24 well cell culture plates (Falcon by Becton Dickinson, NJ, USA) at amount of 20 µl/well with 500 µl of basic media. Cells were cultured in humid atmosphere containing 5% CO_2 at 37°C. Media was changed twice a week. All cell culture experiments were conducted as duplicate.

The BMP-2 was provided by Dr Walter Sebald from University of Wurzburg, Germany. 200ng/ml rhBMP-2 had been preferred for application to every ceramic in 24 well cell culture plate. Totally 12 µg BMP was added into 1200 µl RNAse free water (Invitrogen, New York, USA). 20 µl from mixture (amount of rhBMP-2=200ng/ml/well) was applied into every well that was containing 0.5 ml basic medium.

2.4.1. Tests and Microscope Observation for *In Vitro* Experiments:

2.4.1.1. MTT Test:

MTT test had been preferred by many researchers for observation of cell proliferation rate (Wu et al., 2010).

Different amount of cell suspensions were applied onto the 24 well-plates that contained 0.5 ml basic medium for an MTT calibration curve. The cells were allowed to attach and grow and the basic medium was changed every 4 days.

The MTT test has been used also for cells that were grown on ceramics. These cells were incubated with or without BMP and the assay was performed at days 1, 6, and 12. Content of the ceramic applied cultures was 20 µl of cells and 500 µl of media.

The MTT (3-(4,5-dimethylythiazol-2-yl)-2,5-diphenyltetrazolium bromide) assay was used for measuring cell viability. MTT solution was prepared with Thiazolyl Blue Tetra-zolium Bromide (Sigma-Aldrich, catalog number M2128-1G, Oakville, Canada) and HBSS at 5 mg/ml. After filtration of this solution, 100 µl MTT solution was added onto the cells of MTT calibration assay and ceramic applied cultures at stated days. Multi well plates were put into 37°C and 5% CO_2 incubators for 2 hour. Then supernatant was taken out and 1 ml dimethylsulfoxide (DMSO-(GIBCO-Invitrogen cat.11101-011, Ontario, Canada)) was added into multi well plates. The dissolved samples were transferred into 96 well plates (Corning, New York, USA) at 200 µl/well and absorbance was quantified at 570 nm (Issa Y, 2008) by using the KCjunior™ software(Bio-Tek Instruments, Winooski, USA) in a spectrofotometer (ELx800, BIO-TEK Instruments Inc., Winooski, Vermont, USA).

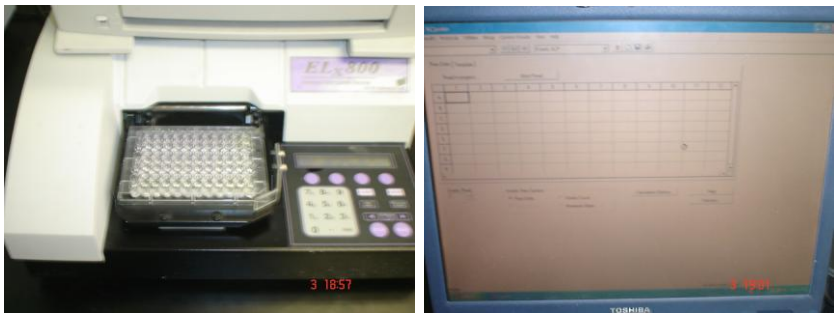

Figure 2.7. Spectrophotometer and the software during measurement.

2.4.1.2. ALP Test:

Typical cytochemical markers of osteoblast differentiation are ALP and mineralized bone nodules (Zamunovic et al., 2004).

ALP tests were made with cells in culture that were prepared for ceramic effect observation. Medium from the wells had been removed and wells were washed with 1 ml HBSS. ALP buffer (0.5 M 2-amino-2 methylpropan-1-ol, 0.1% (v/v) Triton x-100 in distilled water; pH:10.1) was added after removal of HBSS to lyse the cells. The cultures were incubated for 2 hours. 10 mg p-nitrophenyl phosphate (Sigma-Aldrich, catalog number P4744-5G, Oakville, Canada) was dissolved in 5 ml ALP buffer to give 2 mg/mL solution.

50 µl of lyzed cell solution were transferred from culture wells to a new 96 well plate and 50 µl from p-nitrophenyl phosphate solution was added onto them. Kinetic changes in absorbance were quantified at 570 nm by using the KCjunior™ software in a spectrophotometer (Mostafa et al., 2009).

2.4.1.3. DNA Test:

CyQUANT® Cell Proliferation Assay Kit (Invitrogen-Molecular Probes; catalog number C7026, Eugene, Oregon) was used for this aim. The kit contained cell lysis buffer, dye and DNA. Firstly lysis buffer had been

prepared with CyQUANT cell lysis buffer and RNAse free water according to the manufacturer's instructions. 2 ml of solution had been included to calibration study and 18 ml was used later. 6 eppendorf tubes and DNA (10 mg/ml) were used for initial experiment.

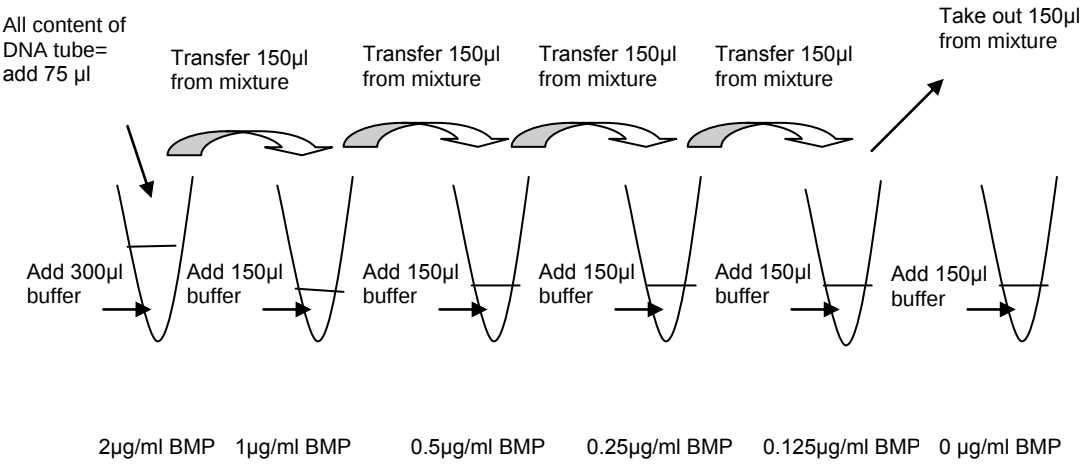

Figure 2.8. Preparation of standard curve samples for the DNA assay.

50 µl from samples and tubes of calibration were put into 96 well plates as duplicate study. Whole content of the dye was mixed to initial 18 ml (lysis buffer+RNAse free water) solution and 50 µl from this solution was added onto all samples in a 96 well-plate. After dye application, 485-527 nm absorbance was run in Fluroskan Ascent Microplate Fluorometer (Fluoroskan Ascent Thermo LabSystems, Helsinki, Finland) and results were followed by using the Ascent software (Varkey et al., 2007).

Figure 2.9. Fluroskan Ascent Microplate Fluorometer and Ascent software.

2.4.1.4. SEM Observation:

After proliferation tests, ceramics were used for SEM observation. Contents of the well that contained cells incubated with ceramics were taken out and rinsed with 1 ml HBSS. 0.5 ml 3% glutaraldehyde in HBSS was added to every well and incubated for 24h. When glutaraldahyde has been removed; 1 ml of 50%, 60%, 70%, 80%, 90% and 100% ethanol was added for each period of dehydration of the samples (Douglas et al., 2010). After incubation with different concentrations of ethanol, the plates were incubated at +4°C until observation. Ceramic tablets were observed with SEM at Alberta University.

2.5. *In Vivo* Experiments:

Ceramics were used alone or combined with growth factors for bone repair (Nunes et al., 1997).

Ceramics that were prepared at Middle East Technical University Department of Metallurgical and Material Engineering were applied to 36 week old female Sprague Dawley rats (range of weight 225-250g) at Hacettepe University Surgical Research Laboratory and housed at 12 h light/dark cycle with room temperature set at 25°C. Rats had adlib food and water. Ethical commission permission (#2007/32) was obtained on March 26, 2007. Housing, animal environment and experimental procedures were approved by the Hacettepe University Experimental Animal Care and Use Committee.

Rats were randomly assigned into experimental groups:

a) HA= rats that had OVX, defect operation and HA ceramic applied to defects.

b) Si-HA= rats that had OVX, defect operation and Si-HA ceramic applied to defects.

c) Sr-Si-HA= rats that had OVX, defect operation and Sr1000ppm-Si-HA ceramic applied to defects.
d) BMP-Si-HA= rats that had OVX, defect operation and BMP-Si-HA composite applied to defects.
e) Sr-BMP-Si-HA= rats that had OVX, defect operation and Sr1000ppm-BMP-Si-HA composite applied to defects.
f) Control= rats that had OVX, defect operation and ceramic was not applied to defects.
g) Control 2=rats that did not have OVX, defect operation or ceramic application operation.

After *in vitro* studies, ceramics were turned to powder form and autoclaved, then sterile rhBMP-2 had been applied to them without effecting from autoclave negatively. Two microgram of rh-BMP-2 was dissolved in 8 µl of injectable sterile water (Carlo Erba, Rodano, Italy), applied to ceramics and dried for 2 hours in room temperature and stayed for 4 days at -20°C (Noshi et al., 2001). Powder form of ceramics was applied to bone defects easily as other studies that used granule type ceramics (Gonda et al., 2009).

2.5.1. Ovariectomy Operation:

Quantity and quality of fracture callus is decreased during early period of fracture healing in OVX rats, so osteoporosis inhibits bone formation and mineralization (Xu et al., 2002). OVX caused osteoporosis results with low rate of fracture healing (Walsh et al., 1997).

Bone mineral densities (BMD) by DXA (DPX-L Lunar Radiation, USA) and XP (Siemens Multix C, Erlangen, Germany) measurements were done at the Middle East Technical University Medical Centre. Measurements were done before OVX, defect operations and continued 2 week and 4 week after defect operations. Analysis of data was done with regions of interest (ROI) at DXA machine. ROI of right tibia, left tibia, right femur, left femur and vertebra were analyzed at every measurement with DXA.

Anteroposterior radiographs were obtained on Agfa Mamoray MR3-II (Belgium) films. The distance of the x ray source to the bones was 100 cm. The setting of the machine was 42 kV and 3.2 mA per second. Films were developed using the Ecomat 21 (ELK Medical Products, Tokyo, Japan) automatic developing machine. Radiographs were evaluated by two independent observers (MB, HK) who were blinded to the groups. They scored the radiographs for periosteal reaction, quality of bone union, bone remodeling and ceramic integration according to a scoring system modified from An (An et al., 1999). Briefly, the score range of periosteal reaction was between 0 for none and 3 for full, the score range for quality of bone union was between 0 for nonunion and 3 for union, the score range for bone remodeling was between 0 for no remodeling and 3 for full remodeling cortex, and the score range for implant integration was between 0 for no change to 3 for fully replacement. The lowest and highest possible scores were 0 and 12, respectively.

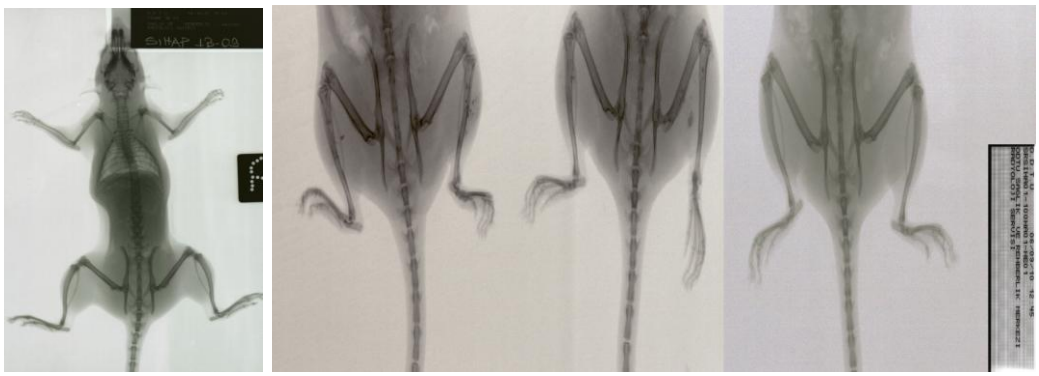

Figure 2.10. XP images of rats.

The groups of *in vivo* study had 2 stages as explained before. Firstly only Si-HA group had been compared with control (defect only) group. The XP values of these groups belong to only before OVX and operation time. This type of analysis helps us to see whether there is deformation before implantation.

The second stage of study was done with other ceramic groups and healthy group. The XP results of these second stage groups were evaluated at operation, operation+2week and operation+4week periods.

Figure 2.11. DXA machine and appearance of results during measurement.

Initially, OVX was applied to healthy rats that had normal BMD, under general anesthesia with Alfamine 10% (contains 100mg/ml Ketamin HCl) and Alfazyne 2% (has 20mg/ml Xylazin(HCl)- Alfasan International B.V., Netherlands). Alfamine (40-60cc intramuscularly) and Alfazyne (5-10cc intraperiotoneally) had been applied for anesthesia. Bilateral incisions were made via the abdominal midline incision and 2 ovaries were ligated from their suspensory ligament and veins.

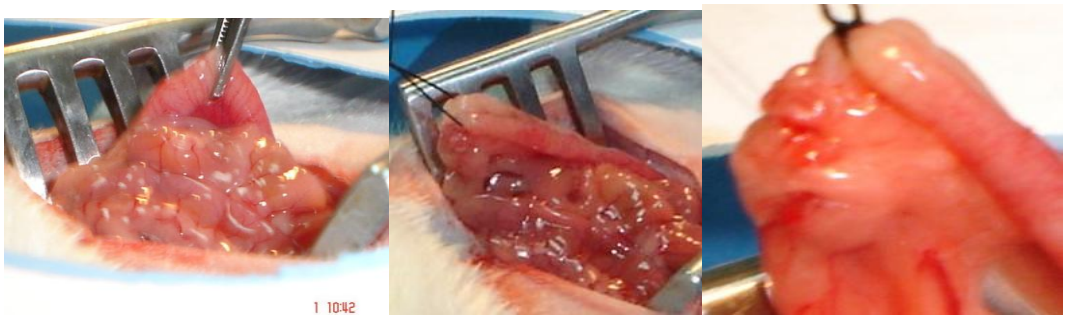

Figure 2.12. The uterus and ligation of the ovaries

After closing the incision with sutures (Silk suture (Noncapillary (3/0 R. cut. edge, autraumatic, nonabsorbable), Boz, Turkey)), spray film (OpSite® spray moisture vapor permeable spray dressing-Smith&Nephew Medical Ltd.

Hull, England) was applied onto the operation site for prevention of bacterial contamination.

2.5.2. Defect Formation:

Rats that had reduced BMD were included into the experiment according to DXA measurement results. Defects were formed in the left and right proximal parts of tibias of the rats. After anesthesia (same anesthetics for OVX operation) longitudinal incision were done from anteromedial site at tibia of rats. The defect was created at the medial cortex of the exposed tibia using a 2.5 mm drill (Dremel® 10.8 V, Lithium-ion, Breda-Netherlands). When the defect areas were cleaned with isotonic sodium clorur, cavities were filled with different type of powder form bioceramics.

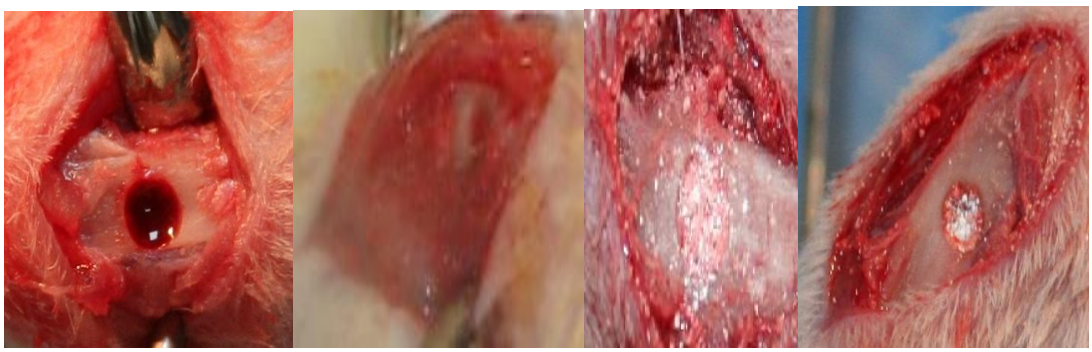

Figure 2.13. Formation of cortical cavity and filling with bioceramics.

Powder form HA, Si-HA and BMP and/or Sr-containing Si-HA ceramics were applied to the cavities. Muscles and skin were closed and Opsite® spray was applied for asepsis.

2.5.3. After Defect Formation:

Rats were allowed free cage activity at 12 hour light and 12 hour darkness with food-water *ad libidum* until they were terminated. BMD, XP

measurements were repeated 2 and 4 weeks after defect operation. Rats were terminated by application of high amount of Alfazyne-Alfamine at 2 and 4 weeks. The tibia samples were put into Formaldehyde.

2.5.4. Tests and Measurements for *In Vivo* Experiments:

After termination, histological tests were done in Hacettepe University Faculty of Medicine Department of Histology-Embryology and observation of defect healing was done by micro CT in Department of Anatomy.

2.5.4.1. Micro CT:

Samples of *in vivo* experiments were evaluated for observation of cavities with X-ray microtomography at Hacettepe University Faculty of Medicine Department of Anatomy. Compact X-ray microtomography (SkyScan 1174, Kontich, Belgium) had been used for this purpose. X-ray tomography system allowed measuring three dimensional object structures with resolution of less than 10 μm. This system uses Windows environment, the final images can be saved in BMP or TIFF formats. After termination, bone samples in formaldehyde were brought to tomography and placed to machine with focusing defect areas. Tomography was set for voltage and current to 50 kV and 800 μA with 2.000° rotation step. After measurement, analysis was done with its software. Firstly ROI areas were drawn at the defect areas and software separates HA and bone at defect areas by different colors. Lastly the percentage of bone healing was calculated as the ratio of bone volume to tissue volume.

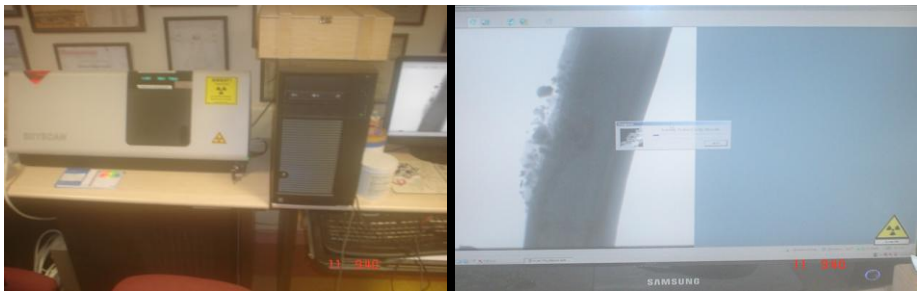

Figure 2.14. Micro CT measurements.

2.5.4.2. Histology and Histomorphometry:

Tibial bones were fixed in 10 % neutral buffered formalin at room temperature and all of the specimens sent to micro CT analysis. After analysis, all specimens were decalcified in De Castro solution (chloral hydrate, nitric acid, distilled water) and embedded in paraffin by using an automated tissue processor with vacum.

Figure 2.15. Samples in DeCastro solution.

Figure 2.16. Semi-enclosed Benchtop Tissue Processor and Modular Tissue Embedding Center.

Figure 2.17. Samples had been embedded with paraffin.

3 μm thick sections were stained with hematoxylin & eosin (HE), Masson's trichrome (MT). MT produces high contrast images with red bone, green osteoid-collagen and purple cell cytoplasm.

Figure 2.18. Sliding microtome that was utilized for taking sections from samples (Samples were collected by microscope slides).

Histomorphometry or quantitative histology is the analysis of histological sections by using bone formation and bone structure parameters. Photomictographs of each defect area were generated by a light microscope (Leica DMR) attached computerized digital camera (Model DFC 480, Leica, Westlar, Germany). Bright-field images of the defect area were captured and analyzed quantitaively by image processing program (Qwin Plus and LAS, Leica Inc., Westlar, Germany). Number of pixels corresponding to new trabecular bone area in each image of defect area was quantified, divided by the total number of pixels corresponding to total defect area and converted to μm^2 in each specimen. The cortical bone thickness was measured within

the defect zone and at the opposite healthy cortical bone site at randomly selected high power fields. The average defect zone cortical bone thickness relative to the normal cortical bone thickness was calculated and are reported as average for each sample. The tissue response to the bioceramics was semiquantitatively evaluated. (Table 2.3, Lu et al. (2004), An et al. (1999)).

Table 2.3. Histological scoring system for the tissue response.

Parameters	Scores				
	4	**3**	**2**	**1**	**0**
Fibrous connective tissue formation	severe deposition of dense collagenous connective tissue around implant.	disruption of normal tissue architecture and presence of moderately dense fibrous connective tissue	presence of moderate connective tissue	presence of delicate spindle shaped cells or mild fibroplasia	no difference from normal control tissue, no presence of connective tissue at or around implant site
Inflammatory cellular infiltration	severe cellular infiltrate response to implant or tissue necrosis at or around the site	presence of large numbers of lymphocytes, macrophages and foreign body giant cells, also notable presence of eosinophils and neutrophils	for presence of several lymphocytes, macrophages with a few foreign body giant cells and a small foci of neutrophils	presence of a few lymphocytes or macrophages, no presence of foreign body giant cells, eosinophil or neutrophils	no difference from normal control tissue, no presence of macrophages, foreign body cells, lymphocytes, eosinophils or neutrophils at or around implant site

2.6. Statistics:

Differences between groups were analyzed by nonparametric tests Kruskal-Wallis and Dunns test. Kruskal-Wallis test shows whether there are differences between groups. Dunns test defines which groups are significantly different from other groups. These statistical tests were performed to results of *in vitro*, micro CT and histology tests. The samples that had those measurements were independent between each other. But for

measuring DXA and XP, same samples had been used. Because of the dependence of samples, for DXA and XP results Friedman, Mann Whitney U and Wilcoxon statistical tests were used. The groups which have p values that were equal and lower than 0.05 were accepted to be different significantly.

CHAPTER 3

RESULTS

3.1. Ceramic Properties

3.1.1. Compression Test:

There were significant differences between compressive strength values of the ceramics used in this study. The HA group resulted with lower compression strength and the value of that group was significantly ($p=0.007$) lower than that of the other ceramics (Table 3.1., Figure 3.1.). Although Sr500-Si-HA ceramic had lower strength than the other ceramics that contained Sr, Sr1000-Si-HA resulted with the highest compressive strength in this study. The difference of Sr500-Si-HA ceramic from Sr250-Si-HA and Sr-1000-Si-HA were significantly lower ($p=0.007$).

Table 3.1. Compressive strength (MPa) (Ave±SD (Range: Min-Max)) of ceramics assessed in this study

	strength(MPa)(Ave±SD (Range: Min-Max))
HA	6.98±1.27 (5.69-8.64)
Si-HA	101.44±20.18 (81.46-129.91)
Sr250-Si-HA	108.26±20.18 (81.92-128.37)
Sr500-Si-HA	75.77±15.14 (62.40-91.88)
Sr1000-Si-HA	117.51±12.39 (99.38-126.49)

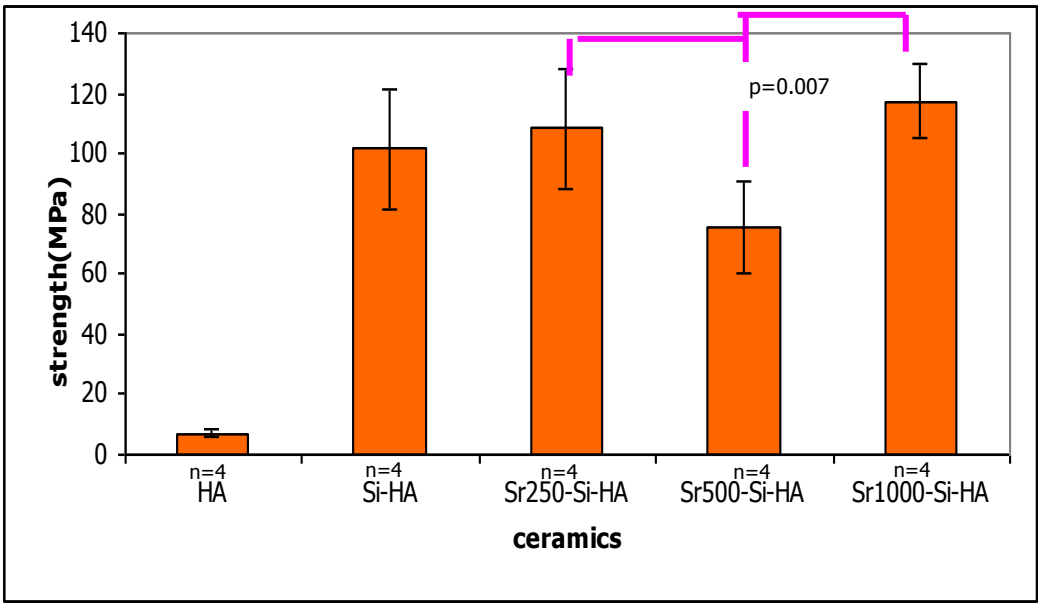

Figure 3.1. Compressive strength (MPa) of ceramics assessed in this study.

3.2. Sr Release Test:

Sr500-Si-HA ceramic released the highest amount of Sr into distilled water on day 3. Sr1000-Si-HA and Sr250-Si-HA followed Sr500-Si-HA by means of Sr release into distilled water at the same time point. Rate of Sr release on day 14 was similar to that of day 3.

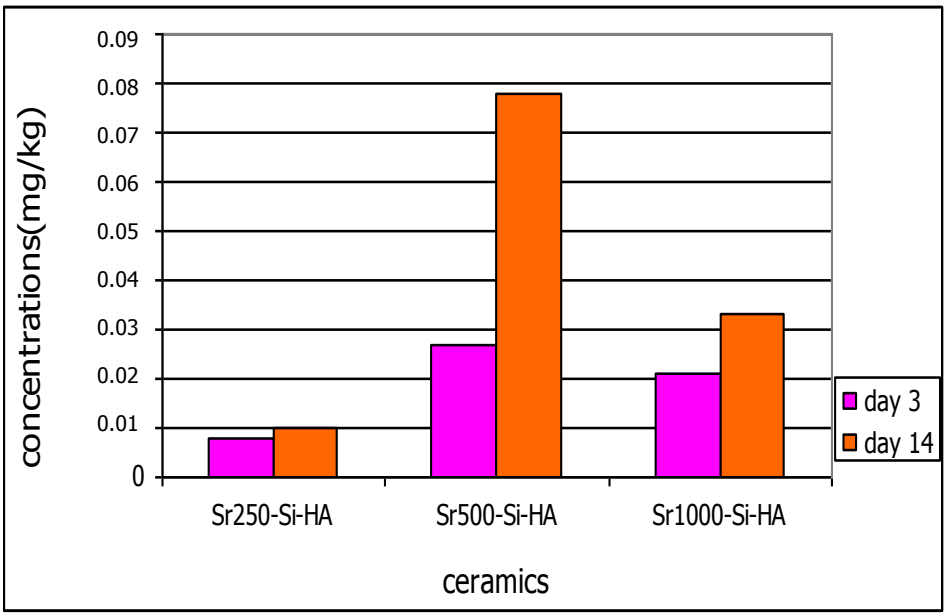

Figure 3.2. Sr release (mg/kg) from ceramics that were incubated in distilled water for 3 and 14 days (n=1 in all groups).

Sr250-Si-HA and Sr1000-Si-HA had more consistent Sr releases than Sr500-Si-HA. Especially at day 14, higher release from Sr500-Si-HA ceramic can be seen clearly (Table 3.2.).

Table 3.2. Sr amount (mg) released from the ceramics into 20 ml distilled water(data was calculated by using results of spectrometry).

		Released Sr amount(mg)		Release %	
	Sr content(mg)	day 3	day 14	day 3	day 14
Sr250-Si-HA	0.05	$16x10^{-5}$	$20x10^{-5}$	0.32	0.4
Sr500-Si-HA	0.1	$54x10^{-5}$	$156x10^{-5}$	0.54	1.56
Sr1000-Si-HA	0.2	$42x10^{-5}$	$66x10^{-5}$	0.21	0.33

Sr amount released into human serum was lower than the detection limit($15x10^{-4}$ mg/kg) of the spectrophotometer.

3.3. *In Vitro* Tests:

3.3.1. Proliferation Test by MTT:

MTT test showed proliferation of cells and biocompatibility of the ceramics and composites. MTT absorbance increased when the number of cells increased at the calibration test of the MTT assay (Figure 3.3).

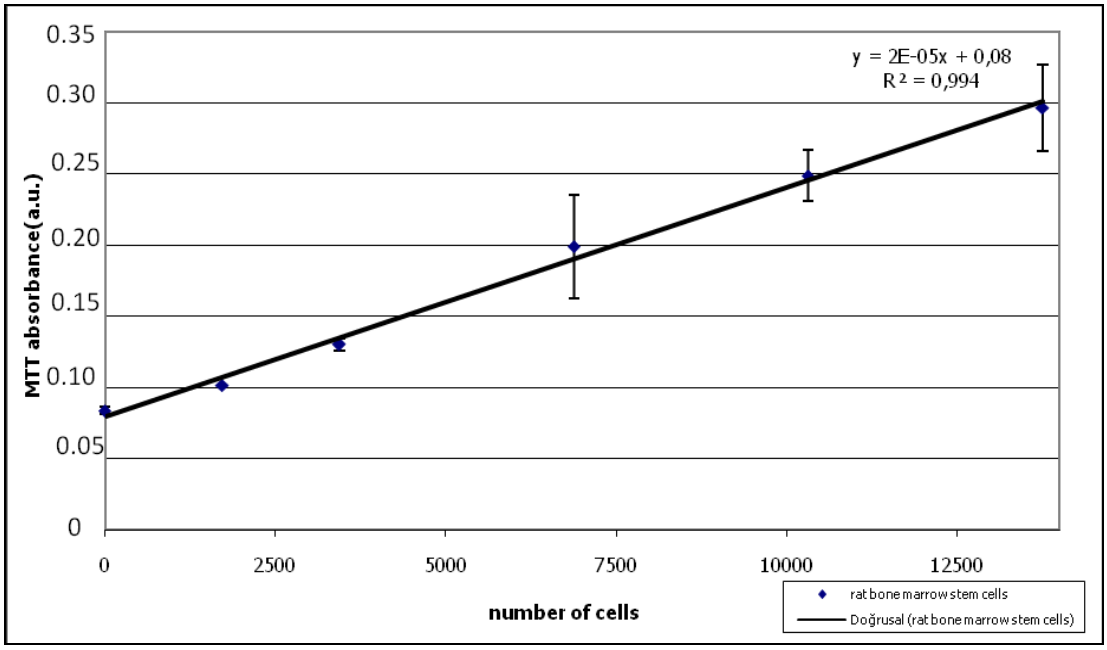

Figure 3.3. MTT calibration revealed increasing number of cells.

MTT assay results increased from day 1 to 6 in all groups but not in the Sr1000-Si-HA group (Figure 3.4). There were significant differences in between groups when they were evaluated among different time points. Cell proliferation rates increased in the Si-HA and the Sr250-Si-HA groups between days 1 and 6 ($p<0.001$). The cell proliferation rate of the Sr1000-Si-HA group however decreased between the same time points ($p<0.001$). At day 12, cell proliferation rates decreased in all groups.

On day 1, MTT absorbance of the Sr1000-Si-HA group was significantly higher ($p=0.035$) than all the other groups. On day 6, the Sr250-Si-HA group presented the highest MTT absorbance, which was

significantly (p=0.042) different from the other groups. On day 12, there was no significant difference between the MTT absorbance of the groups.

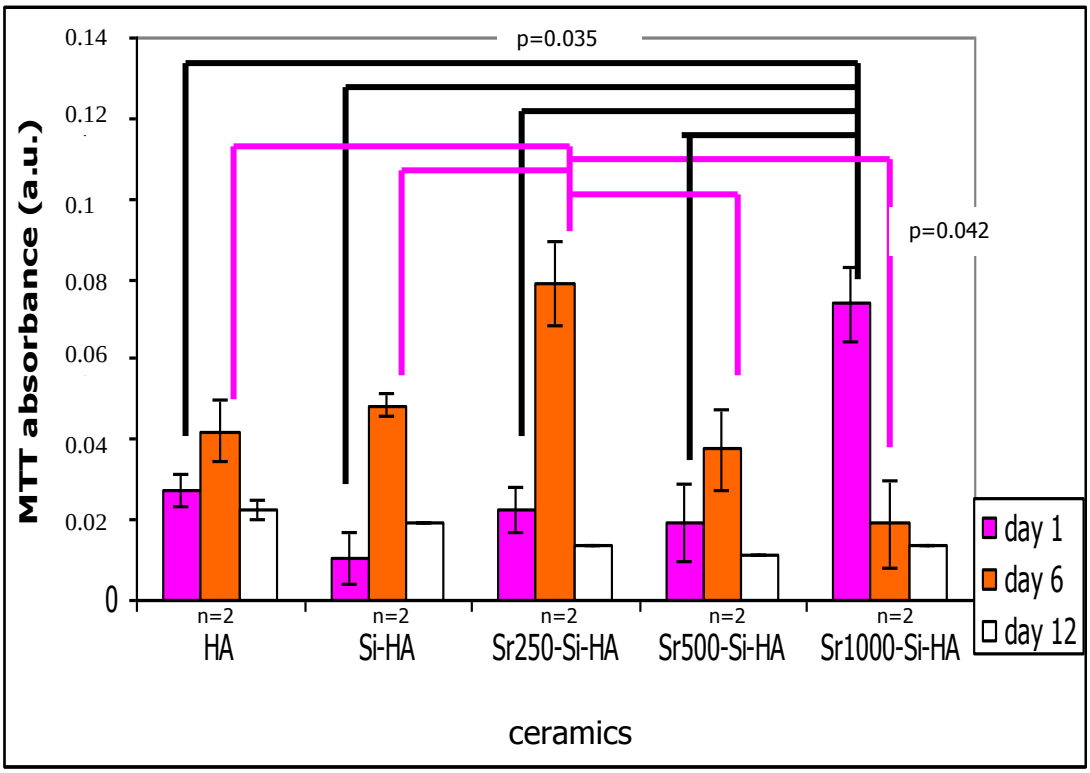

Figure 3.4. MTT assay results (a.u.) of cells that were applied to the ceramics.

When BMP was added to the ceramics, MTT absorbance decreased significantly between days 1 and 12 (Figure 3.5.). BMP-HA (p=0.006) and BMP-Sr1000-SiHA (p=0.05) presented significant MTT absorbance decrease between days 1 and 12. BMP-Si-HA and BMP-Sr250-SiHA groups MTT absorbance on the other hand increased (p=0.05) between days 1 and 6.

On day 1, the BMP-Sr500-SiHA group caused lower (p=0.035) MTT absorbance than that of the BMP-HA and the BMP-Sr1000-Si-HA groups. The results of the BMP containing ceramics had similarities with the not BMP-containing ceramics. Sr500-Si-HA still caused cells to have lower MTT absorbance on day 6. BMP-Si-HA and BMP-Sr250-Si-HA composites resulted with higher MTT absorbance on day 6 and their effects were significantly different from that of the BMP-Sr500-Si-HA composite (p=0.042). The BMP-

Si-HA composite resulted with higher (p=0.035) MTT absorbance than that of the BMP-HA and the BMP-Sr1000-Si-HA composites at the same time point. MTT absorbance of cells of the BMP containing ceramics reduced on day 12. BMP-HA and BMP-Sr1000-Si-HA composites resulted with significantly lower (p=0.006) MTT absorbance than BMP-Si-HA, BMP-Sr250-Si-HA groups.

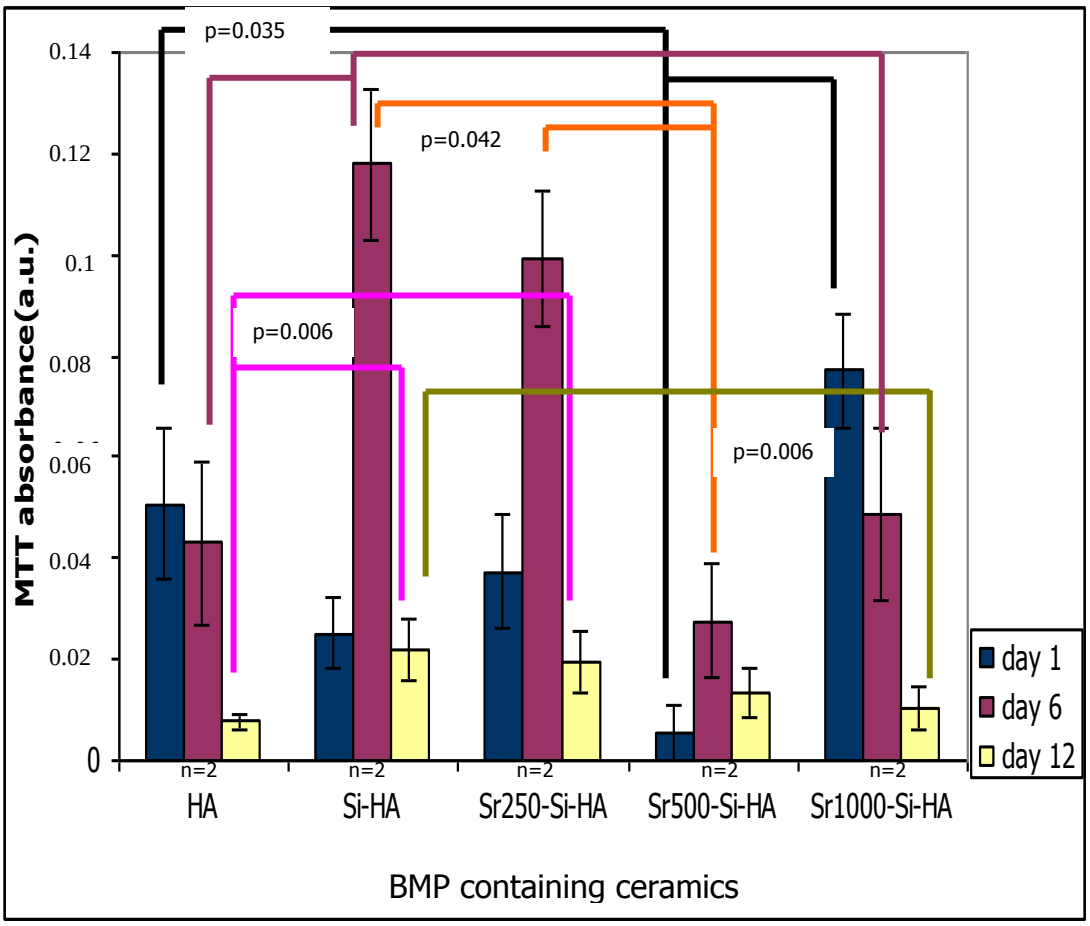

Figure 3.5. MTT assay results (a.u.) of cells that were incubated with BMP containing ceramics.

On day 1, the Si-HA group resulted with significantly lower (p=0.035) MTT absorbance values than the BMP-Sr1000-Si-HA group. The BMP-Sr500-Si-HA group showed lower (p=0.035) results than the Sr1000-Si-HA group at the same time point. On day 6 however, the Sr1000-Si-HA group caused significantly lower (p=0.042) results than the BMP-Si-HA and the BMP-Sr250-Si-HA groups. On day 12, the BMP-HA group had lower (p=0.006) MTT

absorbance than the HA and the Si-HA groups. Significantly lower (p=0.006) MTT absorbance value was obtained in the BMP-Sr1000-Si-HA group than the HA group on the same day.

The proliferation ability of cells that were incubated with the ceramics and composites was lower than the tissue culture polystyrene (tcps) containing wells (results were not shown in graphs).

Cell accumulation on the Sr1000-Si-HA and the BMP containing ceramics were observed on day 1.

Day 1

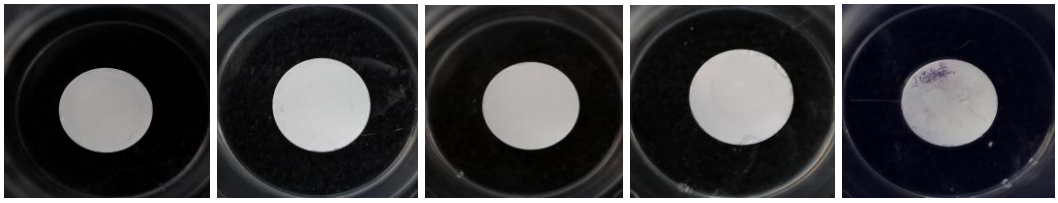

HA Si-HA Sr250-Si-HA Sr500-Si-HA Sr1000-Si-HA

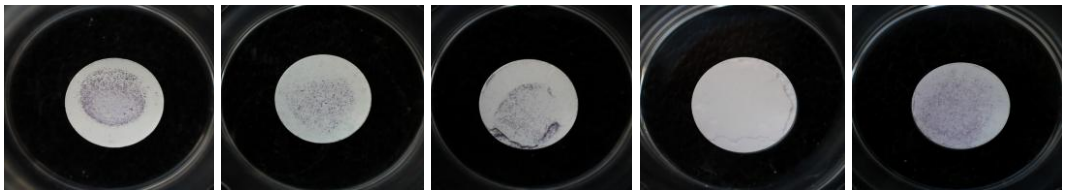

BMP-HA BMP-Si-HA BMP-Sr250-Si-HA BMP-Sr500-Si-HA BMP-Sr1000-Si-HA

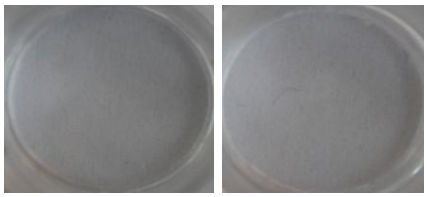

cells cells+BMP

Figure 3.6. Photos of ceramics in wells before MTT test at day 1.

Cells grew well in all groups with BMP on day 6. The well that contained only cells had more cells than the well containing BMP. This result was also observed at the MTT assay.

Day 6

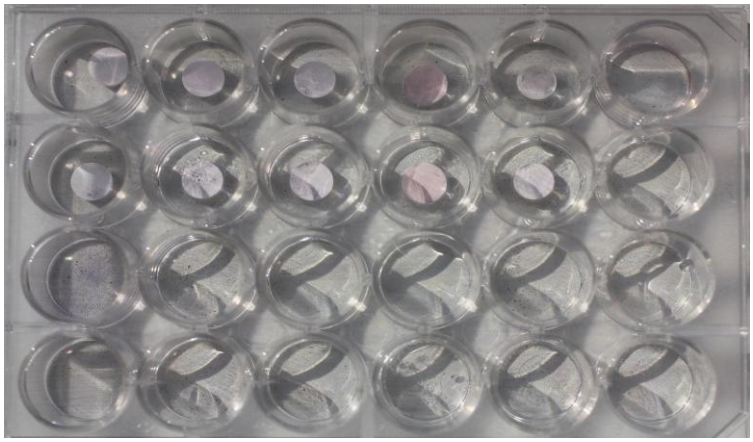

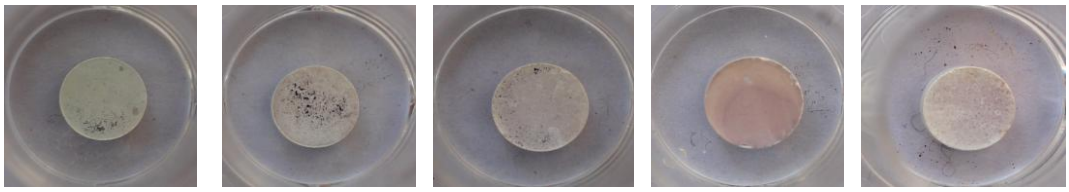

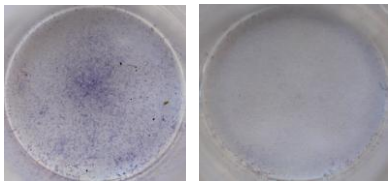

Figure 3.7. Photos of ceramics in wells before MTT test at day 6.

Wells that were containing the Sr1000-Si-HA, the BMP-Si-HA and the BMP-Sr250-Si-HA ceramics had more cell accumulation than the other wells on day 12.

Day 12:

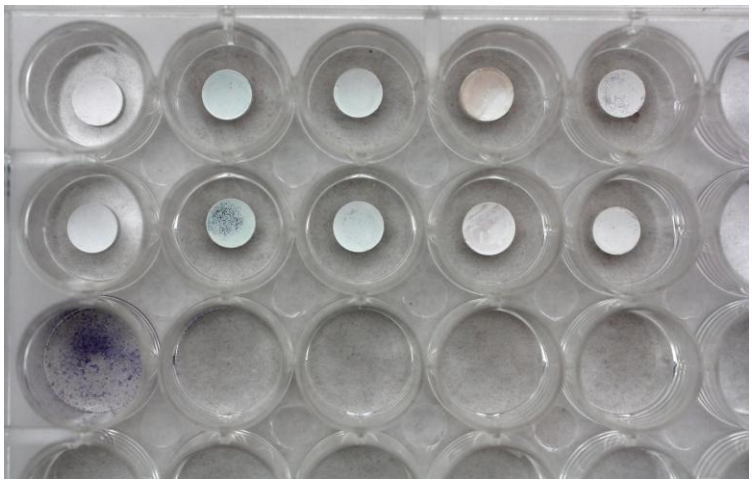

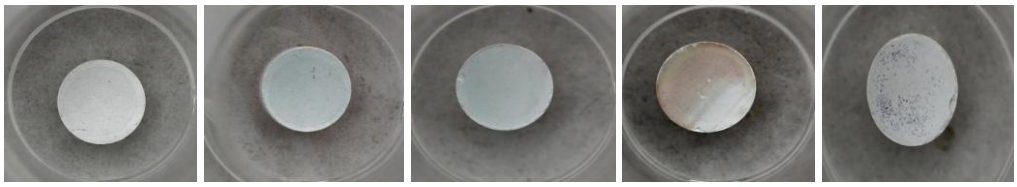

HA Si-HA Sr250-Si-HA Sr500-Si-HA Sr1000-Si-HA

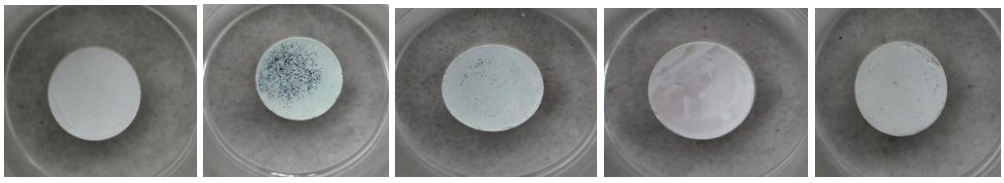

BMP-HA BMP-Si-HA BMP-Sr250-Si-HA BMP-Sr500-Si-HA BMP-Sr1000-Si-HA

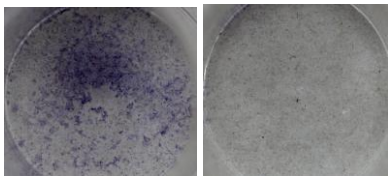

cells cells+BMP

Figure 3.8. Ceramics in wells before the MTT test on day 12.

3.3.2. ALP Tests:

The ALP absorbance difference between days 2 and 6 in the HA group was significant (p=0.019) (Figure 3.9). ALP activity of the cells that were incubated with the Si-HA ceramics significantly (p=0.037) decreased from day 6 to 12. In the Sr250-Si-HA applied cells, ALP activity was decreased between day 2 and 12 (p=0.019). Likewise, difference had been detected at the same time points with the Sr500-Si-HA ceramics (p=0.02). Sr1000-Si-HA ceramics resulted with significant increased (p=0.037) ALP absorbance between days 6 and 12. On day 2, there were significant (p=0.035) differences between the Sr1000-Si-HA, the HA and the Sr500-Si-HA ceramics. Sr1000-Si-HA ceramics presented significantly higher (p<0.001) ALP activity than the other ceramics on day 12.

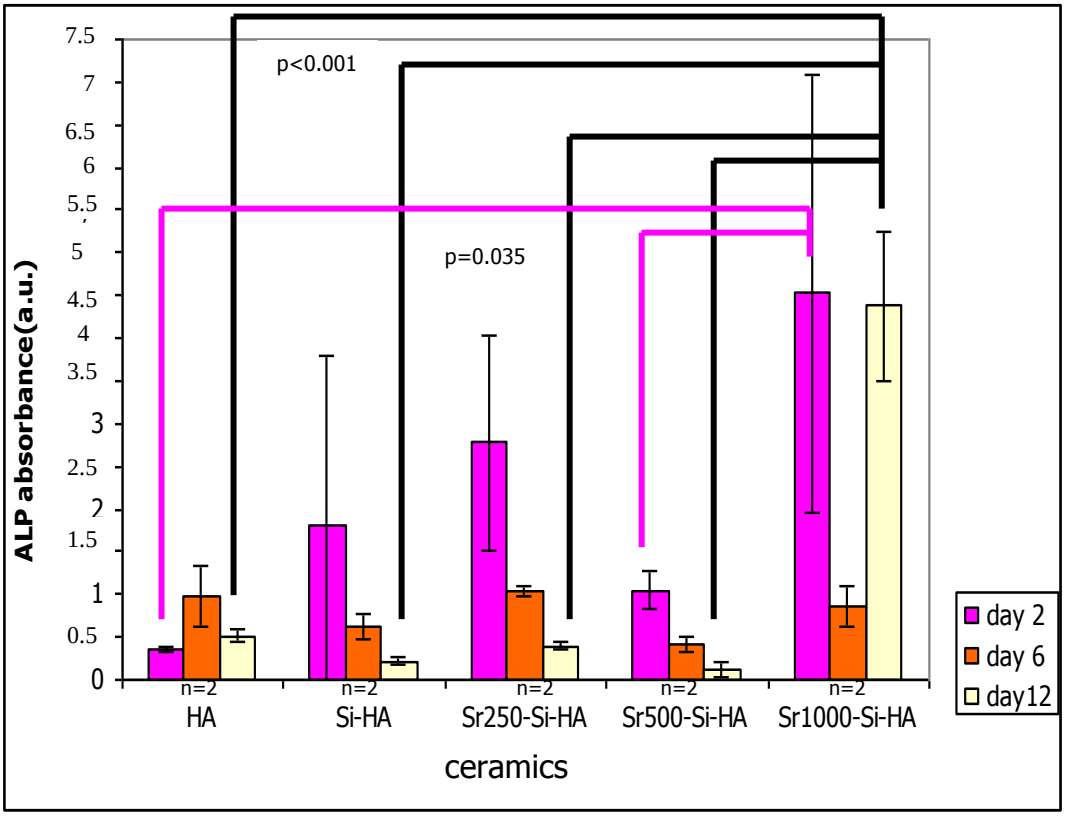

Figure 3.9. ALP assay results (a.u.) of ceramics.

ALP activities of the cells that were combined with the BMP-Sr containing groups reduced with time (Figure 3.10.). The ALP absorbance result of the BMP-HA group was increased between days 6 and 12 ($p=0.02$). Likewise, significant difference at the same time points had been detected with the BMP-Si-HA composites ($p=0.032$).

On day 2, the BMP-Sr1000-Si-HA group showed higher ($p<0.001$) ALP absorbance than the BMP-HA and the BMP-Si-HA groups. On day 6, ALP absorbance of the BMP-Sr500-Si-HA group was significantly lower ($p<0.001$) than the other BMP-containing ceramics. ALP absorbance of the BMP-HA and the BMP-Si-HA groups were also different ($p<0.001$) at the same time point. On day 12, only the BMP-Sr500-Si-HA group showed significant lower ($p<0.001$) results than the BMP-HA and the BMP-Sr250-Si-HA groups.

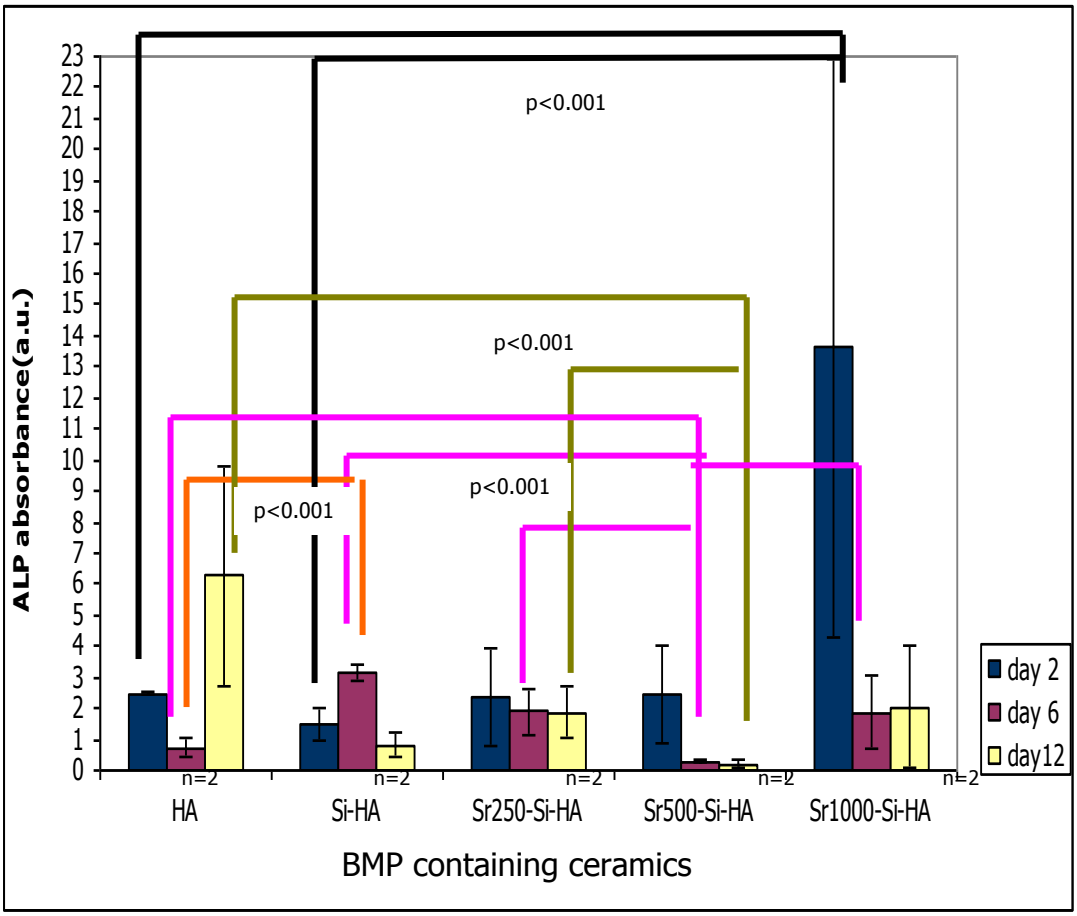

Figure 3.10. ALP assay results (a.u.) of BMP containing ceramics.

The ALP absorbance results of the BMP containing and not containing ceramics were compared. On day 2 there were no significant differences between the groups. On day 6, the BMP-Sr500-Si-HA group resulted with significantly lower ($p<0.001$) absorbance than the HA and the Sr250-Si-HA groups. The Sr500-Si-HA, which was not containing BMP, showed significantly lower ($p<0.001$) absorbance than the BMP-Sr250-Si-HA and the BMP-Sr1000-Si-HA groups. Near these results, BMP-Si-HA showed higher absorbance ($p<0.001$) than the Si-HA, the Sr500-Si-HA and the Sr1000-Si-HA groups. On day 12, ALP absorbance increased in the BMP containing groups. BMP-containing HA group caused higher ($p<0.001$) ALP absorbance than the Si-HA, the Sr250-Si-HA and the Sr500-Si-HA groups. The Si-HA group also showed lower absorbance ($p<0.001$) than the BMP-Sr250-Si-HA group. The Sr500-Si-HA group presented lower absorbance values ($p<0.001$) than the BMP-Si-HA, the BMP-Sr250-Si-HA and the BMP-Sr1000-Si-HA groups. The BMP-Sr500-Si-HA group however had lower absorbance values ($p<0.001$) than the Sr1000-Si-HA group.

On day 6 and 12, the cells that were incubated with the tcps showed higher ($p<0.001$) ALP absorbance than the cells that were applied with the ceramics and composites (results of tcps were not shown in graphs).

3.3.3. DNA Tests:

DNA absorbance increased when the number of cells increased at the calibration test of the DNA test (Figure 3.11).

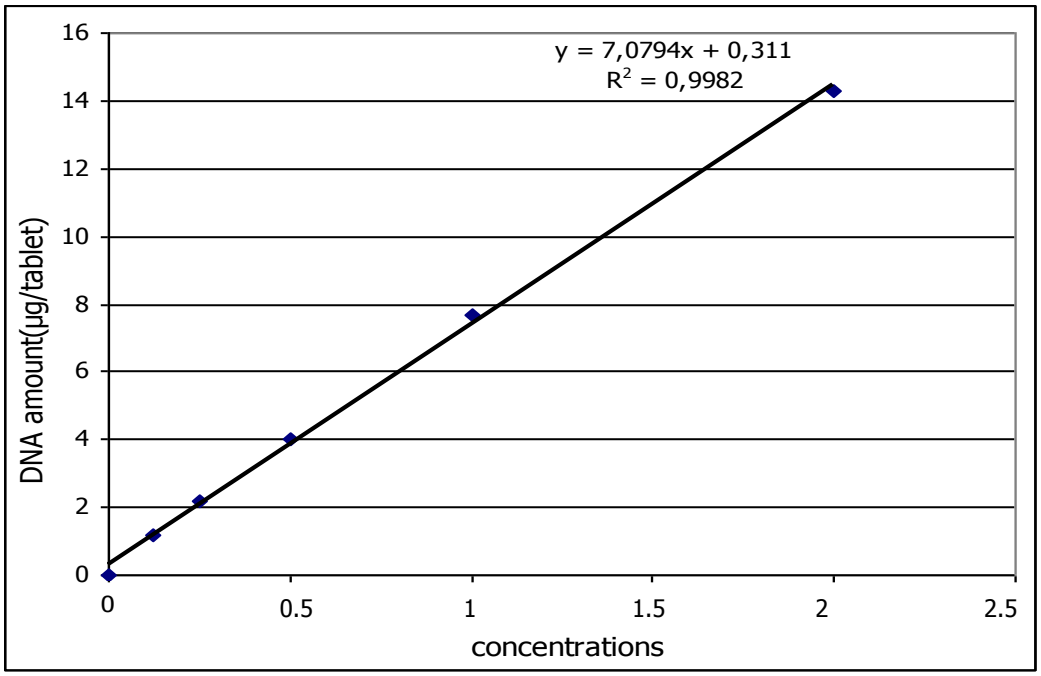

Figure 3.11. Standard curve of the DNA assay.

The difference of DNA amounts between day 2-6 and 2-12 in the HA group was significant (p=0.024) (Figure 3.12). DNA amounts of the cells that were applied together with the Sr250-Si-HA ceramics increased from day 2 to 6 (p=0.01). Likewise, difference had been seen at the cells that were incubated with the Sr500-Si-HA ceramics (p=0.012). In the Sr1000-Si-HA group, DNA amounts increased from day 6 to 12 (p=0.026).

On day 2, the Sr250-Si-HA and the Sr500-Si-HA groups had lower DNA amount than the other groups (p=0.035). On day 12, DNA amount of the Sr1000-Si-HA group was significantly higher from the cells that were incubated with the HA, the Sr250-Si-HA and the Sr500-Si-HA ceramics (p<0.001). Cells that were grown only on tcps showed higher (p<0.001) DNA amounts than the other ceramics on day 12.

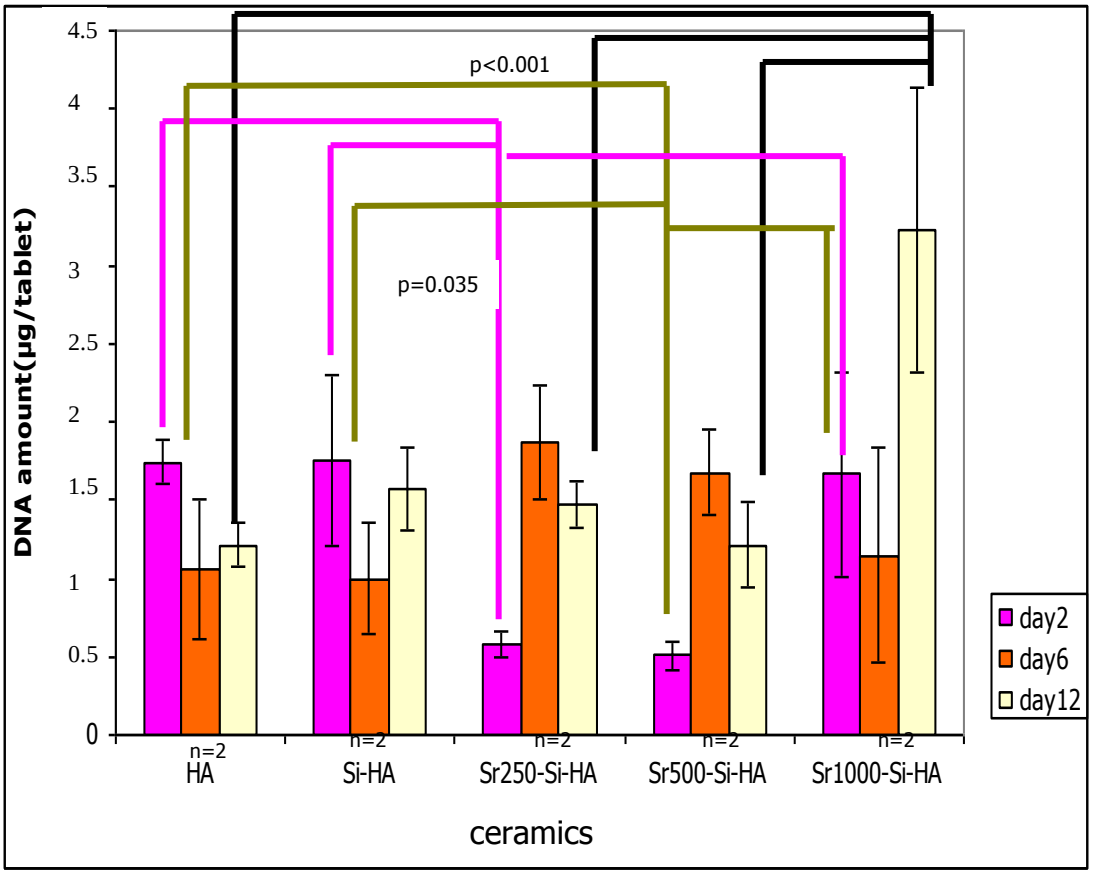

Figure 3.12. DNA assay results (µg/tablet) of the ceramics.

The DNA amount of the BMP-HA group was different (p=0.023) between days 2-6 and 6-12 (Figure 3.13.). Significant decrease in DNA amounts (p=0.012) at the BMP-Sr250-Si-HA group was observed between days 2 and 12. DNA amount difference (p=0.018) at the BMP-Sr500-Si-HA was detected between days 2-6 and 2-12. Significant decrease (p=0.018) in DNA amount at the BMP-Sr1000-Si-HA group was observed between days 2-12 and 6-12.

On day 2, the BMP-Sr500-Si-HA composite caused lower (p<0.001) DNA amount from that of the other composites. The BMP-Si-HA group resulted with higher (p=0.002) DNA amount on day 6 from that of the BMP-HA and the BMP-Sr1000-Si-HA groups. On day 12, the BMP-HA group caused higher DNA amounts than the other groups. The BMP-HA group had significantly higher (p=0.006) DNA amount results than the BMP-Sr250-Si-HA and the BMP-Sr1000-Si-HA groups. The BMP-Sr1000-Si-HA group presented

the lowest absorbance rate (p=0.035) from that of the BMP-Si-HA, the BMP-Sr250-Si-HA and BMP-Sr500-Si-HA groups.

Cells that were grown on tcps showed higher DNA assay results compared to the composites on day 2.

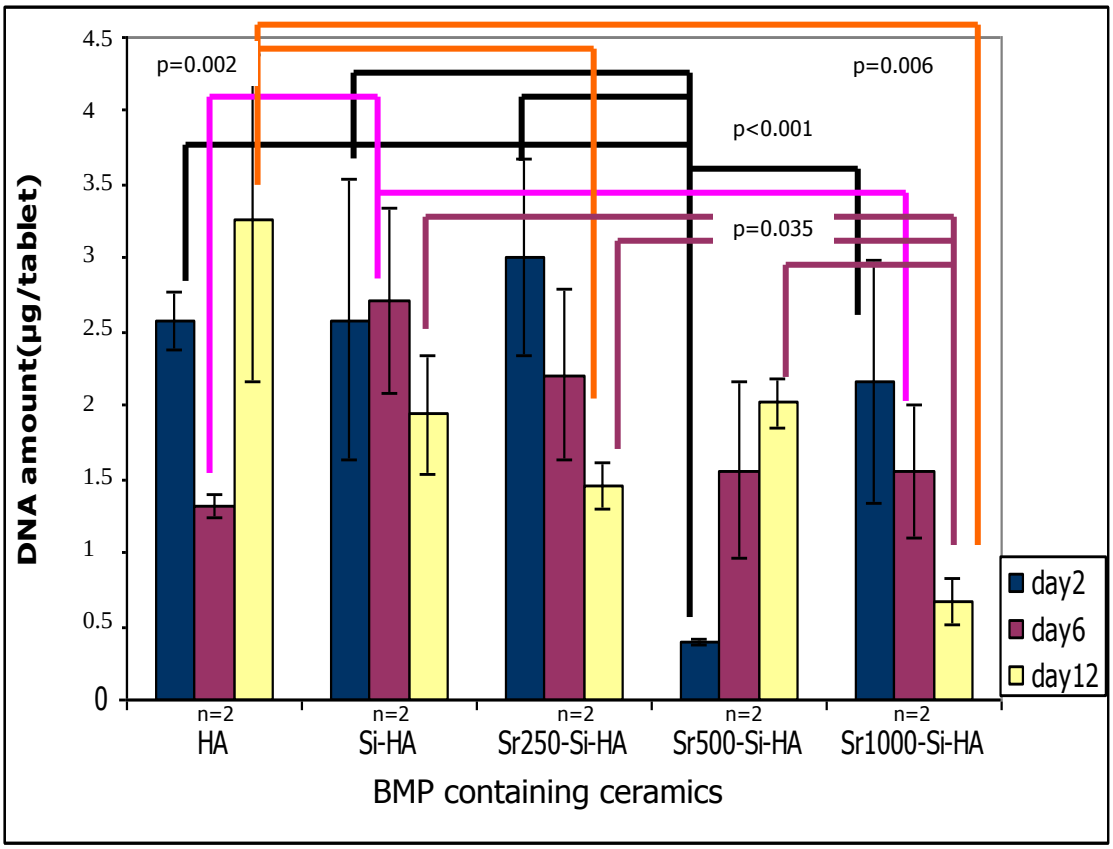

Figure 3.13. DNA assay results (µg/tablet) of the BMP containing ceramics.

BMP containing and not containing groups were compared by using the DNA assay results. On day 2, the HA, the Si-HA and the Sr1000-Si-HA groups had higher DNA amount ($p<0.001$) than the BMP-Sr500-Si-HA group. However, the Sr250-Si-HA group resulted with significantly lower ($p<0.001$) DNA amount than the BMP-HA, the BMP-Si-HA and the BMP-Sr250-Si-HA groups. Likewise, the Sr500-Si-HA group had lower ($p<0.001$) DNA amount than the BMP-HA, the BMP-Si-HA, the BMP-Sr250-Si-HA and the BMP-Sr1000-Si-HA groups. On day 6, the BMP-Sr250-Si-HA group caused higher ($p=0.002$) DNA amount than the HA and the Si-HA groups. Likewise, the

BMP containing Si-HA group had higher ($p=0.002$) DNA amount than the HA, the Si-HA, the Sr1000-Si-HA and the BMP-Sr1000-Si-HA groups. On day 12, the HA group caused lower ($p<0.001$) DNA amount than the BMP-HA, the BMP-Si-HA and the BMP-Sr500-Si-HA groups. The BMP-HA group had higher ($p<0.001$) DNA amounts than the Sr250-Si-HA and the Sr500-Si-HA groups. However, the Sr1000-Si-HA group showed higher ($p<0.001$) DNA amount than the BMP-Sr250-Si-HA, the Sr500-Si-HA and the BMP-Sr1000-Si-HA groups.

3.3.4. ALP/DNA Ratio:

The ALP/DNA ratio was significantly different ($p=0.02$) between days 2-6 and 6-12 in the HA group (Figure 3.14.), Similar differences was detected in the Sr250-Si-HA ($p=0.02$) and the Sr500-Si-HA ($p=0.02$) groups at same time points. The results of day 6 were significantly ($p=0.038$) higher than that of the day 12 in the Si-HA group. Results of day 2 were also significantly ($p=0.042$) higher than that of the day 6 in the Sr1000-Si-HA group. When groups were compared to each other on day 2, the Sr 250-Si-HA and the Sr1000-Si-HA groups presented significantly ($p=0.042$) higher values than the HA group. On day 6, there were no significant differences between groups. On day 12, the Sr1000-Si-HA group had higher values than the Si-HA, the Sr250-Si-HA and the Sr500-Si-HA groups ($p<0.001$).

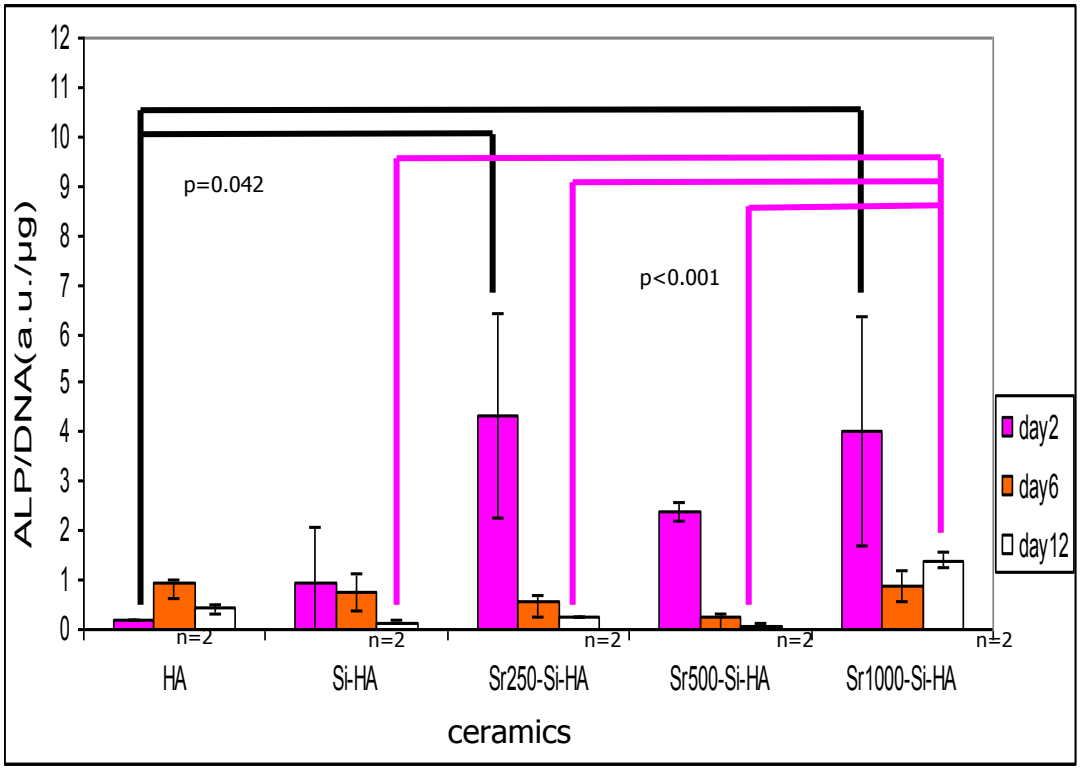

Figure 3.14. The ALP/DNA ratio of cells (a.u./µg) that were incubated with the ceramics.

Results were significantly (p=0.02) different between days 2-6, 6-12 and 2-12 in the BMP-HA group (Figure 3.15.). The day 6 results were higher (p=0.048) than that of the day 12 results of the BMP-Si-HA group. The day 2 results were also higher (p=0.048) than that of the days 6 and 12 results in the BMP-Sr500-Si-HA group. When the groups were compared to each other on day 2, the Sr500-Si-HA and the Sr1000-Si-HA groups had higher (p=0.042) ALP/DNA ratios than the other groups. On day 6, the BMP-Si-HA and the BMP-Sr1000-Si-HA groups had higher (p<0.001) results than the BMP-Sr500-Si-HA group. On day 12, the BMP-HA, the BMP-Sr250-Si-HA and the BMP-Sr1000-Si-HA groups had higher (p<0.001) ALP/DNA ratios than the BMP-Sr500-Si-HA group.

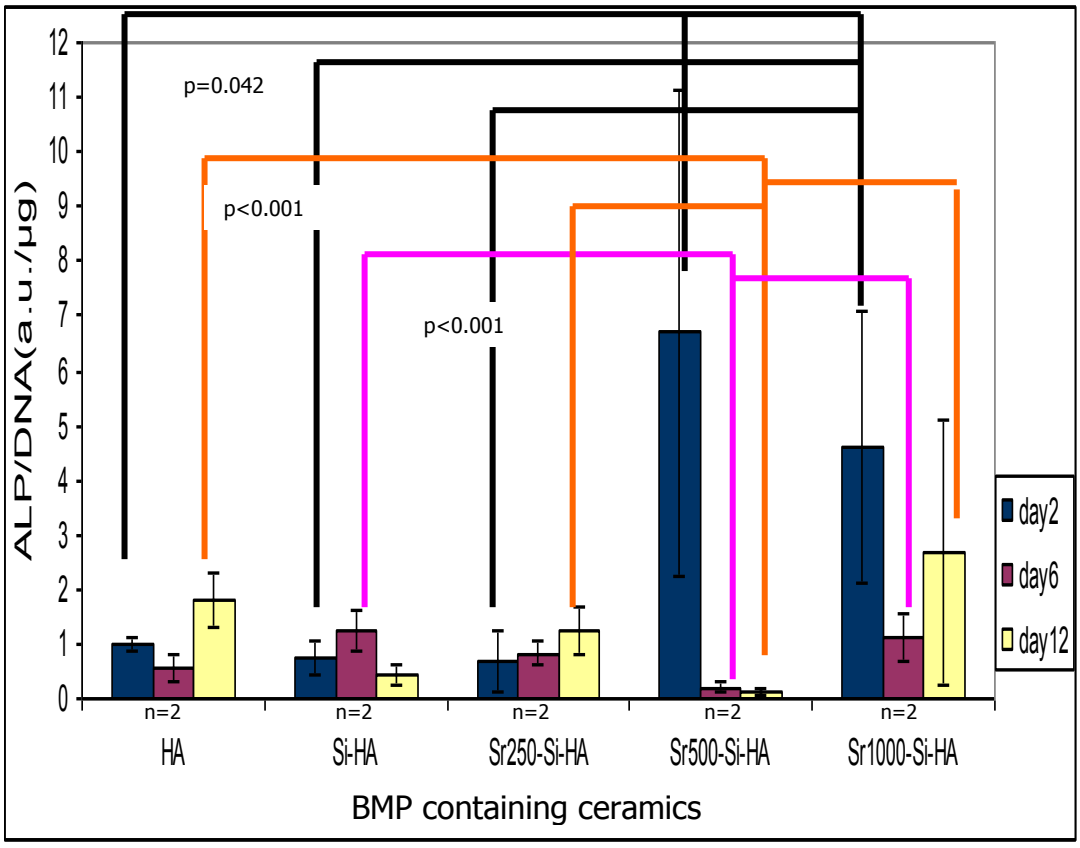

Figure 3.15. ALP/DNA ratio of cells (a.u./µg) that were incubated with the BMP containing ceramics.

When BMP containing and not containing ceramics were compared on day 6, HA groups results were higher ($p<0.001$) than the BMP-Sr500-Si-HA group. Also, the BMP-Si-HA group had higher ($p<0.001$) values than the Sr500-Si-HA group. On day 12, the BMP-HA group had higher ($p<0.001$) ALP/DNA ratios than the Si-HA and the Sr500-Si-HA groups. In addition, the BMP-Sr1000-Si-HA group had higher ($p<0.001$) ALP/DNA ratios than the Si-HA and the Sr500-Si-HA group. The BMP-Sr250-Si-HA group had also higher ($p<0.001$) ALP/DNA ratios than the Sr500-Si-HA group. On the contrary, the Sr1000-Si-HA group resulted with a higher ($p<0.001$) ALP/DNA ratio than the BMP-Sr500-Si-HA group at same time point.

Cells that were grown on tcps had significantly different values at all time points (results of tcps were not shown in graphs). Cells which were

grown on tcps, showed significantly lower ALP/DNA ratios than Sr-Si-HA applied cells on day 2. However cells that were grown on tcps had higher results than other groups on day 6 and 12. Also, BMP applied cells resulted with lower ALP/DNA ratios than other BMP-containing ceramic groups on day 2.

3.3.5. SEM Images:

Attachment of cells to the ceramics had been detected after the MTT assay by SEM photography. Cell adhesions to the HA and the Sr500-Si-HA ceramics were obvious.

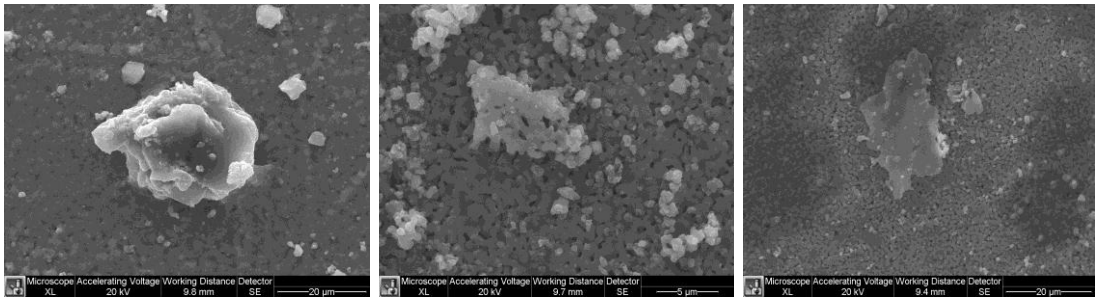

Figure 3.16. SEM pictures of the cells that were incubated with the HA, the Sr250-Si-HA and the Sr500-Si-HA ceramics.

CaP like precipitations were observed at cells that were incubated with the BMP containing ceramics(photos were not shown).

3.4. *In Vivo* Tests:

3.4.1. Radiology:

3.4.1.1. Periosteal Reaction Results:

Decrease in periosteal reaction was observed in the composite implanted groups. The BMP-Si-HA and BMP-Sr-Si-HA groups showed

significant (p=0.017) lower scores than the other groups at two weeks after bioceramic composite implantation (Figure 3.17.). The score of the control 2 group was higher than that of the other groups.

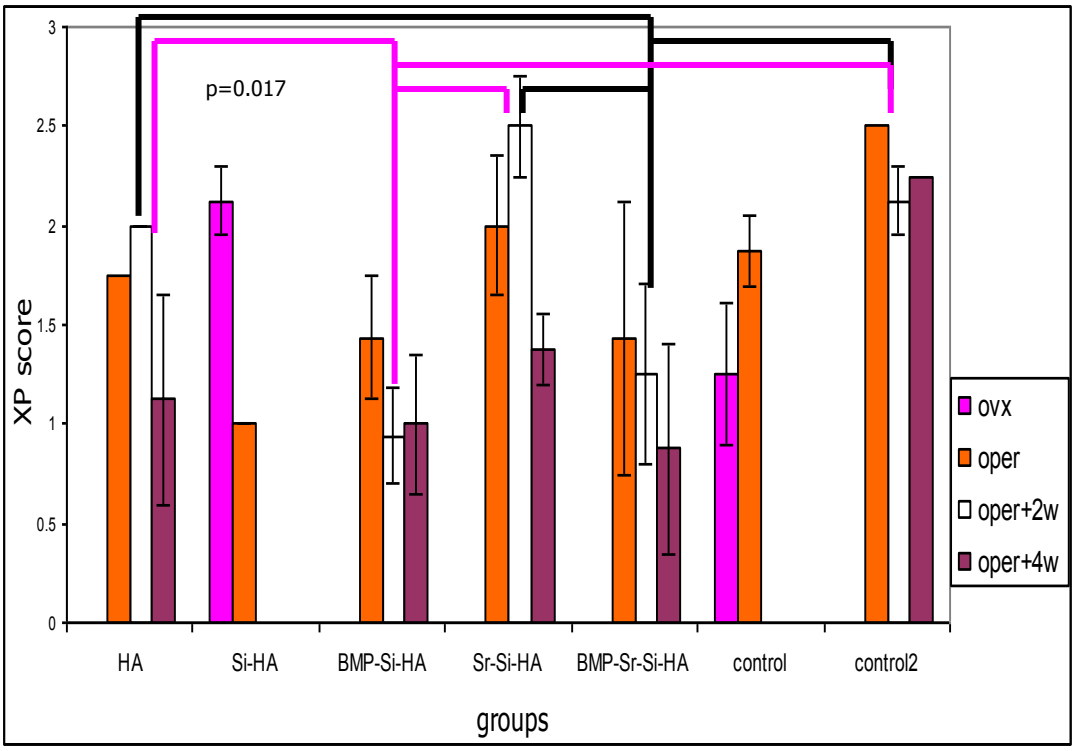

Figure 3.17. Periosteal reaction results of the tibiae (control:defect only ; control2:normal bone) of the groups.

3.4.1.2. Bone Union Results:

There were no significant bone union score differences between groups at the same time point. Bone union scores did not change along the experiments (Figure 3.18.).

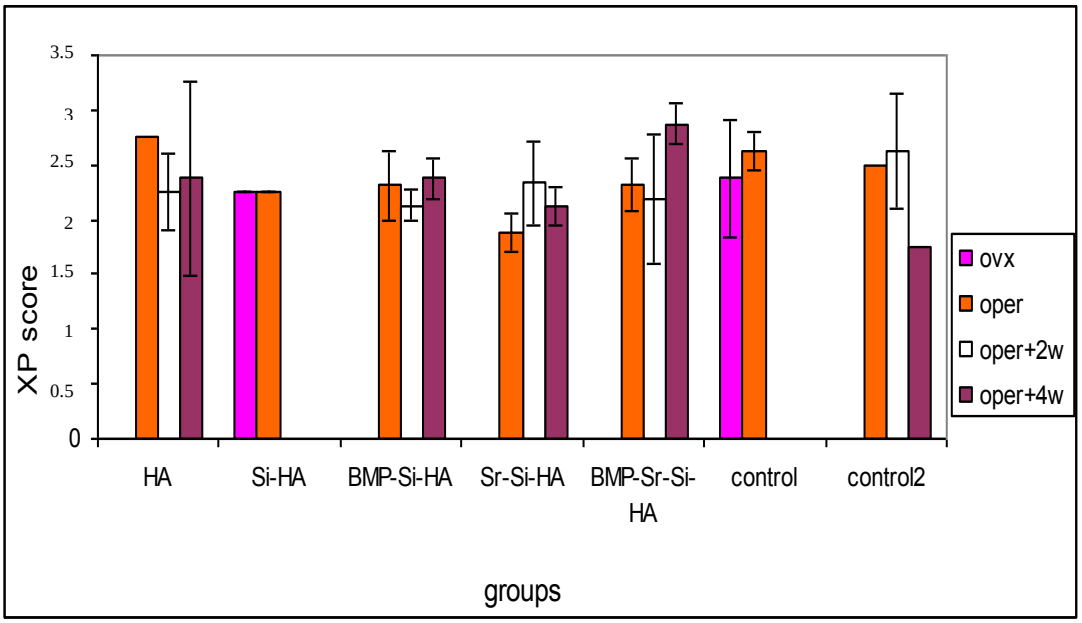

Figure 3.18. Bone union scores of the tibiae (control: defect only; control 2: normal bone) of the groups.

3.4.1.3. Remodeling Results:

There were significant remodeling differences between groups two weeks after bioceramic implantation (Figure 3.19.). The BMP-Si-HA group had significant ($p=0.03$) lower scores than the HA, the Sr-Si-HA and the control 2 groups. The HA and the control 2 groups also had higher ($p=0.03$) remodeling scores than the BMP-Sr-Si-HA group at same time point.

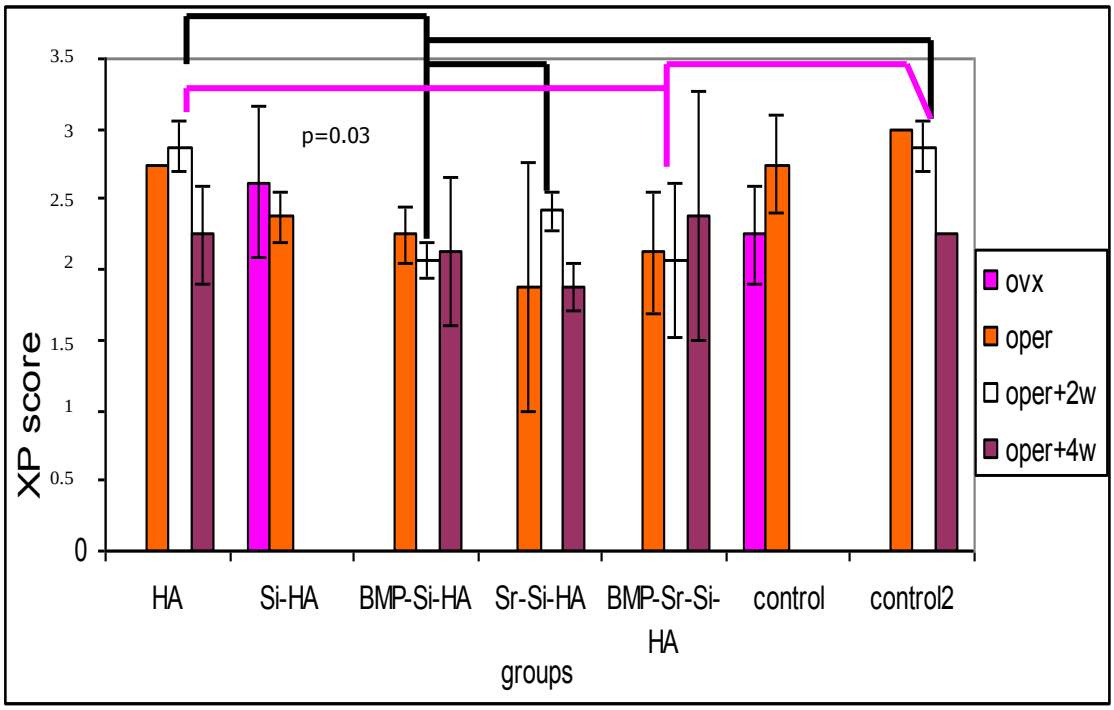

Figure 3.19. Remodeling results of tibiae (control: defect only; control 2: normal bone) of the groups.

3.4.1.4. Implant Integration Results:

The HA, The BMP and/or Sr-containing Si-HA groups had lower implant integration scores than the Control 2 group (Figure 3.20.). The differences between groups at the same time points were not significantly different.

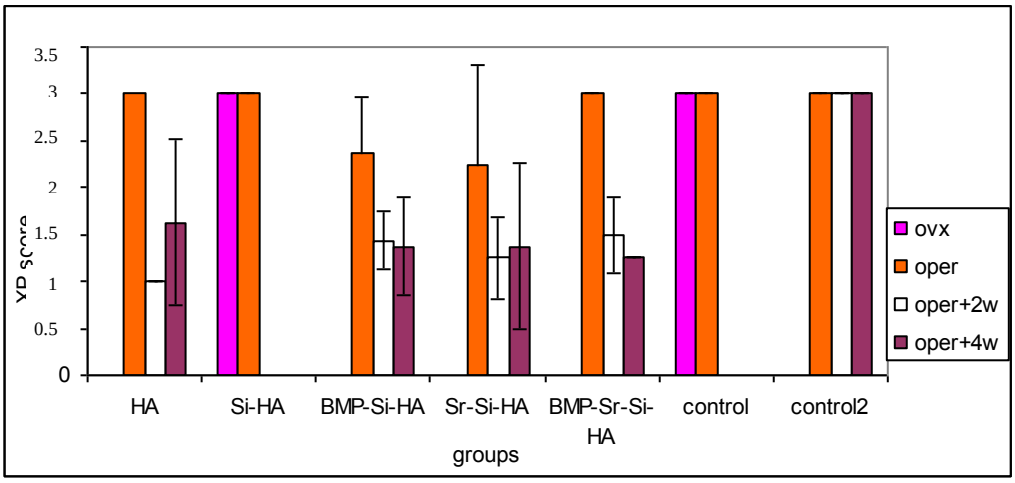

Figure 3.20. Implant integration results of tibiae (control: defect only; control 2: normal bone) of the groups.

3.4.1.5. Overall Radiological Scores:

There were significant differences between groups two weeks after bioceramic implantation by means of periosteal reaction and remodeling. The BMP-Si-HA and the BMP-Sr-Si-HA groups had lower (p=0.03) scores than the HA, the Sr-Si-HA and the control2 groups.

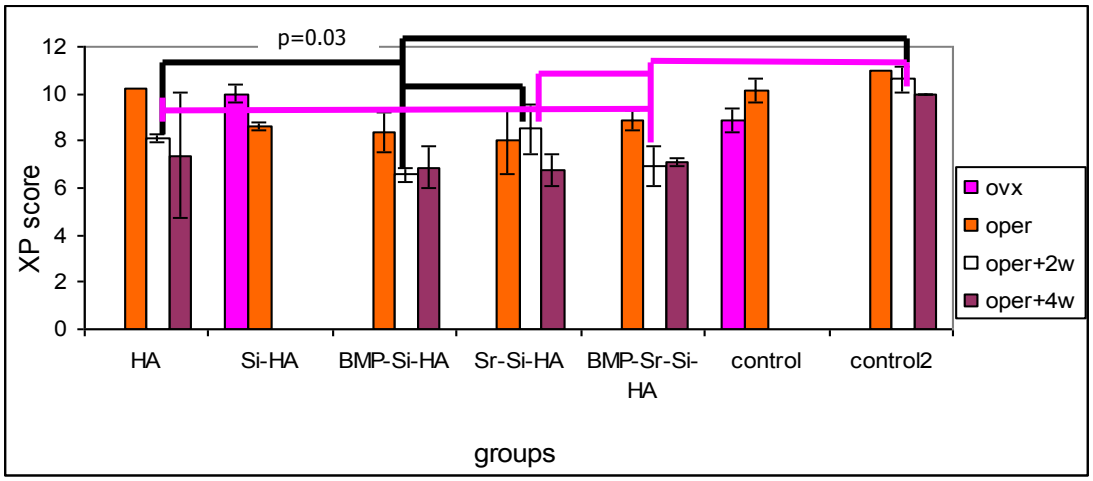

Figure 3.21. Overall radiological scores of the tibiae (control: defect only; control 2: normal bone) of the groups.

3.4.2. DXA Results:

3.4.2.1. DXA Results of First Stage Experiments:

BMD values of the Si-HA ceramic implanted and defect created groups were not different than each other at all time points (Table 3.3.). Although tibiae BMD decreased from OVX to bioceramic implantation time, the differences were not significant. An increase in tibiae BMD values of the Si-HA implanted group was observed between bioceramic implantation and termination at 31 weeks time. The difference however was not significant again.

3.4.2.2. DXA Results of Second Stage Experiments:

BMD of the operated tibia measured by DXA improved after implantation in all groups (Table 3.4). The BMD of the tibia increased at most in the BMP-Sr-Si-HA group from composite implantation to termination at 4 weeks. BMD of the operated tibia also increased in the BMP-Si-HA and the Sr-Si-HA groups however changes were not statistically significant.

The BMD values of the femur and the vertebra were examined for evaluation of osteoporosis formation (Table 3.5. and Table 3.6.). According to the femur BMD results, BMD values of the OVX groups were decreased than that of the non-OVX group between OVX and implantation time. The difference was not significant statistically.

Table 3.3. Bone mineral density (g/cm^2) of the Si-HA implanted and defect created tibia Ave±SD (Range: Min-Max).

	Si-HA	Control
ovx	0.304± 0.02 (0.252-0.325)	0.299± 0.0009 (0.298-0.3)
oper	0.295± 0.02 (0.261-0.334)	0.289± 0.01 (0.272-0.298)
oper+2w	0.298± 0.01 (0.275-0.319)	0.294± 0.002 (0.291-0.297)
oper+4w	0.292± 0.02 (0.234-0.328)	0.297± 0.01 (0.282-0.313)
oper+8w	0.287± 0.004 (0.284-0.291)	0.292± 0.009 (0.281-0.302)
oper+17w	0.303± 0.015 (0.286-0.32)	0.299± 0.01 (0.29-0.316)
oper+31w	0.304± 0.007 (0.296-0.313)	0.288± 0.009 (0.278-0.3)

Table 3.4. Bone mineral density (g/cm^2) of the bioceramic implanted tibia Ave±SD (Range: Min-Max).

	ovx	oper	oper+2w	oper+4w
HA	0.287± 0.02 (0.251-0.344)	0.264± 0.01 (0.238-0.286)	0.284± 0.01(0.266-0.308)	0.274± 0.02(0.251-0.308)
Si-HA	0.304± 0.02 (0.252-0.325)	0.295± 0.02 (0.261-0.334)	0.298± 0.01 (0.275-0.319)	0.292± 0.02 (0.234-0.328)
BMP-Si-HA	0.277± 0.015 (0.259-0.307)	0.264± 0.02 (0.231-0.293)	0.325± 0.04 (0.28-0.37)	0.287± 0.01 (0.272-0.296)
Sr-Si-HA	0.292± 0.02 (0.267-0.327)	0.252± 0.01 (0.229-0.289)	0.276± 0.02 (0.251-0.312)	0.279± 0.02 (0.262-0.305)
BMP-Sr-Si-HA	0.294± 0.02 (0.256-0.333)	0.267± 0.01 (0.251-0.292)	0.26± 0.008 (0.248-0.267)	0.304± 0.02 (0.279-0.319)
control	0.299± 0.0009 (0.298-0.3)	0.289± 0.01 (0.272-0.298)	0.294± 0.002 (0.291-0.297)	0.297± 0.01 (0.282-0.313)
control2	0.284± 0.02 (0.253-0.329)	0.287± 0.02 (0.251-0.315)	0.290± 0.04 (0.261-0.349)	0.25± 0.01 (0.242-0.258)

Table 3.5. BMD results of the femur to assess OVX and time related changes.

	ovx	oper	oper+2w	oper+4w
ovariectomized	0.333± 0.03 (0.284-0.391)	0.321± 0.02 (0.267-0.377)	0.323± 0.03 (0.287-0.379)	0.317± 0.02 (0.285-0.377)
non-ovariectomized	0.304± 0.01 (0.285-0.326)	0.322± 0.02 (0.288-0.344)	0.313± 0.03 (0.274-0.364)	0.314± 0.01 (0.306-0.322)

Table 3.6. BMD results of the vertebra to assess OVX and time related changes.

	ovx	oper	oper+2w	oper+4w
ovariectomized	0.278± 0.01 (0.228-0.295)	0.277± 0.01 (0.249-0.298)	0.275± 0.008 (0.263-0.291)	0.271± 0.008 (0.253-0.287)
non-ovariectomized	0.274± 0.003 (0.272-0.279)	0.279± 0.0007 (0.279-0.28)	0.266± 0.01 (0.257-0.275)	0.28 ± 0.002 (0.278-0.282)

3.4.3. Micro CT:

Percent of bone volume/total volume (BV/TV) ratio of the bioceramic implanted defect area was calculated by micro CT and new bone formation was quantified. At 4 weeks, new bone formation had been observed at the edge of the defects. The BMP-Sr-Si-HA group leaded to new bone formation when compared to the HA group however the difference was not significant (Figures 3.22 and 3.23).

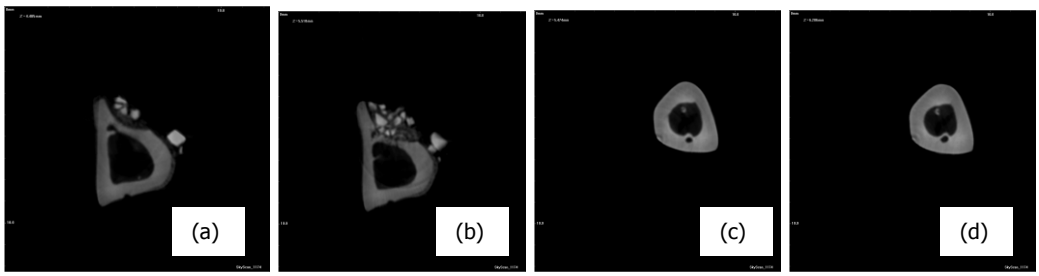

Figure 3.22. Micro CT images of the ceramic implanted into cortical defect group (a, b) and normal bones (c, d).

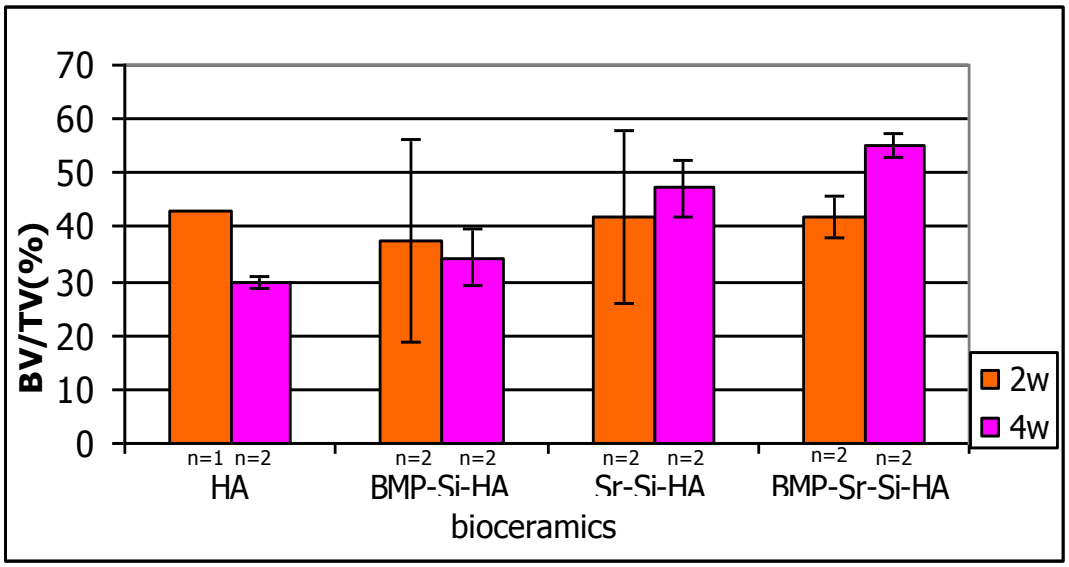

Figure 3.23. Percent bone volume/total volume ratio results of samples that were bioceramic implanted.

3.4.4. Histology and Histomorphometry:

In the first stage of *in vivo* experiments, effect of Si-HA ceramic was evaluated until 31 weeks after implantation. According to histological sections, the cavities in bone seemed ossified and the ceramic was biocompatible (Figure 3.24.).

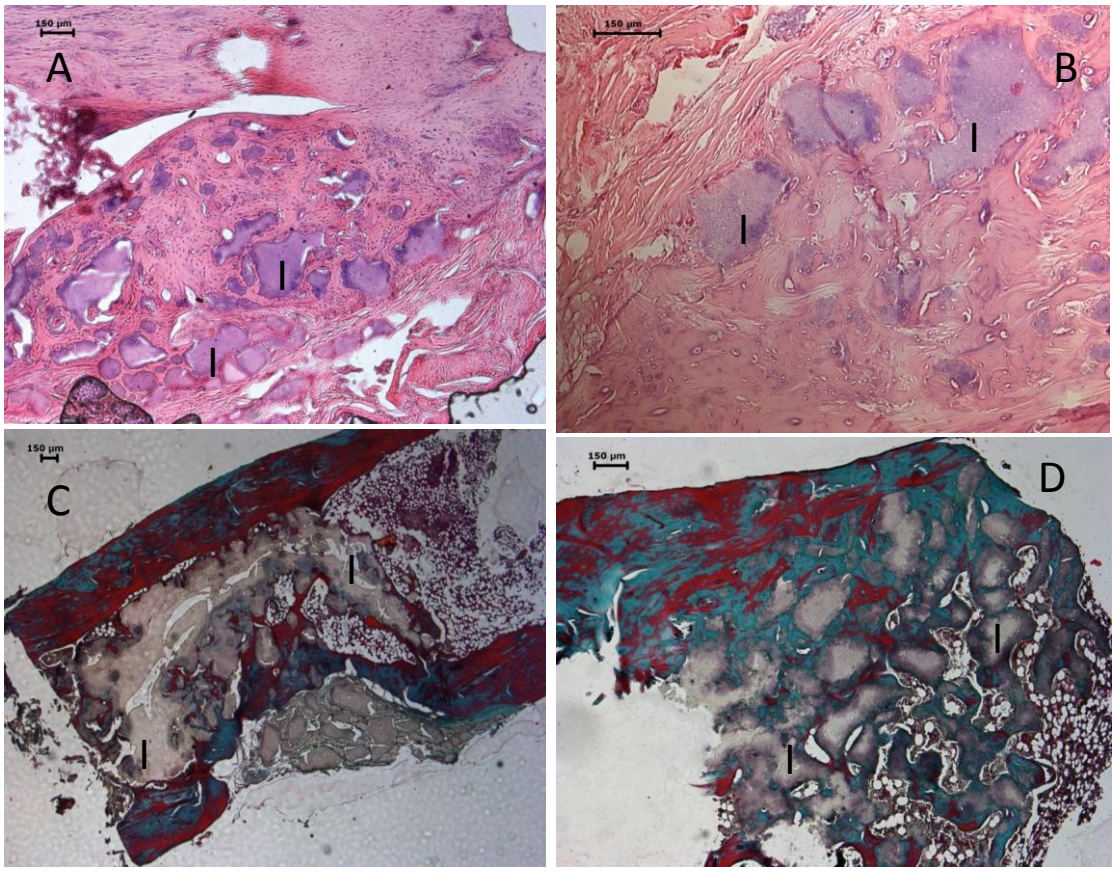

Figure 3.24. A to B (HE stained) and C to D (MT stained) show longterm (31week) implanted Si-HA ceramics. I: Implant, HE: Hematoxylin & Eosin, MT: Masson's Trichrome.

Descriptive statistical data were presented in Table 3.7. for the bone defect healing measurements and the tissue response to the implant. No statistically significant difference was detected between the bioceramic implanted and the control groups regarding the defect healing parameters (defcbt/nbt and ntb/defarea) on weeks 2 and 4. Tissue response scores did

not differ between groups. Neither necrosis nor severe foreign body reaction was noted in any of the samples at any time point.

Table 3.7. Results of histomorphometrical analysis are presented as raw data. defcbt/nbt: ratio of cortical bone thickness at defect area to normal cortical bone thickness, ntb/defarea: ratio of the new trabecular bone area in the defect/total defect area).

	defcbt/nbt		ntb/defarea		tissue response	
	2 week	4 week	2 week	4week	2week	4week
HA	0.389	0.766	0.460	0.644	1	1
		0.714		0.710		1
BMP-Si-HA	0.370	0.919	0.573	0.738	1	1
	0.495	0.967	0.676	0.901	1	1
Sr-Si-HA	0.548	0.831	0.578	0.791	1	2
	0.476	0.805	0.636	0.665	1	1
BMP-Sr-Si-HA	0.776	0.844	0.577	0.909	1	1
	0.704	0.865	0.745	0.855	1	1
Control(defect only)	0.273	0.471	0.226	0.408	0	0

On the other hand, the new bone per total defect area ratio and the cortical bone thickness ratio were higher in the bioceramic implanted groups comparing to that of the control (defect) group. The BMP-Sr-Si-HA, the BMP-Si-HA and the Sr-Si-HA groups provided better new bone formation rates when compared to the defect only and the HA groups at 2 week and 4 week (statistically not significant).

Diverse intramembraneous and at some areas stages of endochondral ossification were observed within the defect area of bioceramic implanted groups. The bioceramics provided an osteoconductive environment at the defect site initiating a mild inflammation that was characterized mainly by mononuclear phagocytic cells, lymphocytes and fibroblasts. The thin fibrous encapsulation consisted of thin collagen fibers with blood vessels adjacent to the degrading ceramic particles. The capsule allowed nearby new bone formation. The bioceramic particles are in close relation with the newly

forming bone trabecules in the implant groups. The bioceramics initiated the huge bony callus formations in all experimental groups (Figure 3.25.). The bioceramic particles being in close relation with the newly forming bone trabecules fill the ossified defect area, also the bony callus protrude into the marrow cavity and to the surrounding periosteum in the implant applied groups (Figure 3.26.).

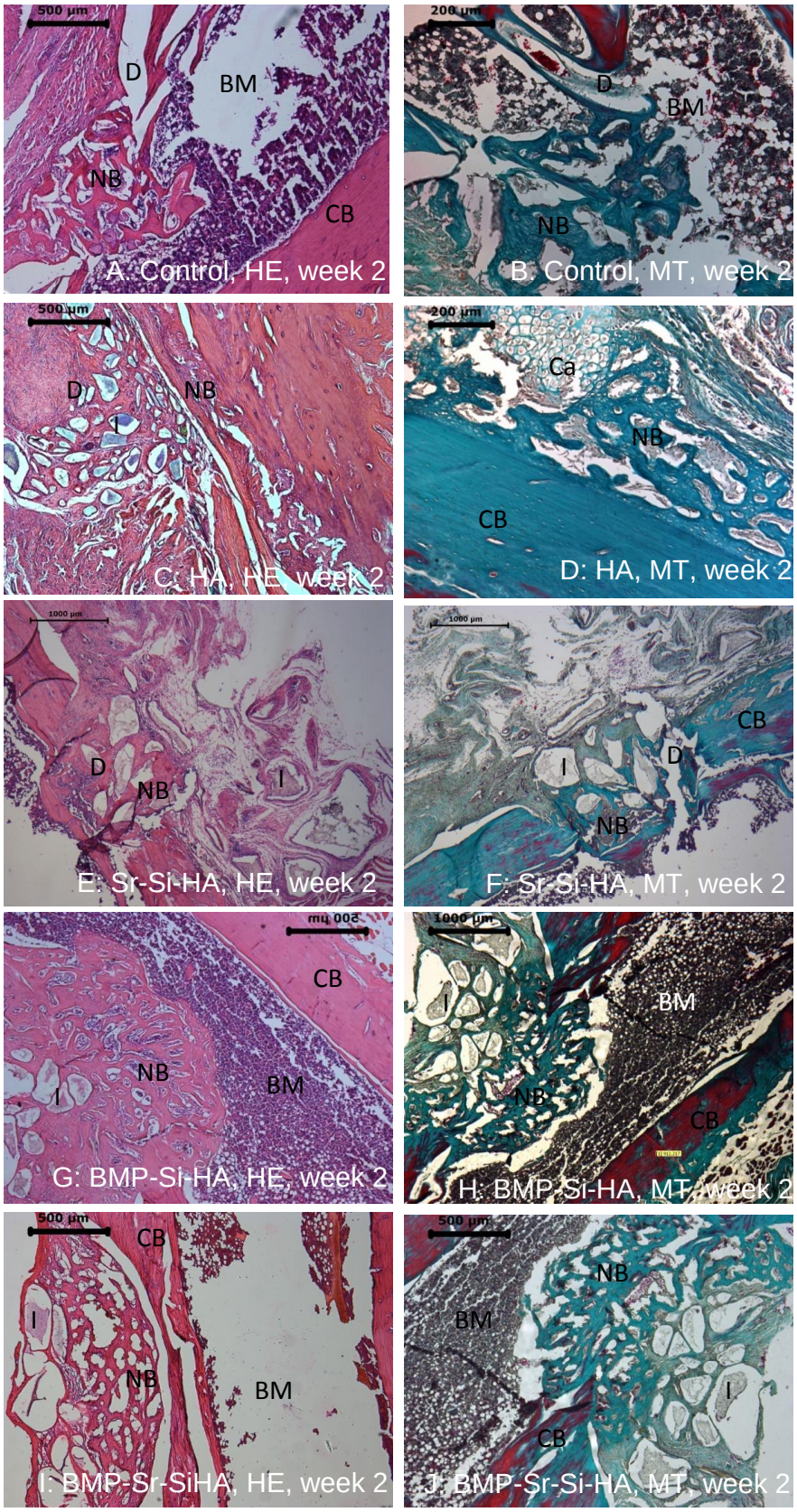

Fig. 3.25. Endochondral (in D) and intramembranous (A-C, E-J) ossification steps are noted within the defect site of implant applied and control groups.
I: Implant, NB: New bone, CB: Cortical bone, BM: Bone marrow, Ca: Cartilage, D:Defect, HE: Hematoxylin Eosin, MT: Masson's Trichrome.

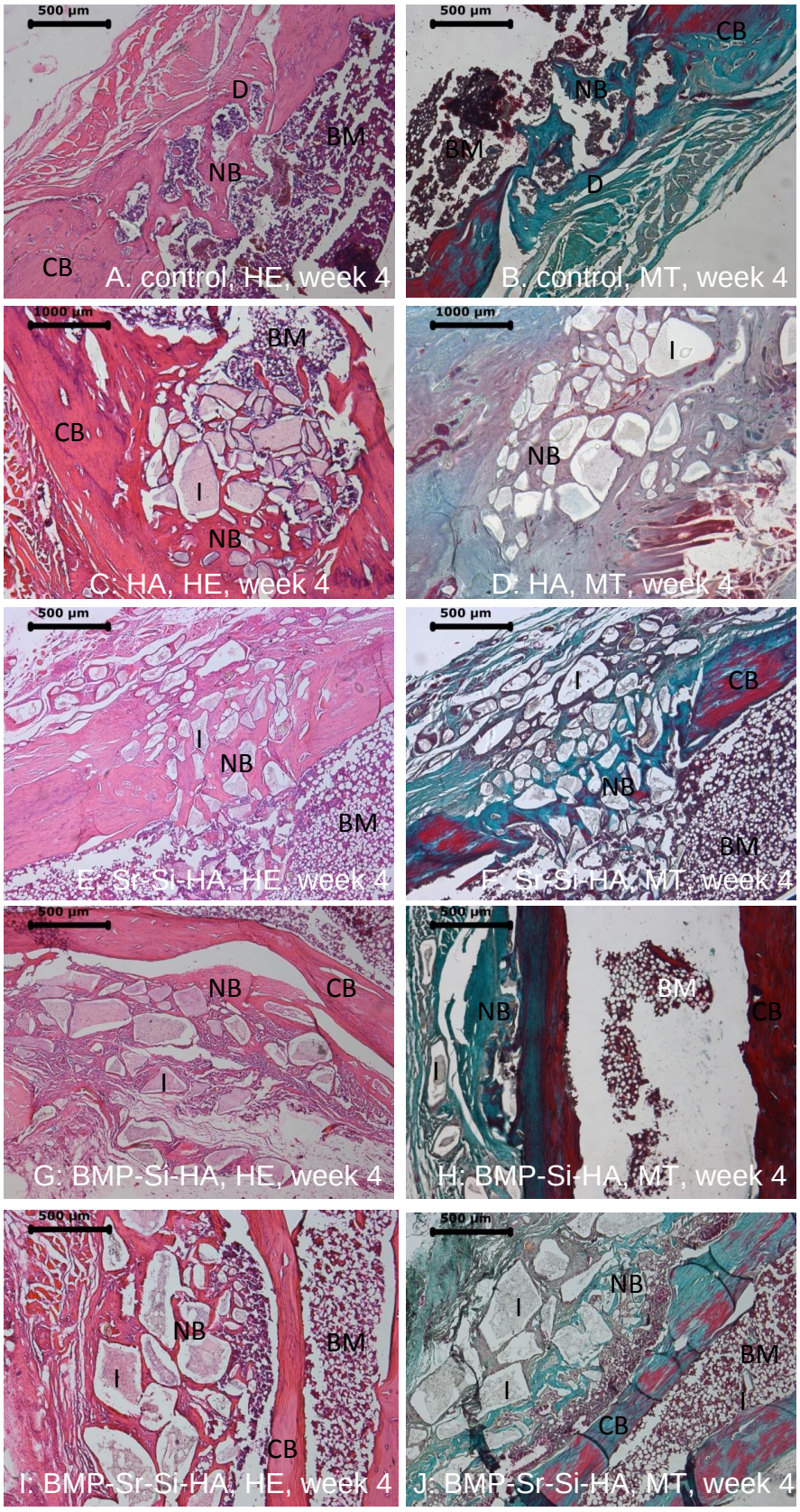

Fig. 3.26. The defect area is nearly totally ossified in all groups.
I: Implant, NB: New bone, CB: Cortical bone, BM: Bone marrow, D:Defect, HE: Hematoxylin Eosin, MT: Masson's Trichrome.

CHAPTER 4

DISCUSSION

XRD and porosity tests were conducted to characterize the ceramics. Compression strength measurement was performed to the ceramics after mechanical characterization.

According to the XRD results, the pattern of the HA ceramic ceramics were in agreement with the JCPDS. There were no peaks that belonged to CaO or TCP. This was a valuable result for supporting the Ca:P ratio. XRD peak intensities were lower in the Si-HA ceramics than the HA ceramics. This result was in line with other studies (Kim et al., 2003). Addition of Si into HA might have changed the peak intensity. XRD peak intensities decreased in the Sr250-Si-HA ceramics when compared to the Si-HA ceramics. Intensities however increased in the Sr500-Si-HA and the Sr1000-Si-HA ceramics. The reason for decrease in intensity of the Sr250-Si-HA was an unexpected result as the XRD results of the Sr1000-Si-HA ceramic was almost similar to that of HA. A possible explanation for the increase at intensities with Sr addition is that Sr is heavier and contains more electrons than Ca and scatter X-rays may occur more effectively (O'Donnell et al. (2008), Terra et al. (2009)). The X-ray pattern obtained from the Sr containing ceramics presented broader diffraction peaks as in other studies (Capuccini et al. (2009), Landi et al. (2007), Li et al. (2007), Li et al. (2010), Mardziah et al. (2008)). The broadening of the X-ray spectrum width indicated the incorporation of Sr to the structure (Li et al., 2007). Appearances of peaks at Sr-containing ceramics were also similar to the peaks obtained at the study of Dagang

(Dagang et al., 2010). Sr-100%HA which was sintered at 1200°C at that study had similar peaks at 2θ values (Dagang et al., 2010).

After XRD characterization, porosity percentages of ceramics were obtained. The bulk densities of ceramics seemed to be lower than the theoretical density of HA as these ceramics had 36.9 – 41.6 % porosity. Sintering conditions were thought to be the causative factor of this porosity range. Decrease in density of the materials may result in increase of biodegradability (Weiss et al., 2003) as density is closely related with porosity. HA materials that are fully dense are accepted to be biocompatible but resorb slowly in the body (Sun et al., 1998, 1999). Microporosity is necessary for cell ingrowth and nutrition when implanted into biological environments. Micropores were prerequisite for *in vivo* osteoconduction of CaP materials (Klawitter et al. (1971), Padilla et al. (2002), Chang et al. (2000), Lu et al. (1999). Expansion of osteoblasts onto porous surface of ceramics was observed in SEM photos in *in vitro* experiments. Our findings were in line with the study of Sennerby (Sennerby et al., 2005). Porosity is also an important factor for scaffold vascularization (Hing et al., 2004, 2005) and beneficial for biomineralization. Cellular events for bone formation occur on porous structures as can be seen from *in vitro* experiment results of this study.

Porosity test was performed in one sample and this was a limitation of our material characterization studies.

HA resulted with significantly lower compression strength (7.0 MPa) when compared to the other ceramics produced and evaluated in this study. Sr incorporation to Si-HA ceramics increased compression strength excluding the Sr500-Si-HA group (75.8 MPa). Sr1000-Si-HA ceramics had the highest compression strength (117.5 MPa) although significantly different result than the Si-HA ceramics was not obtained. Synthetic CaP has reduced mechanical properties because of increased porosity (Douglas et al., 2010). Sr-

incorporated HA based ceramic caused increase in compression strength and this finding was in line with that of the study of Guo (Guo et al., 2005). Compressive strength of HA materials decreased with the increase in sintering temperature according to researchers. The major problems of ceramic materials are their weak mechanical properties related with sintering conditions when compared with bone (Rezwan et al. (2006), Chen et al. (2006)). The compressive strength of HA in this study was significantly low. In Gupta's study, different concentrations of Silica-CaP nanocomposites were evaluated (Gupta et al., 2007). The nanocomposite(diameter 13 mm x 8 mm) which had 32% porosity and lower Si% content than other groups achieved higher compressive strengths. In another study, compressive strength of 5% SiO_2-containing HA pellets(6mm diameter, 12mm height) was 79.09 MPa (Oktar et al., 2007). This value is lower than compressive strength of Si-HA ceramics of our study. Highly porous poly(L-lactic acid)(PLA) coated HA tube containing HA spherules(3–4 cm in length, 1–1.5 cm in diameter) was developed in Peng' study (Peng et al., 2010). According to compression tests, pure HA scaffold had 0.28 MPa compression strength. However, in Cordell's study PMMA-incorporated HA (6.36-6.48 mm in diameter, 12.7-13.1 mm in height) showed 110 MPa (Cordell et al., 2009). This value was higher than the strength obtained for HA in this study. Also, in another study (Dagang et al., 2010), Sr-100% HA group (inner diameter 10.5mm, height 17mm) had compressive strength value around 9 MPa with 44.2% microporosity. The Sr-containing material in this study had better compressive strength values although there were no differences between porosity percentages. Adding Sr to CaP materials enhanced compression strength values in another study (Dagang et al., 2010). The highest strength in this study was obtained with the Sr1000-Si-HA ceramics. In Liu's study, compression strength of the Sr-HA materials(6 mm diameter, 12 mm length) was 144.5 MPa (Liu et al., 2010). Compressive strengths of human cortical bone and cancellous bone are 130-180 MPa (Seal et al. (2001), Keaveny et al. (1993), Zioupos et al. (1998)) and 2-12 MPa (Giesen et al. (2001), Yeni et

al. (2001)), respectively. In this study, Sr1000-Si-HA ceramics were found to be good option for bone replacement. Surface of the Si-HA ceramics was more regular than the other ceramic groups in this study. According to another study (Rosa et al., 2003) irregular surface topography formed on scaffolds when porosity increased. Mean crystal size was negatively effected when Sr amount increased in the ceramics (Verberckmoes et al., 2004). Sr incorporation to ceramics resulted with more disperse appearance when compared with other ceramics in this study. Similar dispersion was observed in the Sr-100%HA composites in another study (Dagang et al., 2010). Decrease in bone mineral crystallinity was evaluated as bone strength increased in Sr treated patients (Marie et al., 2001). Sr incorporation into HA ceramics resulted with adequate compression strengths which caused them to be preferred for bone replacement.

According to the released amounts of Sr from ceramics, Sr250-Si-HA and Sr1000-Si-HA showed consistent release between days 3 and 14. For Sr250-Si-HA the released Sr amount on day 14 was 125% of that of day 3. For Sr500-Si-HA released Sr amount on day 14 was 288% of that of day 3. And for Sr1000-Si-HA, released Sr amount on day 14 was 157% of that of day 3 in this study. Sr release from the ceramics were thought to present a linear increase until a treshold however according to our results, the Sr500-Si-HA ceramic presented a higher release than expected. In this study, the Sr1000-Si-HA ceramic retained the Sr in its structure. According to the Ca release test from ceramics, the Sr1000-Si-HA ceramic released higher Ca amount than the other Sr-containing groups (Figure 4.1.). If the Sr content replaced Ca in the content of the ceramics, this amount of Ca release from the Sr1000-Si-HA ceramics was accepted to be normal.

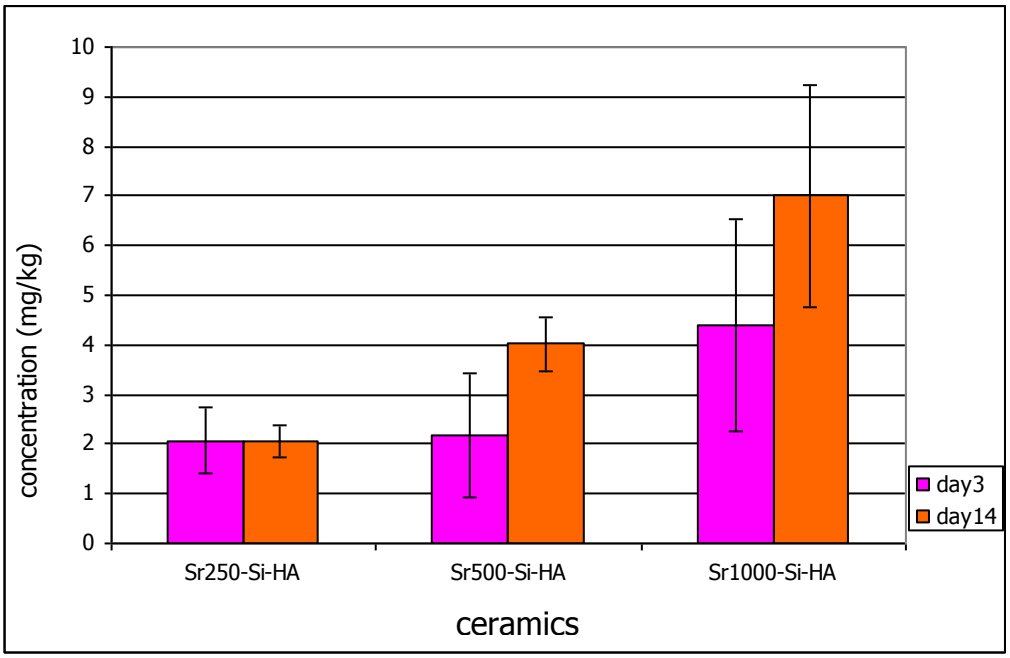

Figure 4.1. Ca release (mg/kg) from ceramics that were incubated in distilled water for 3 and 14 days (n=2 in all groups).

These results supported our selection of Sr1000-Si-HA ceramic for our *in vitro* and *in vivo* applications. Limitation of our Sr release test was the limited number of ceramics tested in this study. Furthermore Sr did not release from the ceramics in serum. This finding indicated that the release of Sr from bioceramics implanted to bone would be limited. Our initial aim for adding Sr into the bioceramics was not to release but improve biocompatibility. Therefore, the release rate of Sr was a descriptive finding for our study.

MTT test results presented deposition of cells on the ceramics. Increase at cell proliferation(based on higher cellular activity) had been observed until day 6 but decreased on day 12. Cells that were incubated with the Si-HA and the Sr250-Si-HA ceramics proliferated until day 6. However, on day 12, all ceramics showed decrease in cell proliferation rates. This indicated that cells reached to confluence or stopped dividing in a week. Higher absorbance was detected with the Sr1000-Si-HA ceramics on day 1.

The effect of Sr-250-Si-HA ceramic was significantly different than the other groups on day 6. Increase of cell proliferation rates in the Si-HA and the Sr250-Si-HA groups that were containing BMP were detected between day 1 and 6. The BMP-Si-HA composites also had higher proliferation rates than the BMP-Sr1000-Si-HA group on day 12. On day 1, cell attachment rate of the BMP-containing Sr1000-Si-HA composites was significantly higher than BMP free Si-HA group when BMP containing and not containing ceramics were compared. However, BMP-Si-HA and BMP-Sr250-Si-HA resulted with more proliferation rates on day 6. On day 12, HA ceramics resulted with more MTT absorbance than the other groups. According to the overall MTT results, BMP addition to ceramics enhanced cell proliferation rates at all time points excluding day 12. Although the Sr1000-Si-HA ceramics had significantly higher results on day 1, the Si-HA and the Sr250-Si-HA groups showed better results on later days. The Sr-HA ceramics showed better cell proliferation rates than the HA ceramics but the difference was not significant (Dagang et al., 2010). Boyd applied grafts containing different concentrations of Ca-Sr-Zn-Si-glass to fibroblast-like cells (Boyd et al., 2009). The graft that was containing higher amount of Sr caused the highest cell viability on day 7. On day 30 however cell viability decreased in the Sr containing grafts. Sr free grafts caused the highest cell viability at 30 days when compared to other grafts in that study. Authors explained this Sr related reduced cell viability by the effect of glass dissolution and accumulation of Zn-Sr in the medium with sequencing cytotoxicity. This finding was in line with our findings. Similarly, the Sr containing ceramics showed higher cell proliferation results at initial time points in this study. Sr free HA ceramics had better MTT absorbance than all the other groups on day 12. Although moderate proliferation rates were observed in the Sr1000-Si-HA ceramics on day 12 in this study, the HA ceramics which had higher Sr content resulted with better proliferation rates up to 14 days in another study (Capuccini et al., 2009). HA and TCP were compared in cell culture conditions in John's study (John et al., 2009). Cell number on the HA scaffold

was lower than that of the TCP scaffold until day 28. Cell amount on the HA scaffolds however increased at later times (John et al., 2009). Si addition to the HA ceramics improved the cell proliferation rate further in this study. This result was in line with other studies and the role of Si for enhancement of bone function was reported before (Keeting et al. (1990), Reffitt et al. (2003)). Si-rich SCPC50 resulted with stimulation of osteoblast phenotypic expression (Gupta et al., 2007).

ALP activity of cells decreased with time in all but not the Sr1000-Si-HA group. MTT absorbance of the Sr1000-Si-HA group decreased during this period. However according to the ALP test, the results of day 12 almost reached the high results of day 2 of that the cells were incubated with the Sr1000-Si-HA ceramics. Sr1000-Si-HA ceramics triggered more ALP absorbance than the other ceramics on days 2 and 12 when groups were compared. According to the ALP test results of the BMP containing composites, the BMP-Sr1000-Si-HA composite had more ALP activity on day 2. ALP absorbance decreased in all BMP containing Sr-bioceramic composites on days 6 and 12. The BMP-Sr500-Si-HA composite resulted with the lowest ALP activity than the other groups on days 6 and 12. When BMP containing and not containing ceramics were compared on day 6, both the Sr500-Si-HA groups (BMP containing or not containing) again resulted with significantly lower ALP activities than the other groups. Besides, BMP-Si-HA composites showed higher ALP absorbance than the BMP free Si-HA, Sr500-Si-HA and Sr1000-Si-HA ceramics at the same time point. On day 12, BMP's improving effect for ALP absorbance continued in the BMP-HA, BMP-Sr250-Si-HA and BMP-Sr1000-Si-HA groups. HA resulted with good ALP activity in this study. In a study (Nishio et al., 2000), pure Titanium (Ti) disks were compared with alkali-heat treated Ti(AH-Ti) or soaked AH-Ti (in simulated body fluid to deposit crystalline HA on the surface) disks and the ALP activities of cells that were incubated with all type disks were low at day 7. According to the XRD test, apatite layers formed on the soaked AH-Ti disks and higher ALP activity

was seen in cells than were applied with those disks than other type disks in that study. The raise in ALP activity might also be related to the Sr amount in the ceramics of this study. Sr1000-Si-HA's stimulating effect could not be maintained until day 12 according to the MTT test. According to the ALP test, the Sr1000-Si-HA group resulted with good ALP absorbance rates. Capuccini investigated the effect of Sr-doped HA at OB like MG63 cells and Oc cultures (Capuccini et al., 2009). HA composites, which had higher Sr content, caused increase at cell proliferation rate and ALP activity in MG63 cells and decrease at proliferation of Oc(s) especially up to 14 days. Peng (Peng et al., 2009) had similar observations recently. ALP activity increased in higher amount of Sr applied groups on day 14 (Peng et al., 2009). According to the overall ALP results of this study, BMP addition to ceramics resulted with increased ALP activity of cells. Although BMP addition did not stimulate cell proliferation until day 12, its enhancing effect was observed in the ALP test. BMP effect to ceramics had been researched before (Watanabe et al. (1990), Ono et al. (1992, 1995), Takaoka et al. (1989), Urist et al. (1981)). Higher ALP activity was observed in the BMP-HA groups when compared to the BMP free HA groups in 2 weeks (Alam et al., 2001). Noshi also observed increased ALP activity by adding BMP to the HA with osteoblasts at 2 weeks (Noshi et al., 2001) which were in line with this study.

Cells that were incubated on tcps resulted with better *in vitro* values than cells applied with ceramics in this study. The effect of polystyrene on cell proliferation had been observed by Douglas et al in their study by comparing with HA-TCP microspheres (Douglas et al., 2010). They explained the reason as the flat surface form of tcps triggered more cell proliferation than 3D structure of biomaterials. This aspect can be valid for ceramics of this study, too. Porosity properties of ceramics may have affected the cell proliferation rates as well. According to some researchers (Anselme et al. (2000), Deligianni et al. (2001)), cell proliferation and ALP activity can be negatively influenced from irregular porous surfaces. Rosa applied HA discs with 5, 15, 30% porosity to cells in culture conditions (Rosa et al., 2003). HA

that had lower porosity percentage, which caused more cell proliferation at day 7 and 14 than other groups. Also, HA that had lower porosity percentage that resulted with higher ALP activity than HA having higher porosity percentage. According to researchers, cell response can be caused by difference of protein adsorption (Zeng et al., 1999) and reorganization of proteins on ceramic samples can be affected by physcochemical properties of the ceramic surface and their profile can be changed (Deligianni et al., 2001).

Although the Sr250-Si-HA and the Sr500-Si-HA ceramics showed lower DNA amount than the HA and the Si-HA ceramics on day 2, they showed higher results on day 6. Sr1000-Si-HA had moderate values at those time points. On day 12, the Sr1000-Si-HA ceramics triggered significantly higher DNA amounts than other ceramics. In addition, the BMP-Sr500-Si-HA composites showed significantly lower values than other composites on day 2. BMP-Si-HA composite caused higher DNA amount on day 6 and the BMP-HA group resulted with more DNA amount than the other groups on day 12. When BMP containing and not containing ceramics were compared, both the Sr500-Si-HA ceramics (BMP containing or not containing) had lower values than the other groups on day 2. BMP addition to ceramics enhanced the DNA amounts of cells especially in the BMP-Si-HA and the BMP-Sr250-Si-HA composites on day 6. These results were parallel to the MTT and the ALP test results. On day 12, although the BMP-HA composites had significantly higher DNA values, the BMP free Sr1000-Si-HA ceramics had better results than other ceramics. HA based material that have higher Sr amount triggered more cell proliferation rates in another study (Capuccini et al., 2009). Also, the DNA assay results of the Si-HA and the Sr250-Si-HA groups were parallel to that of the MTT assay. In addition, DNA test results supported the ALP test results for the Sr500-Si-HA ceramics.

According to the results of ALP activity per DNA of the cells, Sr1000-Si-HA and Sr250-Si-HA ceramics showed better results than the other

groups. BMP-Sr1000-Si-HA composites resulted with good percentages than some of the other groups. The ALP/DNA ratio of with soaked alkali-heat treated titanium disks was examined in another study (Nishio et al., 2000). Crystalline HA deposition on the surfaces of disks was aimed by soaking disks into simulated body fluid. The disks that had apatitic surface resulted with higher ALP/DNA ratio at days 7 and 14. Findings of Nishio et al. (Nishio et al., 2000) were similar to the findings of this study.

As a consequence of *in vitro* experiments, according to the MTT and DNA test results, BMP triggered proliferation rates of cells in initial time points. Sr1000-Si-HA ceramics caused more absorbance rates than other ceramics. Also, the Si-HA and the Sr250-Si-HA ceramics presented favorable MTT, DNA and ALP results. Osteoblastic cells showed typical polygonal shapes and adhered to the surface of the ceramics in SEM evaluations. The ceramics were processed for SEM analysis, however they waited for too long until SEM observation. Because of this reason, the cells on the ceramics could not be seen clearly. This was another limitation of our *in vitro* study. Sr500-Si-HA ceramics had lower absorbance values almost in all *in vitro* tests. According to the results of the Sr release test, the Sr500-Si-HA ceramic released more Sr than the other ceramics. Higher Sr release to the cell culture environment may have triggered the occurrence of the unexpected results. In Boyd's study, decrease at cell viability thought to be related with the accumulation of zinc-Sr in the medium which resulted in cytotoxicity (Boyd et al., 2009). High amount of Sr accumulation in the medium might have affected the proliferation rates of cells in this study.

In vivo XP results of all groups had been evaluated for periosteal reaction, quality of bone union, remodeling, implant integration and total radiological scores at OVX, bioceramic implantation, 2 and 4 weeks after bioceramic implantation. For periosteal reaction and total radiological scores, the HA and Sr-Si-HA groups showed higher values than the BMP-Si-HA and BMP-Sr-Si-HA groups at 2 weeks after bioceramic implantation. Lower

radiological scores of the BMP-Si-HA group were observed at remodeling too. The control 2 group showed better results than the other groups in radiological scores at all time points as this group did not underwent OVX or defect operations. The scores of all bioceramic applied groups were around minimum 1 or 1.5. As the highest radiological score was 4, the results were considered as acceptable in this setting.

DXA results of femur and vertebra showed that, BMD values of the OVX groups were close to the non-ovariectomized group on 4 weeks after operation. OVX operations were applied to the rats for inducing osteoporosis. According to the DXA results, bioceramic implanted rats had increase in their BMD values 16 weeks after their OVX operations. However, limitation of the *in vivo* experiments in this study was the non statistical difference between time points.

According to micro CT analysis, BMP-Sr-Si-HA group had more new bone formation areas than the other groups 2 and 4 weeks after bioceramic implantation. This result was supporting DXA results of same group. But the differences between BV/TV% values of groups were not significant statistically. The effect of Sr addition to the scaffolds was observed using micro CT tests in other studies. In Li's study, Sr added HA group had higher BV/TV% than Sr absent group (Li et al., 2010). In Warnke's study, HA blocks were implanted to the rats (Warnke et al., 2010). Another implant was inserted to the rats later and BMP-2 was applied to both implants on second implantation time. According to CT observations of that study, lower bone densities were seen at delayed BMP-2 applied group. In this study, BMP-2 was applied to rats through composites simultaneously and BMP-2 added composites resulted in more BV/TV% values than other groups.

According to the results of histological investigation, the BMP-Sr-Si-HA, Sr-Si-HA and BMP-Si-HA bioceramic implanted groups resulted in higher new

bone formation rates than the other groups on 2 and 4 weeks. The HA implanted group showed lower bone formation rates than the other groups in this study. Similarly, in another study (Noshi et al., 2001) the alone HA ceramic did not trigger good histology results. In Noshi's study, HA, BMP-HA and MSC-BMP-HA materials were applied subcutaneously to rats (Noshi et al., 2001). HA and BMP-HA resulted without bone formation on 4 weeks after implantation. Besides, Sr addition was observed to increase new bone forming sites in another studies (Grynpas et al., 1996). Likewise, in this study Sr1000-Si-HA ceramics resulted with more bone formation areas. In this study, the Sr1000-Si-HA ceramics were preferred according to the *in vitro* test results. Also, the Si content of the ceramics might have increased new bone formation. According to some researches, Si enhanced solubility of HA (Porter et al., 2003) scaffolds. In addition, Si was known to improve bone mineralization and metabolism (Reffitt et al., 2003). In Uludağ's study, rhBMP-2-containing Helistat (colagen sponge) showed bone formation at 2 weeks (Uludağ et al., 2000). BMP addition to scaffolds enhanced bone formation while no bone formation areas were detected at BMP absent groups in another study (Alam et al., 2001). The results of this study were in line with that study. Enhancing effect of Sr was examined in other studies. Sr application resulted with increase at trabecular bone volume in Ammann's study (Ammann et al., 2004). In Zreiqat's study, Sr–Hardystonite (Sr–$Ca_2ZnSi_2O_7$, Sr–HT) were compared to Hardystonite (HT) which were implantated to tibial bone defects of rats (Zreiqat et al., 2010). New bone formation areas were seen at periphery of Sr-HT implants on 3 weeks after implantation at that study.

According to observation of histological sections, mild inflammation with thin fibrous encapsulation was seen in this study. Ceramic particles mingled with bone and inflammatory reaction was not occured. These results were important to show integration and biocompatibility of the bioceramics. Powder form of bioceramics might have affected the response of body. Because, CaP ceramics have risk to be accepted as foreign material by

immune system because of their brittleness properties (Anderson JM, 1988). Therefore, powder form of ceramics was preferred more against irritation of mucosal layers that could be formed by small particles of materials (de Groot K (1988), Douglas et al. (2010)).

CHAPTER 5

CONCLUSION

As a conclusion, we were able to prepare and characterize Sr containing ceramics and combined them with BMP in this study. The ceramics were evaluated by compression test mechanically after their characterization. According to our results, addition of Sr into Si-HA ceramics increased their compressive strength. Ceramics, which had more Sr content resulted with more compressive strength.

Sr release studies revealed that trace amount of Sr is released to distilled water in 3 and 14 days. However, Sr release into serum stayed under detection limits which indicated that the release of Sr from the ceramics will be limited when ceramics will be implanted into bone.

In vitro studies results showed that these ceramics were biocompatible. They stimulated rat OB proliferation. ALP activity and DNA amounts of cells increased parallel to the proliferation rate of cell especially in the Sr1000-Si-HA ceramic applied wells. In addition, BMP caused an increase in cellular activities when BMP was added into the ceramics.

In vivo results displayed that when BMP-Sr-Si-HA and Sr-Si-HA ceramics were implanted into rat tibia, they enhanced bone defect healing. Radiology was insufficient to quantify healing however micro CT and histological findings support *in vivo* biocompatibility and osteontegrity. Consequently, in this study, the ceramics displayed increased mechanical strength and allowed cell attachment (especially Sr-Si-HA ceramics). New bone formation increased with the BMP-Sr-Si-HA bioceramic composites in

bone defects. The results of this study promote future research on Sr containing bioceramics in treatment of orthopedic problems.

REFERENCES

1. Akao M, Aoki H, Kato K. "Mechanical properties of sintered hydroxyapatite for prosthetic applications" Journal of Materials Science, 1981; 16; 809-12
2. Alam I, Asahina I, Ohmamiuda K, Takahashi K, Yokota S, Enomoto S. Evaluation of ceramics composed of different hydroxyapatite to tricalcium phosphate ratios as carriers for rhBMP-2, Biomaterials 2001; 22; 1643-1651
3. Ambrosio AM, Sahota JS, Khan Y, Laurencin CT. A novel amorphous calcium phosphate polymer ceramic for bone repair: I. Synthesis and characterization. Journal of Biomedical Materials Research 2001; 58; 295–301
4. Ammann P. Rizzoli R, Muller K, Slosman D, Bonjour J-P. IGF-I and parnidroiiate increase bone mineral density in ovariectomized adult rats. Am J Physiol 1993; 265; E770 6.
5. Ammann P, Shen V, Robin B, Mauras Y, Bonjour JP, Rizzoli R. Strontium ranelate improves bone resistance by increasing bone mass and improving architecture in intact female rats. J Bone Miner Res 2004; 19; 2012–20.
6. An YH, Friedman RJ. Animal models of bone defect repair. In Animal Models in Orthopaedic Surgery. Eds. An YH, Fredman RJ, CRC Press, Boca Raton, USA, 1999, pp: 241-260.
7. Anderson JM. Inflammatory response to implants. Trans Am Soc Artif Intern Organs 1988; 34; 101–7
8. Andreshak JL, Rabin SI, Patwardhan AG, Wezeman FH. Tibial segmental defect repair: chondrogenesis and biomechanical strength

modulated by basic fibroblast growth factor. Anat Rec. 1997 Jun; 248(2); 198-204

9. Angeli A, Guglielmi G, Dovio A, Capelli G, de Feo D, Giannini S, Giorgino R, Moro L & Giustina A. High prevalence of asymptomatic vertebral fractures in post-menopausal women receiving chronic glucocorticoid therapy: a cross-sectional outpatient study. Bone 2006; 39; 253–259.
10. Anselme K, Bigerelle M, Noel B, Dufresne E, Judas D, Iost A, Hardouin P. Qualitative and quantitative study of human osteoblast adhesion on materials with various surface roughnesses. J Biomed Mater Res 2000; 49; 155–66.
11. Aoki H, Okayama S, Akao M. "Processing of the fourth international symposium on ceramics in medicine, London, UK,Sept. 1987,", Bioceramics 1991; vol. 4; p 87
12. Aoshima K, Fan J, Cai Y, Katoh T, Teranishi H, Kasuya M. Assessment of bone metabolism in cadmium-induced renal tubular dysfunction by measurements of biochemical markers. Toxicol. Lett. 2003; 136; 183–192.
13. Bagi CM, Brommage R, Deleon L, Adams S, Rosen D, Sommer A. Benefit of systemically administered rhIGF-I and rhlGF-l/ IGFBP-3 on cancellous bone in ovariectomized rats. J Bone Miner Res 1994; 9; 1301-12
14. Bagi CM, Ammann P, Rizzoli R, Miller SC. Effect of estrogen deficiency on cancellous and cortical bone structure and strength of the femoral neck in rats. Calcif Tissue Int 1997; 61; 336–344
15. Bajpai AK, Bundela H. γ-Radiation Assisted Fabrication of Hydroxyapatite_Polyacrylamide Nanocomposites with Possible Application, in Bone Implantology, Journal of Composite Materials, 2010; Vol. 44; No. 6
16. Banerjee SS, Tarafder S, Davies NM, Bandyopadhyay A, Bose S. Understanding the influence of MgO and SrO binary doping on the

mechanical and biological properties of b-TCP ceramics, Acta Biomaterialia 2010; 6; 4167–4174

17. Baron R, Tsouderos Y. In vitro effects of S12911-2 on osteoclast function and bone marrow macrophage differentiation. Eur J Pharmacol. 2002 Aug 16; 450(1), 11-7
18. Baron TD, Teitlebaum SL, Bergfeld MA, Parker G, Cruvant EM, Avoli LV. Effect of alcohol ingestion on bone and mineral metabolism in rats. Am J Physiol 1980; 238; E5007-E510
19. Barrett-Connor E, Nielson CM, Orwoll E, Bauer DC, Cauley JA. Epidemiology of rib fractures in older men: Osteoporotic Fractures in Men (MrOS) prospective cohort study, BMJ 2010; 340; c1069
20. Be'ery-Lipperman M, Gefen A. Contribution of muscular weakness to osteoporosis: Computational and animal models, Clinical Biomechanics 2005; 20; 984–997
21. Black LJ, Sato M, Rowley ER, Magee DE, Bekele A, Williams DC, Cullnan GJ, Bendele R, Kauffman RF, Bensch WR, Frolik CA, Termine JD, Bryant HU. Raloxifene (LY139481 HCl) prevents bone loss and reduces serum cholesterol without causing uterine hypertrophy in ovariectomized rats, J. Clin. Invest. 1994; 93; 63–69
22. Bobba R. Dense Membranes for Anode Supported all Perovskite IT-SOFCs, Annual Report (9/15/2005 - 09/14/2006a).
23. Bobba R, Samrat G, Weichang Z, Hrudananda J. Innovative processing of dense LSGM electrolytes for IT-SOFC's, Journal of Power Sources, 2006b; 159; 21-28
24. Bouxsein ML. Determinants of skeletal fragility. Best Pract Res Clin Rheumatol 2005; 19; 897–911
25. Boyd D, Carroll G, Towler MR, Freeman C, Farthing P, Brook IM. Preliminary investigation of novel bone graft substitutes based on strontium-calcium-zinc-silicate glasses, J Mater Sci Mater Med. 2009 Jan; 20(1), 413-20

26. Boyle WJ, Simonet WS, Lacey DL. Osteoclast differentiation and activation, Nature 2003, 423; 337-342
27. Brandi ML. Microarchitecture, the key to bone quality, Rheumatology 2009; 48; iv3–iv8
28. Bronner F, Worrell RV (eds.), Orthopaedics, principles of basic and clinical science.Boca Raton, FL; 1999, CRC.
29. Brzoska MM, Kaminski M, Supernak-Bobko D, Zwierz K, Moniuszko-Jakoniuk J. Changes in the structure and function of the kidney of rats chronically exposed to cadmium. I. Biochemical and histopathological studies. Arch. Toxicol. 2003; 77; 344–352.
30. Brzoska MM, Moniuszko-Jakoniuk J. Low-level exposure to cadmium during the lifetime increases the risk of osteoporosis and fractures of the lumbar spine in the elderly. Studies on a rat model of human environmental exposure. Toxicol Sci. 2004a Dec; 82(2): 468-77.
31. Brzoska MM, Majewska K, Moniuszko-Jakoniuk J. Mineral status and mechanical properties of lumbar spine of female rats chronically exposed to various levels of cadmium. Bone 2004b; 34; 517–526.
32. Bucholz RW. Nonallograft osteoconductive bone graft substitutes, Clin Orthop Relat Res. 2002 Feb; 395; 44-52
33. Buruiana LM, Hadarag E. La nature de l'inhibition de l'heparine sur la phosphatase acide enythrocitaine. Natunwissenschaften, 1958; 45; 293-294.
34. Burge R, Dawson-Hughes B, Solomon DH, Wong JB, King A, Tosteson A. Incidence and economic burden of osteoporosis-related fractures in the United States, 2005-2025, J Bone Miner Res. 2007 Mar; 22(3), 465-75
35. Caetano-Lopes J, Canhão H, Fonseca JE. Osteoblasts and bone formation Acta Reumatol Port. 2007 Apr-Jun; 32(2), 103-10
36. Canalis E, Hott M, Deloffre P, Tsouderos Y, Marie PJ. The divalent strontium salt S12911 enhances bone cell replication and bone formation in vitro Bone 1996; 18(6), 517-23

37. Canalis E, Delany AM. Mechanisms of glucocorticoid action in bone. Annals of the New York Academy of Science 2002; 966; 73–81
38. Capuccini C, Torricelli P, Boanini E, Gazzano M, Giardino R, Bigi A, Interaction of Sr-doped hydroxyapatite nanocrystals with osteoclast and osteoblast-like cells, J Biomed Mater Res 2009; 89A; 594–600
39. Carlisle EM. Silicon: A possible factor in bone calcification. Science 1970; 167; 179–280
40. Carlisle EM. Silicon: A requirement in bone formation independent of vitamin D1. Calc Tissue Int 1981; 33; 27–34
41. Carter DR, Hayes W. The compressive behavior of bone as a two-phase porous structure. J Bone Jt Surg 1977; 59A, 954–62
42. Chalkley SR, Richmond J, Barltrop D, Measurement of vitamin D3 metabolites in smelter workers exposed to lead and cadmium. Occup. Environ. Med. 1998; 55; 446– 452.
43. Chang BS, Lee CK, Hong KS, et al. Osteoconduction at porous hydroxyapatite with various pore configurations. Biomaterials. 2000; 21(12), 1291–8.
44. Chattopadhyay N, Yano S, Tfelt-Hansen J, Rooney P, Kanuparthi D, Bandyopadhyay S, Ren X, Terwilliger E, Brown EM. Mitogenic action of calcium-sensing receptor on rat calvarial osteoblasts, Endocrinology. 2004 Jul; 145(7), 3451-62
45. Chaudhari A, Ron E, Rethman MP, Recombinant human bone morphogenetic protein-2 stimulates differentiation in primary cultures of fetal rat calvarial osteoblasts. Mol Cell Biochem. 1997; 167(1-2), 31-9
46. Chen P, Carrington JL, Hammonds RG, Reddi AH. Stimulation of chondrogenesis in limb bud mesoderm cells by recombinant human bone morphogenetic protein 2B (BMP-2B) and modulation by transforming growth factor beta 1 and beta 2. Exp Cell Res. 1991 Aug; 195(2), 509-15

47. Chen QZ, Thompson ID, Boccaccini AR. 45S5 Bioglass-derived glass-ceramic scaffolds for bone tissue engineering. Biomaterials 2006; 27(11), 2414–25
48. Choi JH, Rhee IK, Park KY, Kim JK, Rhee SJ. Action of green tea catechin on bone metabolic disorders in chronic cadmium-poisoned rats. Life Sci. 2003; 73; 1479– 1489.
49. Chow J, Tobias JH, Colston KW, Chambers TJ. Estrogen maintains trabecular bone volume in rats not only by suppression of bone resorption but also by stimulation of bone formation. J Clin Invest 1997; 89(7), 1-8
50. Cole Z, Dennison E, Cooper C. Update on the treatment of post-menopausal osteoporosis. Br Med Bull. 2008; 86; 129-43.
51. Cooper C. The crippling consequences of fractures and their impact on quality of life. Am J Med 1997; 103; 12S–17S
52. Cordell JM, Vogl ML, Wagoner Johnson AJ. The influence of micropore size on the mechanical properties of bulk hydroxyapatite and hydroxyapatite scaffolds. Journal of the mechanical behavior of biomedical materials 2009; 2; 560-570
53. Cummings SR, Melton LJ. Epidemiology and outcomes of osteoporotic fractures. Lancet 2002; 359; 1761–1767
54. Curzon MEJ, Cutress TW. Strontium. Trace elements and dental disease. London: John Wright, PSG Inc.; 1983, p. 283–304.
55. Çömelekoğlu Ü, Bagış S, Yalın S, Ogenler O, Yıldız A, Şahin NÖ, Oğuz İ, Hatungil R. Biomechanical evaluation in osteoporosis:ovariectomized rat model, Clin Rheumatol 2007; 26; 380–384
56. Daculsi G. Biphasic calcium phosphate concept applied to artificial bone, implant coating and injectable bone substitute. Biomaterials. 1998 Aug; 19(16), 1473-8
57. Dagang G, Kewei X, Yaxiong L. Physicochemical properties and cytotoxicities of Sr-containing biphasic calcium phosphate bone scaffolds. J Mater Sci: Mater Med 2010; 21; 1927–1936

58. Dahl SG, Allain P, Marie PJ, Mauras Y, Boivin G, Ammann P. Incorporation and distribution of strontium in bone. Bone 2001; 28(4), 446-53
59. de Groot K. Effect of porosity and physicochemical properties on the stability, resorption and strength of calcium phosphate ceramics. Ann N Y Acad Sci 1988; 523; 227–33
60. Deckers MM, van Bezooijen RL, van der Horst G, Hoogendam J, van Der Bent C, Papapoulos SE, Löwik CW. Bone morphogenetic proteins stimulate angiogenesis through osteoblast-derived vascular endothelial growth factor A. Endocrinology. 2002 Apr; 143(4), 1545-53
61. Deligianni DD, Katsala ND, Koutsoukos PG, Missirlis YF. Effect of surface roughness of hydoxyapatite on human bone marrow cell adhesion, proliferation, differentiation and detachment strength. Biomaterials 2001; 22; 87–96
62. Delmas PD. Treatment of postmenopausal osteoporosis. Lancet 2002; 359(9322), 2018–2026
63. Dempster DW. Bone histomorphometry in glucocorticoid-induced osteoporosis. J Bone Miner Res. 1989 Apr; 4(2), 137-41
64. Dennison E, Mohamed MA, Cooper C. Epidemiology of osteoporosis. Rheum Dis Clin North Am 2006; 32; 617–629
65. Develioğlu H, Koptagel E, Gedik R, Dupoirieux L. The effect of a biphasic ceramic on calvarial bone regeneration in rats, J Oral Implantol. 2005; 31(6), 309-12
66. Douglas T, Liu Q, Humpe A, Wiltfang J, Sivananthan S, Warnke PH. Novel ceramic bone replacement material CeraBalls seeded with human mesenchymal stem cells, Clin. Oral Impl. Res. 2010; 21; 262–267
67. Driessens F, Verbeeck R. Biomaterials. Boca Raton: CRC Press; 1990
68. Duan Y, Beck TJ, Wang XF, Seeman E. Structural and biomechanical basis of sexual dimorphism in femoral neck fragility has its origins in growth and aging. J Bone Miner Res 2003; 18; 1766–74.

69. Egermann M, Schneider E, Evans CH, Baltzer AW. The potential of gene therapy for fracture healing in osteoporosis. Osteoporos Int. 2005 Mar; 16 Suppl 2, S120-8 Review
70. Elliot JC. Structure and chemistry of the apatites and other calcium orthophosphates. Amsterdam: Elsevier; 1994.
71. Enlow DH. Principles of bone remodeling. Springfield, IL: Charles C Thomas, 1963.
72. Enlow DH. The human face: An account of the postnatal growth and development of the craniofacial skeleton. New York: Harper and Row, 1968
73. ESHRE Capri Workshop Group. Bone fractures after menopause, Human Reproduction Update, 2010, pp. 1–13
74. Evans CH, Palmer GD, Pascher A, Porter R, Kwong FN, Gouze E, Gouze JN, Liu F, Steinert A, Betz O, Betz V, Vrahas M, Ghivizzani SC. Facilitated endogenous repair: making tissue engineering simple, practical, and economical. Tissue Eng. 2007; 13; 1987–1993.
75. Fleisch H, Russell RG, Francis MD. Diphosphonates inhibit hydroxyapatite dissolution in vitro and bone resorption in tissue culture and in vivo. Science 1969; 165(899), 1262-4
76. Frost HM. Dynamics of bone remodeling. In Bone Biodynamics, Boston: Lıttle &Brown 1964; 315
77. Frost HM. Skeletal structural adaptations to mechanical usage (SATMU): 2. Redefining Wolff's law: the remodeling problem. Anat. Rec. 1990; 226; 414–422
78. Frost HM. Introduction to a new skeletal physiology, vol. I and II., Pueblo: Pajaro Group, 1995
79. Fujita R, Yokoyama A, Nodasaka Y, Kohgo T, Kawasaki T. Ultrastructure of ceramic-bone interface using hydroxyapatite and beta-tricalcium phosphate ceramics and replacement mechanism of beta-tricalcium phosphate in bone. Tissue Cell. 2003 Dec; 35(6), 427-40

80. Fukunaka Y, Iwanaga K, Morimoto K, Kakemi M, Tabata Y. Controlled Release of Plasmid DNA from Cationized Gelatin Hydrogels Based on Hydrogel Degradation, J. Control Release, 2002; 23(80), 333–343
81. Garrison KR, Donell S, Ryder J, Shemilt I, Mugford M, Harvey I, Song F. Clinical effectiveness and cost-effectiveness of bone morphogenetic proteins in the non-healing of fractures and spinal fusion: A systematic review. Health Technol Asses 2007; 11(30), 1–150.
82. Genant HK, Cann CE, Ettinger B, Gordan GS. Quantitative computed tomography of vertebral spongiosa: A sensitive method for detecting early bone loss after oophorectomy. Ann Intern Med 1982; 97; 699-705
83. Gentleman E, Fredholm YC, Jell G, Lotfibakhshaiesh N, O'Donnell MD, Hill RG, Stevens MM. The effects of strontium-substituted bioactive glasses on osteoblasts and osteoclasts in vitro, Biomaterials 2010; 31; 3949–3956
84. Gerhard FA, Webster DJ, Van Lenthe GH, Müller R. In silico biology of bone modelling and remodelling: adaptation, Phil. Trans. R. Soc. A 2009; 367; 2011–2030
85. Gibson LJ. The mechanical behavior of cancellous bone. J Biomech 1985; 18; 317–28.
86. Giesen EBW, Ding M, Dalstra M, van Eijden TMGJ. Mechanical properties of cancellous bone in the human mandibular condyle are anisotropic. J Biomech 2001; 34; 799–803.
87. Gonda Y, Ioku K, Shibata Y, Okuda T, Kawachi G, Kamitakahara M, Murayama H, Hideshima K, Kamihira S, Yonezawa I, Kurosawa H, Ikeda T. Stimulatory effect of hydrothermally synthesized biodegradable hydroxyapatite granules on osteogenesis and direct association with osteoclasts, Biomaterials 2009; 30; 4390–4400
88. Grob GN. From Aging to Pathology: The Case of Osteoporosis. Journal of the history of medicine and allied sciences, 2010

89. Gronowicz G, McCarthy MB. Response of Human Osteoblasts to Implant Materials: Integrin-Mediated Adhesion, Journal of Orthopedic Research, 1996 Nov; 14(6), 878-87
90. Grosso A, Douglas I, Hingorani A, MacAllister R, Smeeth L. Post-marketing assessment of the safety of strontium ranelate; a novel case-only approach to the early detection of adverse drug reactions. Br J Clin Pharmacol. 2008 Nov; 66(5); 689-94
91. Grynpas MD, Hamilton E, Cheung R, Tsouderos Y, Deloffre P, Hott M, et al. Strontium increases vertical bone volume in rats at a low dose that doesn't induce detectable mineralization defect. Bone 1996; 18(3), 253-9
92. Guo D, Xu K, Zhao X, Han Y. Development of a strontium-containing hydroxyapatite bone cement, Biomaterials, 2005, Volume 26, Issue 19, Pages 4073-4083
93. Gupta G, El-Ghannam A, Kirakodu S, Khraisheh M, Zbib H, Enhancement of Osteoblast Gene Expression by Mechanically Compatible Porous Si-Rich Nanocomposite, J Biomed Mater Res Part B: Appl Biomater 2007; 81B, 387–396
94. Hamdan Alkhraisat M, Moseke C, Blanco M, Barralet JE, Lopez-Carbacos E, Gbureck U. Strontium modified biocements with zero order release kinetics, Biomaterials 2008; 29(35), 4691-7
95. Hansen MA, Hasseger C, Overgaard K, Marslew U, Riis BJ, Christiansen C. Dual-energy X-ray absorptiometry: A precise method of measuring bone mineral denisty in the lumbar spine. J Nucl Med 1990; 31; 1156-1162
96. Hay E, Hott M, Graulet AM, Lomri A, Marie PJ. Effects of bone morphogenetic protein-2 on human neonatal calvaria cell differentiation. J Cell Biochem. 1999 Jan 1; 72(1); 81-93.
97. Hearn AP, Silber E. Osteoporosis in multiple sclerosis, Mult Scler 2010; 16; 1031

98. Hegge KA, Fornoff AS, Gutierres SL, Haack SL, New therapies for osteoporosis, Journal of Pharmacy Practice 2009; Vol 22 No:1,
99. Hench LL, Wilson J, editors "An introduction to bioceramics", advanced series in ceramics. vol 1. Singapore, World Scientific, 1993
100. Hernández L, Gurruchaga M, Goñi I. Injectable acrylic bone cements for vertebroplasty based on a radiopaque hydroxyapatite. Formulation and rheological behaviour. J Mater Sci Mater Med. 2009 Jan, 20(1), 89-97.
101. Hing KA, Saeed S, Buckland T, Rerell PA. Microporosity affects bioactivity of macroporous hydroxyapatite bone graft substitutes. Key Eng Materials 2004; 273–276
102. Hing KA, Annaz B, Saeed S, Rerell PA, Buckland T. Microporosity enhances bioactivity of synthetic bone graft substitutes. J Mater Sci Mater Med 2005; 16; 467–475.
103. Hing KA, Revell PA, Smith N, Buckland T. Effect of silicon level on rate, quality and progression of bone healing within silicate-substituted porous hydroxyapatite scaffolds, Biomaterials 2006; 27; 5014–5026
104. Hirata I, Nomura Y, Ito M, Shimazu A, Okazaki M. Acceleration of bone formation with BMP2 in frame-reinforced carbonate apatite–collagen sponge scaffolds, J Artif Organs 2007; 10; 212–217
105. Hofbauer LC, Khosla S, Dunstan CR, Lacey DL, Boyle WS, Riggs BL, The roles of osteoprotegerin and osteoprotegerin ligand in the paracrine regulation of bone resorption, J Bone Miner Res 2000; 15; 2-12
106. Hogan BL. Bone morphogenetic proteins: multifunctional regulators of vertebrate development. Genes and Development 1996; 10; 1580–1594.
107. Hott M, Deloffre P, Tsouderos Y, et al. S12911-2 reduces bone loss induced by short-term immobilization in rats. Bone. 2003; 33; 115–23.

108. Hulley PA, Gordon F, Hough FS. Inhibition of mitogen-activated protein kinase activity and proliferation of an early osteoblast cell line (MBA 15.4) by dexamethasone: role of protein phosphatases. Endocrinology 1998; 139; 2423–2431.

109. Hutmacher DW. Polymeric scaffolds in tissue engineering bone and cartilage. Biomaterials 2000; 21; 2529–2543.

110. Ioannidis G, Papaioannou A, Hopman WM, Akhtar-Danesh N, Anastassiades T, Pickard L, Kennedy CC, Prior JC, Olszynski WP, Davison KS, Goltzman D, Thabane L, Gafni A, Papadimitropoulos EA, Brown JP, Josse RG, Hanley DA, Adachi JD. Relation between fractures and mortality: results from the Canadian Multicentre Osteoporosis Study CMAJ, 2009 Sep 1; 181(5), 265-71

111. Issa Y, Brunton P, Waters CM, Watts DC. Cytotoxicity of metal ions to human oligodendroglial cells and human gingival fibroblasts assessed by mitochondrial dehydrogenase activity. Dent Mater 2008; 24(2), 281–7

112. JCPDS, PDF card: no 9-432, ICDD(JCPDS) Newton square, Pennsylvania, USA

113. Jallot E, Benhayoune H, Weber G, Balossier G, Bonhomme P. Characterization of the interfacebetween hydroxyapatite coating film and bone: use of a new expression tocorrect matrix effects for PIXE measurements in thick samples embedded in resin. J. Phys. D: Appl. Phys. 2000; 33; 321–326

114. Javaid MK, Holt RIG. Understanding osteoporosis. Journal of Physchopharmacology 2008; 22(2), 38-45

115. Jee WSS. Structure and function of bone tissue. In: Bronner F, Worrell RV, editors. Orthopaedics, principles of basic and clinical science, Boca Raton, FL: CRS Press[Chapter 1], 1999

116. John A, Varma HK, Vijayan S, Bernhardt A, Lode A, Vogel A, Burmeister B, Hanke Th, Domaschke H, Gelinsky M, In vitro

investigations of bone remodeling on a transparent hydroxyapatite ceramic, Biomed. Mater. 2009; 4; 015007, 9pp

117. Johnell O, Kanis JA, Oden A, Johansson H, De Laet C, Delmas P, Eisman JA, Fujiwara S, Kroger H, Mellstrom D, Meunier PJ, Melton III LJ, O'Neill T, Pols H, Reeve J, Silman A, Tenenhouse A. Predictive Value of BMD for Hip and Other Fractures, J Bone Miner Res 2005; 20; 1185-94

118. Jones AL, Bucholz RW, Bosse MJ, Mirza SK, Lyon TR, Webb LX, Pollak AN, Golden JD, Valentin-Opran A; BMP-2 Evaluation in Surgery for Tibial Trauma-Allgraft (BESTT-ALL) Study Group. Recombinant human BMP-2 and allograft compared with autogenous bone graft for reconstruction of diaphyseal tibial fractures with cortical defects. A randomized, controlled trial. J Bone Joint Surg Am. 2006 Jul; 88(7), 1431-41.

119. Jugdaohsingh R, Tucker KL, Qiao N, Cupples LA, Kiel DP, Powell JJ. Dietary silicon intake is positively associated with bone mineral density in men and premenopausal women of the Framingham Offspring cohort. J Bone Miner Res 2004; 19(2), 297–307.

120. Kamitakahara M, Ohtsuki C, Miyazaki T. Review Paper: Behavior of Ceramic Biomaterials Derived from Tricalcium Phosphate in Physiological Condition, J Biomater Appl 2008; 23; 197

121. Kanis JA, Johnell O. Requirements for DXA for the management of osteoporosis in Europe. Osteoporos Int 2005; 16; 229-238

122. Katagiri T, Yamaguchi A, Ikeda T, Yoshiki S, Wozney JM, Rosen V, Wang EA, Tanaka H, Omura S, Suda T. The non-osteogenic mouse pluripotent cell line C3H10T1/2 is induced to differentiate into osteoblastic cells by recombinant human bone morphogenetic protein-2. Biochem. Biophys. Res. Commun. 1990; 172; 295–299.

123. Kawamura J, Yoshida O, Nishino K, Itokawa I. Disturbances in kidney functions and calcium and phosphate metabolism in cadmiumpoisoned rats. Nephron 1978; 20; 101– 110.

124. Keaveny TM, Hayes WC. Mechanical properties of cortical and trabecular bone. In: Hall BK, editor. Bone growth. Boca Raton, FL: CRC Press, 1993, p. 285–344

125. Keeting PE, Oursler MJ, Wiegand KE, Bonde SK, Spelsberg TC, Riggs BL. Zeolite A increases proliferation, differentiation, and transforming growth factor b production in normal adult human osteoblast-like cells in vitro. J Bone Mineral Res 1990; 7; 1281–1289.

126. Kempen DHR, Lu L, Hefferan TE, Creemers LB, Maran A, Classic KL, Dhert WJA, Yaszemski MJ. Retention of in vitro and in vivo BMP-2 bioactivities in sustained delivery vehicles for bone tissue engineering, Biomaterials 2008; 29; 3245–3252

127. Kenley RA, Yim K, Abrams J, Ron E, Turek T, Marden LJ, Hollinger JO. Biotechnology and bone graft substitutes. Pharm Res 1993; 10; 1393–1401.

128. Kim SR, Lee JH, Kim YT, Riu DH, Jung SJ, Lee YJ, et al: Synthesis of Si, Mg substituted hydroxyapatites and their sintering behaviors. Biomaterials 2003; 24; 1389–1398

129. Kim SS, Gwak SJ, Kim BS. Orthotopic bone formation by implantation of apatite-coated poly(lactide-co glycolide)/ hydroxyapatite composite particulates and bone morphogenetic protein-2, J Biomed Mater Res 2008; 87A: 245–253

130. Klawitter JJ, Hulbert SF. Application of porous ceramics for the attachment of load baring orthopaedic applications. J Biomed Mater Res. 1971; 2(2), 161–7.

131. Klein-Nulend J, van der Plas A, Semeins CM, Ajubi NE, Frangos JA, Nijweide PJ, Burger EH. Sensitivity of osteocytes to biomechanical stress in vitro. FASEB J. 1995; 9; 441–445

132. Kochi G, Sato S, Fukuyama T, Morita C, Honda K, Arai Y, Ito K. Analysis on the guided bone augmentation in the rat calvarium using a microfocus computerized tomography analysis. Oral Surg Oral Med Oral Pathol Oral Radiol Endod. 2009 Jun; 107(6), e42-8

133. Koç N, Timuçin M, Korkusuz F. Fabrication and characterization of porous tricalcium phosphate ceramics. Ceramics International 2004; 30; 205–211

134. Köse N, Presentation slides, School of Basic Knowledge and Research about Orthopaedy and Traumatology, Turkish Orthopaedy and Traumatology Association, February 17-20, 2010.

135. Krajewski A, Ravaglioli A, Roncari E, Pinasco, P. Porous ceramic bodies for drug delivery. J Mater Sci Mater Med. 2000 Dec; 11(12); 763-71

136. Kubo T, Shiga T, Hashimoto J, Yoshioka M, Honjo H, Urabe M, Kitajima I, Semba I, Hirasawa Y. Osteoporosis influences the late period of fracture healing in a rat model prepared by ovariectomy and low calcium diet. J Steroid Biochem & Mol Biol 1999; 68; 197-202

137. Kwan MD, Wan DC, Skeletal tissue engineering. In: Principles of Tissue Engineering eds. Lanza RP, Vacanti J. Academic Press, 2007

138. Kwan MD, Slater BJ, Wan DC, Longaker MT. Cell-based therapies for skeletal regenerative medicine. Hum Mol Genet. 2008 Apr 15; 17(R1), R93-8. Review

139. Lacey DL, Timms E, Tan HL, Kelley MJ, Dunstan CR, Burgess T, Elliott R, Colombero A, Elliott G, Scully S, Hsu H, Sullivan J, Hawkins N, Davy E, Capparelli C, Eli A, Qian YX, Kaufman S, Sarosi I, Shalhoub V, Senaldi G, Guo J, Delaney J, Boyle WJ. Osteoprotegerin ligand is a cytokine that regulates osteoclast differentiation and activation. Cell 1998; 93; 165–76.

140. Landi E, Celotti G, Logroscino G, Tampieri A. Carbonated hydroxyapatite as bone substitute. J Eur Ceram Soc 2003; 23; 293

141. Landi E, Tampieri A, Celotti G, Sprio S, Sandri M, Logroscino G. Sr-substituted hydroxyapatites for osteoporotic bone replacement. Acta Biomaterialia 2007; 3; 961–969

142. LeGeros RZ. Properties of osteoconductive biomaterials: calcium phosphates. Clin Orthop Relat Res. 2002 Feb; 395; 81-98. Review

143. Lee HY, Lie D, Lim KS, Thirumoorthy T, Pang SM. Strontium ranelate-induced toxic epidermal necrolysis in a patient with post-menopausal osteoporosis. Osteoporosis Int 2009 Jan; 20(1), 161-2

144. Lee SH, Shin H. Matrices and scaffolds for delivery of bioactive molecules in bone and cartilage tissue engineering. Adv. Drug Deliv. Rev. 2007; 59; 339–359

145. Lehnerdt F. Beitrage zur Pathologishen Anatomie und Allgemeinen Pathologie. Ziegler, 1910; 47; 215-247.

146. Levy BT, Hartz A, Woodworth G, Xu Y, Sinift S. Interventions to Improving Osteoporosis Screening: An Iowa Research Network (IRENE) Study, JABFM 2009; 22; 360-7

147. Lewiecki EM. Managing osteoporosis: Challenges and strategies, Cleveland clinic Journal of Medicine, 2009; 76(8), 457-466

148. Li Y, Li Q, Zhu S, Luo E, Li J, Feng G, Liao Y, Hu J. The effect of strontium-substituted hydroxyapatite coating on implant fixation in ovariectomized rats, Biomaterials 2010; 31; 9006-9014

149. Li ZY, Lam WM, Yang C, Xu B, Ni GX, Abbah SA, Cheung KMC, Luk KDK, Lu WW. Chemical composition, crystal size and lattice structural changes after incorporation of strontium into biomimetic apatite, Biomaterials 2007; 28; 1452–1460

150. Lindsay R, Hart DM, Forrest C, Baird C. Prevention of spinal osteoporosis in oophorectomised women. Lancet 1980; 2; 1151-4.

151. Lindsay R. Sex steroids in the pathogenesis and prevention of osteoporosis. In: Riggs BL (ed) Osteoporosis: Etiology, Diagnosis and Management. Raven Press, New York, 1988, pp 333–358

152. Liu C-C, Kalu DN. Human parathyroid hormone- (1-34) prevents bone loss and augments bone formation in sexually mature ovariectomized rats. J Bone Miner Res 199O; 5; 973-82

153. Liu WC, Wong CT, Fong MK, Cheung WS, Kao RY, Luk KD, Lu WW. Gentamicin-loaded strontium-containing hydroxyapatite bioactive

bone cement--an efficient bioactive antibiotic drug delivery system. J Biomed Mater Res B Appl Biomater. 2010 Nov; 95(2); 397-406

154. Looker AC, Orwoll ES, Johnston CC Jr, et al. Prevalence of low femoral bone density in older U.S. adults from NHANES III. J Bone Miner Res 1997; 12; 1761-8

155. Lu JX, Flautre B, Anselme K, et al. Role of interconnections in porous bioceramics on bone recolonization in vitro and in vivo. J Mater Sci Mater Med. 1999; 10(1), 111–20

156. Lu M, Rabie ABM. Quantitative assessment of early healing of intramembranous and endochondral autogenous bone grafts using micro-computed tomography and Qwin image analyzer. Int J Oral Maxillofac. Surg, 2004; 33; 369-376

157. Manolagas SC. Birth and death of bone cells: basic regulatory mechanisms and implications for the pathogenesis and treatment of osteoporosis. Endocr Rev 2000; 21; 115–37

158. Marcus CS, Lengemann FW. Absorption of Ca45 and Sr85 from solid and liquid food at various levels of the alimentary tract of the rat. J Nutr. 1962 Jun; 77; 155-60

159. Mardas N, Stavropoulos A, Karring T. Calvarial bone regeneration by a combination of natural anorganic bovine-derived hydroxyapatite matrix coupled with a synthetic cell-binding peptide (PepGent): an experimental study in rats. Clin Oral Implants Res. 2008 Oct; 19(10), 1010-5

160. Mardziah CM, Sopyan I, Hamdi M, Ramesh S. Synthesis and characterization of strontium-doped hydroxyapatite powder via sol-gel method. Med J Malaysia 2008; 63(Suppl. A), 79-80

161. Marie PJ, Hott M, Modrowski D, De Pollak C, Guillemain J, Deloffre P, Tsouderos Y. An uncoupling agent containing strontium prevents bone loss by depressing bone resorption and maintaining bone formation in estrogendeficient rats. J Bone Miner Res 1993; 8; 607–15.

162. Marie PJ, Ammann P, Boivin G, Rey C. Mechanisms of actions and therapeutic potential of strontium in bone. Calcif Tissue Int 2001; 69; 121-9

163. Marra KG, Szem JW, Kumta PN, DiMilla PA, Weiss LE. In vitro analysis of biodegradable polymer blend/hydroxyapatite composites for bone tissue engineering. Journal of Biomedical Materials Research 1999; 47; 324–335

164. Martin FC. Next steps for falls and fracture reduction. Age Ageing. 2009 Nov; 38(6); 640-3

165. Matsumoto G, Omi Y, Kubota E, Ozono S, Tsuzuki H, Kinoshita Y, Yamamoto M, Tabata Y. Enhanced regeneration of critical bone defects using a biodegradable gelatin sponge and beta-tricalcium phosphate with bone morphogenetic protein-2. J Biomater Appl. 2009 Nov; 24(4); 327-42.

166. Mazess RB: On aging bone loss. Clin Orthop 1982; 165; 239-52

167. McCaslin FE Jr, Janes JM. The effect of strontium lactate in the treatment of osteoporosis. Proc Staff Meetings Mayo Clin, 1959; 34; 329-334

168. Meunier PJ, Lorenc RS, Smith IG et al. Strontium ranelate:new efficient antiosteoporotic agent for treatment of vertebral osteoporosis in postmenopausal women. Osteoporos Int 2002; 13(Suppl); 66

169. Meunier PJ, Roux C, Seeman E, Ortolani S, Badurski JE, Spector TD, Cannata J, Balogh A, Lemmel EM, Pors Nielsen S, Rizzoli R, Genant HK, Reginster JY. The effects of strontium ranelate on the risk of vertebral fracture in women with postemenopausal osteoporosis. N Engl J Med 2004, 350:459-68.

170. Mori H, Manabe M, Kurachi Y, Nagamo M, Osteointegration of dental implants in rabbit bone with low bone mineral density. J Oral Maxillofacial Surgery 1997; 55; 351-61

171. Mostafa NZ, Uludag H, Dederich DN, Doschak MR, El-Bialy TH. Anabolic effects of low-intensity pulsed ultrasound on human gingival fibroblasts, Archives of Oral Biology 2009; 54; 743–748

172. Mullender MG, Tan SD, Vico L, Alexandre C, Klein-Nulend J. Differences in osteocyte density and bone histomorphometry between men and women and between healthy and osteoporotic subjects. Calcif Tissue Int 2005; 77(5), 291–296

173. Murata M, Akazawa T, Tazaki J, Ito K, Sasaki T, Yamamoto M, Tabata Y, Arisue M. Blood Permeability of a Novel Ceramic Scaffold for Bone Morphogenetic Protein-2, J Biomed Mater Res Part B: Appl Biomater 2007; 81B, 469–475

174. Namgung R, Mimouni F, Campaigne BN, Ho ML, Tsang RC. Low bone mineral content in summer-born compared with winter-born infants. J Pediatr Gastroenterol Nutr. 1992 Oct; 15(3), 285-8.

175. National Osteoporosis Foundation, http://www.nof.org (last visited on December 30, 2010)

176. Naves-Diaz M, Diaz-Lopez J, Gomez-Alonso C, Altadill- Arregui A, Rodriguez-Rebollar A, Cannata- Andia J. Study of incidence of osteoporotic fractures in a cohort of individuals older than 50 years from Asturias, Spain, after a 6 year follow-up period. Med Clin (Barc) 2000; 115; 650–3

177. Ni GX, Lu WW, Xu B, Chiu KY, Yang C, Li ZY, Lam WM, Luk KDK. Interfacial behaviour of strontium-containing hydroxyapatite cement with cancellous and cortical bone. Biomaterials 2006; 27; 5127–5133

178. Nishio K, Neo M, Akiyama H, Nishiguchi S, Kim HM, Kokubo T, Nakamura T. The effect of alkali- and heat-treated titanium and apatite-formed titanium on osteoblastic differentiation of one marrow cells,J Biomed Mater Res, 2000; 52; 652–661

179. Nordberg G, Jin T, Bernard A, Fierens S, Buchet JP, Ye T, Kong Q, Wang H. Low bone density and renal dysfunction following environmental cadmium exposure in China. Ambio 2002; 31; 478–481.

180. Noshi T, Yoshikawa T, Dohi Y, Ikeuchi M, Horiuchi K, Ichijima K, Sugimura M, Yonemasu K, Ohgushi H. Recombinant Human Bone Morphogenetic Protein-2 Potentiates the In Vivo Osteogenic Ability of Marrow/Hydroxyapatite Composites, Artificial Organs, 2001; 25(3), 201-8

181. Nunes CR, Simske SJ, Sachdeva R, Wolford LM. Long-term ingrowth and apposition of porous hydroxyapatite implants. J Biomed Mater Res 1997; 36; 560–563.

182. O'Donnell MD, Fredholm Y, de Rouffignac A, Hill RG. Structural analysis of a series of strontium-substituted apatites, Acta Biomaterialia 2008; 4; 1455–1464

183. O'Neill T, Felsenberg D, Varlow J, Cooper C, Kanis J, Silman A. The prevalence of vertebral deformity in European men and women: the European Vertebral Osteoporosis Study. J Bone Miner Res 1996; 11; 1010– 8

184. Ogoshi K, Moriyama T, Nanzai Y. Decrease in the mechanical strength of bones of rats administered cadmium. Arch. Toxicol. 1989; 63; 320–324

185. Ogoshi K, Nanzai Y, Moriyama T. Decrease in bone strength of cadmium-treated young and old rats. Arch. Toxicol. 1992; 66; 315–320

186. Ohgushi H, Goldberg VM, Caplan AI. Repair of bone defects with marrow and porous ceramic. Acta Orthop Scand 1989; 60; 334–9.

187. Ohta H, Yamauchi Y, Nakakita M, Tanaka H, Asami S, Seki Y, Yoshikawa H. Relationship between renal dysfunction and bone metabolism disorder in male rats after long-term oral quantitative cadmium administration. Ind. Health 2000; 38; 339–355.

188. Oktar FN, Agathopoulos S, Ozyegin LS, Gunduz O, Demirkol N, Bozkurt Y, Salman S. Mechanical properties of bovine hydroxyapatite (BHA) composites doped with SiO_2, MgO, Al_2O_3, and ZrO_2. J Mater Sci Mater Med 2007; 18; 2137–2143

189. Ono I, Ohura T, Murata M, Yamaguchi H, Ohnuma Y, Kuboki Y. A study on bone induction in hydroxyapatite combined with bone morphogeneticprotein. Plast Reconstr Surg 1992; 90; 870-9.

190. Ono I, Gunji H, Kaneko F, Saito T, Kuboki Y. Efficacy of hydroxyapatite ceramics as a carrier of recombinant human bone morphogeticprotein. J Craniofac Surg 1995; 6; 238-44

191. Padilla S, Roman J, Vallet-Regi M. Synthesis of porous hydroxyapatites by combination of gelcasting and foams burn out methods. J Mater Sci Mater Med. 2002;13(10); 1193–7.

192. Parfitt AM, Mathews CHE, Villanueva AR, Kleerekoper M. Relationships between surface, volume, and thickness of iliac trabecular bone in aging and osteoporosis. J Clin Invest 1983; 72; 1396–1409

193. Parfitt AM. Bone remodeling: Relationship to the amount and structure of bone, and the pathogenesis and prevention of fractures. In Riggs BL, Melton U III (Eds): Osteoporosis: Etiology, Diagnosis, and Management. New York, Raven Press, 1988, pp 45-94.

194. Parfitt AM. Osteonal and hemi-osteonal remodeling: The spatial and temporal framework for signal traffic in adult human bone. J Cell Biochem 1994; 55; 273–286.

195. Patel N, Best SM, Bonfield W, Gibson IR, Hing KA, Damien E, Revell PA. A comparative study on the in vivo behavior of hydroxyapatite and silicon substituted hydroxyapatite granules, J Mater Sci Mater Med 2002; 13(12); 1199-206

196. Peng S, Zhou G, Luk KDK, Cheung KMC, Li Z, Lam WM, Zhou Z, Lu WW. Strontium Promotes Osteogenic Differentiation of

Mesenchymal Stem Cells Through the Ras/MAPK Signaling Pathway, Cell Physiol Biochem 2009; 23; 165-174

197. Peng TC, Cooper CW, Munson PL. The hypocalcemic effect of alcohol in rats and dogs, Endocrinol 1972; 91; 586-593

198. Peng TC, Gitelman HJ. Ethanol-induced hypocalcemia, hypermagnesemia and inhibition of serum calcium-raising effect of parathyroid hormone in rats. Endocrinol 1974; 94; 608-611

199. Peng Q, Jiang F, Huang P, Zhou S, Weng J, Bao C, Zhang C, Yu H, A novel porous bioceramics scaffold by accumulating hydroxyapatite spherules for large bone tissue engineering in vivo. I. Preparation and characterization of scaffold, J Biomed Mater Res 2010; 93A, 920–929

200. Pi M, Quarles LD. A Novel Cation-Sensing Mechanism in Osteoblasts Is a Molecular Target for Strontium. J Bone Miner Res. 2004 May; 19(5), 862-9

201. Pors Nielsen S. The biological role of strontium. Bone 2004; 35; 583-88

202. Porter AE, Patel N, Skepper JN, Best SM, Bonfield W. Comparison of in vivo dissolution processes in hydroxyapatite and siliconsubstituted hydroxyapatite bioceramics. Biomaterials 2003; 24(25), 4609–20.

203. Prabha Shankar B. Osteoporosis- a silent epidemic. Pharma. Times 2002; 34; 21–22

204. Qiu K, Zhao XJ, Wan CX, Zhao CS, Chen YW. Effect of strontium ions on the growth of ROS17/2.8 cells on porous calcium polyphosphate scaffolds. Biomaterials 2006; 27; 1277–1286

205. Reddi AH. Symbiosis of Biotechnology and Biomaterials: Applications in Tissue Engineering of Bone and Cartilage, J. Cell Biochem. 1994; 56(2); 192–195.

206. Reddi AH. Bone morphogenetic proteins: an unconventional approach to isolation of first mammalian morphogens, Cytokine Growth Factor Dev 1997; 8C, 11-20

207. Reddi AH. Bone morphogenetic proteins: from basic science to clinical applications. J Bone Joint Surg Am. 2001; 83-A Suppl 1(Pt 1), S1-6

208. Rees SG, Hughes Wassel DT, Waddington RJ, Embery G. Interaction of bone proteoglycans and proteoglycan components with hydroxyapatite. Biochim Biophys Acta. 2001 Dec 5; 1568(2), 118-28

209. Reffitt DM, Ogston N, Jugdaosingh R, Cheung HFJ, Evans BAJ, Thompson RPH, Powel JJ, Hampson GN. Orthosilicic acid stimulates collagen type 1 synthesis and osteoblastic differentiation in human osteoblast-like cells in vitro. Bone 2003; 32, 127–135

210. Reginster JY, Seeman E, De Vernejoul MC, Adami S, Compston J, Phenekos C, Devogelaer JP, Curiel MD, Sawicki A, Goemaere S, Sorensen OH, Felsenberg D, Meunier PJ. Strontium ranelate reduces the risk of nonvertebral fractures in postmenopausal women with osteoporosis: Treatment of Peripheral Osteoporosis (TROPOS) study. J Clin Endocrinol Metab 2005; 90; 2816–2822

211. Rezwan K, Chen QZ, Blaker JJ, Boccaccini AR. Biodegradable and bioactive porous polymer/inorganic composite scaffolds for bone tissue engineering. Biomaterials 2006; 27(18), 3413–31

212. Rho JY, Kuhn-Spearing L, Zioupos P. Mechanical properties and the hierarchical structure of bone, Medical Engineering & Physics 1998; 20; 92-102

213. Riggs BL, Wahner HW, Dunn WL, Mazess RB, Offord KP, Melton LJ 3rd. Differential changes in bone mineral density of the appendicular and axial skeleton with aging: relationship to spinal osteoporosis. J Clin Invest. 1981 Feb; 67(2), 328-35

214. Riggs BL, Melton LJ III. Medical progress series: Involutional osteoporosis. N Engl J Med 1986; 314; 1676

215. Riggs BL. Overview of Osteoporosis, West J Med 1991; 154; 63-77

216. Rodríguez JP, Garat S, Gajardo H, Pino AM, Seitz G. Abnormal osteogenesis in osteoporotic patients is reflected by altered mesenchymal stem cells dynamics. J Cell Biochem. 1999 Dec 1; 75(3), 414-23

217. Ron E, Schaub RG, Turek TJ. Formulations of blood-clot polymer matrix for delivery of osteogenic proteins. U.S. patent 5171579; 1992

218. Rosa AL, Beloti MM, van Noort R. Osteoblastic differentiation of cultured rat bone marrow cells on hydroxyapatite with different surface topography. Dental Materials 2003; 19; 768–772

219. Rosen V, Nove J, Song JJ, Thies RS, Cox K, Wozney JM. Responsiveness of clonal limb bud cell lines to bone morphogenetic protein 2 reveals a sequential relationship between cartilage and bone cell phenotypes. J Bone Miner Res. 1994 Nov; 9(11), 1759-68

220. Rosenthal HL, Eves MM, Cochran OA. Common strontium concentration of mineralized tissues from marine and sweet water animals. Comp Biochem Physiol. 1970 Feb 1; 32(3), 445-50

221. Rosenthal HL, Cochran OA, Eves MM. Strontium content of mammalian bone, diet and excreta. Environ Res. 1972 Jun; 5(2), 182-91

222. Roux C. Strontium ranelate: short- and long-term benefits for post-menopausal women with osteoporosis. Rheumatology (Oxford). 2008 Jul; 47 Suppl 4, iv20-22

223. Salata LA, Franke-Stenport V, Rasmusson L. Recent outcomes and perspectives of the application of bone morphogenetic proteins in implant dentistry. Clin Implant Dent Relat Res. 2002; 4(1), 27-32

224. Sanson G. The myth of osteoporosis. Ann Arbor, MI:MCD Century Publications, 2003

225. Sanz-Herrera JA, Kasper C, van Griensven M, Garcia-Aznar JM, Ochoa I, Doblare M. Mechanical and flow characterization of Sponceram carriers: Evaluation by homogenization theory and experimental validation. J Biomed Mater Res B Appl Biomater 2008 Oct; 87(1), 42-8.

226. Sanz-Herrera JA, García-Aznar JM, Doblaré M. A mathematical approach to bone tissue engineering. Philos Transact A Math Phys Eng Sci. 2009 May 28; 367(1895), 2055-78.

227. Saville PD, Lieber CS. Effect of alcohol on growth, bone density and muscle magnesium in the rat. J Nutri 1965; 87; 477-484

228. Schmitt JM, Hwang K, Winn SR, Hollinger JO. Bone Morphogenetic Proteins: An Update on Basic Biology and Clinical Relevance, J. Orthop. Res. 1999; 17(2), 269–278

229. Schneiders W, Reinstorf A, Ruhnow M, Rehberg S, Heineck J, Hinterseher I, Biewener A, Zwipp H, Rammelt S. Effect of chondroitin sulphate on material properties and bone remodelling around hydroxyapatite/collagen composites. J Biomed Mater Res A. 2008 Jun 1; 85(3), 638-45

230. Schroeder HA, Tıpton IH, Nason AP. Trace metals in man: strontium and barium. J Chronic Dis. 1972 Sep; 25(9), 491-517

231. Schwarz K. A bound form of silicon in glycosaminoglycans and polyuronides. Proc Natl Acad Sci U S A. 1973 May; 70(5), 1608-12

232. Seal BL, Otero TC, Panitch A. Polymeric biomaterials for tissue and organ regeneration. Mater Sci Eng: R: Rep 2001; 34, 147–230

233. Seeman E. Growth in bone mass and size are racial and gender differences in bone mineral density more apparent than real? J Clin Endocrinol Metab.1998 May; 83(5), 1414-9

234. Seeman E. Pathogenesis of bone fragility in women and men. Lancet 2002; 359; 1841–1850

235. Seeman E, Delmas PD. Bone quality--the material and structural basis of bone strength and fragility. N Engl J Med. 2006a May 25; 354(21), 2250-61

236. Seeman E, Vellas B, Benhamou C, Aquino JP, Semler J, Kaufman JM, Hoszowski K, Varela AR, Fiore C, Brixen K, Reginster JY, Boonen S. Strontium ranelate reduces the risk of vertebral and nonvertebral fractures in women eighty years of age and older. J Bone Miner Res. 2006b Jul; 21(7), 1113-20

237. Seeman E. Structural basis of growth-related gain and age-related loss of bone strength. Rheumatology (Oxford). 2008 Jul; 47 Suppl 4, iv2-8. Review

238. Sennerby L, Dasmah A, Larsson B, Iverhed M. Bone tissue responses to surface-modified zirconia implants: a histomorphometric and removal torque study in the rabbit. Clin Implant Dent Relat Res 2005; 7(Suppl 1), S13–20

239. Shorr E, Carter AC. The usefulness of strontium as an adjuvant to calcium in the remineralization of the skeleton in man. Bull Hosp Joint Dis. 1952 Apr; 13(1), 59-66.

240. Skerry TM, Suswillo R, el Haj AJ, Ali NN, Dodds RA, Lanyon LE. Load-induced proteoglycan orientation in bone tissue in vivo and in vitro. Calcif Tissue Int 1990; 46; 318-326

241. Skoryna SC. Metabolic aspects of the pharmacologic uses of trace elements in human subjects with specific references to stable strontium. Trace Subst. Enviorn Health.1984; 18, 3-23

242. Stayton PS, Drobny GP, Shaw WJ, Long JR, Gilbert M. Molecular recognition at the protein-hydroxyapatite interface. Crit Rev Oral Biol Med. 2003; 14(5), 370-6. Review

243. Sun JS, Liu HC, Chang WHS, Li J, Lin FH, Tai HC. Influence of hydroxyapatite particle size on bone cell activities: An in vitro study. J Biomed Mater Res 1998; 39; 390–397

244. Sun JS, Lin FH, Hung TY, Tsuang YH, Chang WHS, Li J, Liu HC. The influence of hydroxyapatite particles on osteoclast cell activities. J Biomed Mater Res. 1999 Jun 15; 45(4), 311-21.

245. Takahashi N, Sasaki T, Tsouderos Y, Suda T. S 12911-2 inhibits osteoclastic bone resorption in vitro. J Bone Miner Res. 2003 Jun; 18(6), 1082-7.

246. Takaoka T, Nakahara H, Yoshikawa H, Masuhara K, Tsuda T, Ono K. Ectopic bone induction on and in porous hydroxyapatite combined with collagen and bone morphogenetic protein. Clin Orthop 1989; 234; 250-4.

247. Tang BMP, Eslick GD, Nowson C, Smith C, Bensoussan A. Use of calcium or calcium in combination with vitamin D supplementation to prevent fractures and bone loss in people aged 50 years and older: a meta-analysis, Lancet 2007; 370; 657–66

248. Tanko LB, Sondergaard BC, Oestergaard S, Karsdal MA, Christiansen C. An update review of cellular mechanisms conferring the indirect and direct effects of estrogen on articular cartilage. Climacteric 2008; 11; 4–16

249. Temenoff JS, Mikos AG. Injectable biodegradable materials for orthopedic tissue engineering. Biomaterials 2000; 21; 2405-2412

250. Terra J, Dourado ER, Eon JG, Ellis DE, Gonzalez G, Rossi AM. The structure of strontium-doped hydroxyapatite: an experimental and theoretical study. Phys Chem Chem Phys. 2009 Jan 21; 11(3), 568-77.

251. Thies RS, Bauduy M, Ashton BA, Kurtzberg L, Wozney JM, Rosen V. Recombinant human bone morphogenetic protein-2 induces osteoblastic differentiation in W-20-17 stromal cells. Endocrinology. 1992 Mar; 130(3), 1318-24.

252. Thompson RC Jr. Heparin osteoporosis,:an experimental model using rats, J Bone Joint Surg A 1973; 55; 606-612

253. Turkey, Health Interview Survey, 2008, http://www.turkstat.gov.tr/PreTablo.do?tb_id=6&ust_id=1 (last visited on August 16, 2010)

254. Turner RT, Greene VS, Bell NH. Demonstration that ethanol inhibits bone matrix synthesis and mineralization in the rat. Bone Min Res 2:6 1-66 (1987)

255. Turner RT, Aloia RC, Segel LD, Hannon KS, Bell NH. Chronic alcohol treatment results in disturbed vitamin D metabolism and skeletal abnormalities in rats. Alcohol Clin Exp Res 1988; 12; 159-162.

256. Turner RT, Riggs BL, Spelsberg TC. Skeletal effects of estrogen. Endocr Rev 1994; 15; 275–300.

257. Turner RT, Maran A, Lotinun S, Hefferan T, Evans GL, Zhang M, Sibonga JD. Animal models for osteoporosis. Rev Endocr Metab Disord 2001; 2; 117–127

258. Uludag H, D'Augusta D, Golden J, Li J, Timony G, Riedel R, Wozney JM, Implantation of recombinant human bone morphogenetic proteins with biomaterial carriers: A correlation between protein pharmacokinetics and osteoinduction in the rat ectopic model,J Biomed Mater Res 2000; 50; 227–238,

259. Urist MR. Bone: formation by autoinduction. Science. 1965 Nov 12; 150(698), 893-9

260. Urist MR, Lietze A, Dawson E. Beta-tricalcium phosphate delivery system for bone morphogeneticprotein. Clin Orthop 1981; 157; 259-77.

261. Uriu K, Morimoto I, Kai K, Okazaki Y, Okada Y, Qie Y L, Okimoto N, Kaizu K, Nakamura T, Eto S. Uncoupling between bone formation and resorption in ovariectomized rats with chronic cadmium exposure. Toxicol. Appl. Pharmacol. 2000; 164; 264–272

262. Van Staa TP, Leufkens HG, Abenhaim L, Zhang B, Cooper C. Use of oral corticosteroids and risk of fractures. Journal of Bone and Mineral Research 2000; 15; 993–1000.

263. Vanderschueren D, Gaytant J, Boonen S, Venken K. Androgens and bone. Curr Opin Endocrinol Diabetes Obes 2008; 15; 250–254

264. Venken K, Callewaert F, Boonen F, Vanderschueren D. Sex Hormones, their receptors and bone health. Osteoporos Int 2008; 19; 1517–1525

265. Vestergaard P, Schwartz K, Pinholt EM, Rejnmark L, Mosekilde L, Use of bisphosphonates and raloxifene and risk of deep venous thromboembolism and pulmonary embolism, Osteoporos Int 2010; 21; 1591–1597

266. Volek-Smith H, Urist MR. Recombinant human bone morphogenetic protein (rhBMP) induced heterotopic bone development in vivo and in vitro. Proc Soc Exp Biol Med. 1996 Mar; 211(3); 265-72

267. Wahner HW, Dunn WL, Brown ML, Morin ML, Riggs BL. Comparison of dual energy x-ray absorptiometry (DEXA) and dual photon absorptiometry (DPA) for bone mineral measurements of the lumbar spine. Mayo Clin Proc 1988; 63; 1075-84

268. Walsh WR, Sherman P, Howlett CR, Sonnabend DH, Ehrlich MG. Fracture healing in a rat osteopenia model. Clin Orthop 1997; 342; 218–227

269. Wang EA, Rosen V, D'Alessandro JS, Bauduy M, Cordes P, Harada T, Israel DI, Hewick RM, Kerns KM, LaPan P, et al. Recombinant human bone morphogenetic protein induces bone formation. Proc Natl Acad Sci U S A. 1990 Mar; 87(6), 2220-4

270. Wang EA, Israel DI, Kelly S, Luxenberg DP. Bone morphogenetic protein-2 causes commitment and differentiation in C3H10T1/2 and 3T3 cells. Growth Factors. 1993; 9(1), 57-71.

271. Warnke PH, Bolte H, Schünemann K, Nitsche T,Sivananthan S, Sherry E, Douglas T, Wiltfang J,Becker ST. Endocultivation: Does delayed application of BMP improve intramuscular heterotopic bone formation? Journal of Cranio-Maxillofacial Surgery 2010; 38; 54-59

272. Varkey M, Kucharski C, Doschak MR, Winn SR, Brochmann EJ, Murray S, Matyas JR, Zernicke RF, Uludag H.Osteogenic response of bone marrow stromal cells from normal and ovariectomized rats treated with a low dose of basic fibroblast growth factor. Tissue Eng. 2007 Apr; 13(4); 809-17

273. Watanabe M, Harada K, Asahina I, Enomoto S. Implantation of hydroxyapatite granules mixed with atelocollagen and bone inductive protein in rat skull defects. In: Yamamuro T, Hench LL, Wilson JJ, editors. CRC handbook of bioactive ceramics, vol. II. Boca Raton, FL: CRC Press, 1990, p. 223-8.

274. Weiss P, Obadia L, Magne D, Bourges X, Rau C, Weitkamp T, Khairoun I, Bouler JM, Chappard D, Gauthier O, Daculsi G. Synchrotron X-ray microtomography (on a micron scale) provides three-dimensional imaging representation of bone ingrowth in calcium phaspate biomaterials. Biomaterials 2003; 24; 4591–4601.

275. Westerlind KC, Wronski TJ, Ritman EL, Luo ZP, An KN, Bell NH, Turner RT. Estrogen regulates the rate of bone turnover but bone balance in ovariectomized rats is modulated by prevailing mechanical strain. Proc Natl Acad Sci U S A. 1997 Apr 15; 94(8), 4199-204

276. White AP, Vaccaro AR, Hall JA, Whang PG, Friel BC, McKee MD. Clinical applications of BMP-7/OP-1 in fractures, nonunions and spinal fusion. Int Orthop. 2007 Dec; 31(6): 735-41. Review

277. Wong KL, Wong CT, Liu WC, Pan HB, Fong MK, Lam WM, Cheung WL, Tang WM, Chiu KY, Luk KDK, Lu WW. Mechanical properties and in vitro response of strontium-containing hydroxyapatite/ polyetheretherketone composites. Biomaterials 2009; 30; 3810–3817

278. World Health Organisation, Environmental Health Criteria 134, Cadmium. International Programme on Chemical Safety (IPCS) WHO, 1992, Geneva

279. Wozney JM, Rosen V, Celeste AJ, Mitsock LM, Whitters MJ, Kriz RW, Hewick RM, Wang EA.Novel regulators of bone formation: molecular clones and activities. Science. 1988 Dec 16; 242(4885), 1528-34

280. Wozney JM, Rosen V. Bone morphogenetic protein and bone morphogenetic protein gene family in bone formation and repair. Clin Orthop Relat Res. 1998 Jan; 346; 26-37. Review

281. Wu Y, Jiang W, Wen X, He B, Zeng X, Wang G, Gu Z. A novel calcium phosphate ceramic–magnetic nanoparticle composite as a potential bone substitute, Biomed. Mater 2010; 5(1):15001

282. Xu SW, Yu R, Zhao GF, Wang JW. Early period of fracture healing in ovariectomized rats. Chin J Traumatol 2003 Jun; 6(3), 160-6

283. Yamaguchi A. Regulation of differentiation pathway of skeletal mesenchymal cells in cell lines by transforming growth factor-beta superfamily. Semin Cell Biol. 1995 Jun; 6(3), 165-73. Review

284. Yamaguchi A, Ishizuya T, Kintou N, Wada Y, Katagiri T, Wozney JM, Rosen V, Yoshiki S.Effects of BMP-2, BMP-4, and BMP-6 on osteoblastic differentiation of bone marrow-derived stromal cell lines, ST2 and MC3T3-G2/PA6. Biochem Biophys Res Commun. 1996 Mar 18; 220(2), 366-71

285. Yasuda H, Shima N, Nakagawa N, Yamaguchi K, Kinosaki M, Mochizuki S, et al. Osteoclast differentiation factor is a ligand for osteoprotegerin/osteoclastogenesis-inhibitory factor and is identical to TRANCE/RANKL. Proc Natl Acad Sci U S A 1998; 95; 3597–602.

286. Yeni YN, Fyhrie DP. Finite element calculated uniaxial apparent stiffness is a consistent predictor of uniaxial apparent strength in human vertebral cancellous bone tested with different boundary conditions. J Biomech 2001; 34; 1649–54

287. Yoshimura N, Muraki S, Oka H, Kawaguchi H, Nakamura K, Akune T, Cohort Profile: Research on Osteoarthritis/Osteoporosis

Against Disability study, International Journal of Epidemiology 2010; 39; 988–995

288. Zamunovic N Cappellen D, Rohner D, Susa M. The Journal of Biological Chemistry, 2004 Vol 279, No 36, Issue of September 3, pp 37704-37715

289. Zeng H, Chittur KK, Lacefield WR. Analysis of bovine serum albumin adsorption on calcium phosphate and titanium surfaces. Biomaterials 1999; 20; 377–84.

290. Zhang C, Li C, Huang S, Hou Z, Cheng Z, Yang P, Peng C, Lin J. Self-activated luminescent and mesoporous strontium hydroxyapatite nanorods for drug delivery, Biomaterials 2010; 31; 3374–3383

291. Zhang M, Zhai W, Lin K, Pan H, Lu W, Chang J. Synthesis, in vitro hydroxyapatite forming ability, and cytocompatibility of strontium silicate powders, J Biomed Mater Res Part B: Appl Biomater 2010; 93B, 252–257

292. Zhong JP, Greenspan DC, Feng JW, "A microstructural examination of apatite induced by Bioglass in vitro", Journal of Materials Science: Materials in Medicine 2002; 13; pp321-26

293. Zhou Z, Ren Y, Yang D, Nie J. Performance improvement of injectable poly(ethylene glycol) dimethacrylate-based hydrogels with finely dispersed hydroxyapatite. Biomed Mater. 2009 Jun; 4(3), 035007

294. Zioupos P, Currey JD. Changes in the stiffness, strength, and toughness of human cortical bone with age. Bone 1998; 22; 57–66

295. Zreiqat H, Ramaswamy Y, Wu C, Paschalidis A, Lu ZF, James B, Birke O, McDonald M, Little D, Dunstan CR. The incorporation of strontium and zinc into a calcium–silicon ceramic for bone tissue engineering, Biomaterials 2010; 31; 3175–3184

APPENDIX

ETHICAL COMMITTEE APPROVAL

HACETTEPE ÜNİVERSİTESİ

DENEY HAYVANLARI ETİK KURULU

Hacettepe 06100, ANKARA

Sayı : B.30.2.HAC.0.01.00.05/ 50

DENEY HAYVANLARI ETİK KURUL KARARI

TOPLANTI TARİHİ	: 26.03.2007 (PAZARTESİ)
TOPLANTI SAYISI	: 2007/4
DOSYA KAYIT NUMARASI	: 2007/32
KARAR NUMARASI	: 2007/32 – 14
YARDIMCI ARAŞTIRMACILAR	: Vet. Hek. Gözde Kemsan, Vet. Hek. Dr. İlyas Onbaşılar, Prof. Dr. Feza Korkusuz, Prof. Dr. Muharrem Timuçin, Prof. Dr. Aykut Özkul.
HAYVAN TÜRÜ ve SAYISI	: 60 adet rat.

Üniversitemiz Tıp Fakültesi Histoloji ve Embriyoloji Anabilim Dalı öğretim üyelerinden Doç. Dr. Petek Korkusuz'un araştırma yürütücüsü olduğu 2007/32 kayıt numaralı ve *"Stronsiyum ve/veya Kemik Morfojenik Proteini (BMP) İçeren Biyoseramik Matriksin (hipaluronan, hidroksiapatit ve silikonun) Ratlarda Osteoporotik Kırık İyileşmesine Etkileri"* konulu çalışma; Deney Hayvanları Etik Kurulu Yönergesi'ne göre uygun bulunarak onaylanmasına karar verilmiştir.

Prof. Dr. Metin Dağdeviren (Başkan)

Prof. Dr. Sevim Dalkara (Üye) — Prof. Dr. Hakan Orer (Üye)

KATILMADI
Prof. Dr. Sema Çalış (Üye) — Doç.Dr. Nuket Örnek Bükan (Üye)

Prof.Dr. Ömer Gündüyusu (Üye) — Doç.Dr. Nuray Er (Üye)

Doç.Dr. Kaya Yorgancı (Üye) — Doç.Dr. Mehmet Ali Onur (Üye)

Dr.V. H. İlyas Onbaşılar (Üye) — Avukat Oya Söyüer (Üye)

CURRICULUM VITAE

Personal Informations:
Name : Gözde
Surname : Kerman
Place of Birth : Ankara
Date of Birth : Jan 15, 1981
e-mail : gozdekerman@hotmail.com

Education Informations:

2004- : Middle East Technical University
Natural and Applied Sciences-Biotechnology-PhD student
1998-2003 : Ankara University
Faculty of Veterinary Medicine
1991-1998 : Çankaya Milli Piyango Anatolian High School- Ankara
Polatlı Anatolian High School-Polatlı/Ankara

Projects:

1. Kerman G, Bilgili H, Kürüm B, Yardımcı C, Soysal Y, Yıldız C, Deveci S, Bahçe M. Autologous Chondrocyte Transplantation:Clinical and experimental study in knee joints of dogs (Project results have been presented in 4th National Veterinary Medicine Students Research Congress(2002))

2. Kerman G, Yardımcı C, Pişkin E, Bilgili H. Biomechanical comparison of two different restoration techniques on cruciate anterior ligaments: Experimental study on rabbit knee joint (project results have been presented in 4th National Veterinary Medicine Students Research Congress(2002))

3. Kerman G, Korkusuz P, Hakkı SS, Puralı N, Koç N, Timuçin M, Korkusuz F. Evaluation of MC3T3-E1 Cells applied to bioceramics by scanning electron microscope(SEM) and confocal microscope (CM) (Project results have been presented in 18th National Electron Microscope Congress(2007))

4. Kerman G, Korkusuz P, Hakkı SS, Puralı N, Timuçin M, Koc N, Korkusuz F. Observation of MC3T3-E1 Cells Applied Bioceramics by Scanning Electron Microscope and Confocal Microscope(Project results have been presented 11th Ceramic, Cells and Tissues Congress(2007))

Joined Congresses in Turkey:

- 4th National Veterinary Medicine Students Research Congress , May 9-11, 2002, Istanbul
- 2nd Eurasian IWRC Wildlife Rehabilitation Symposium, May 16-20, 2002, Ankara
- Basic course in Laboratory Animals Science, Nov 1-2, 2003, Kayseri
- 11th Biomedical Science and Technology Symposium, Sep 6-10, 2004, Hacettepe University, Ankara
- 4th Ankara University Biotechnology days, October, 2005, Ankara University, Ankara
- Nanotechnology Conference, NanoTR, May 3-5, 2006, Middle East Technical University, Ankara
- Cutting Edge Science in Medical Informatics and Medicine, June 22-23, 2006, Middle East Technical University, Ankara
- Transmission Electron Microscopy(TEM) Course, April 26-27, 2007, Hacettepe University, Ankara
- Immunohistochemistry Course, May 24-25, 2007, Hacettepe University, Ankara
- NanoTR III, Nanoscience and Nanotechnology Conference, June 11-14, 2007, Bilkent University, Ankara
- 18th National Electron Microscope Congress, August 26-29, 2007, Anadolu University, Eskisehir
- 3rd Stem Cell Symposium, October 5, 2007, Hacettepe University, Ankara
- Workshop on alternative methods(Reduction, Refinement, Replacement to Animal tests), Nov 12-13, 2007, Hacettepe University, Ankara
- Clinical Orthopaedics and Related Research Writing Workshop, April 18-20, 2008, Istanbul
- International Symposium on Biotechnology:Developments and Trends, September 27-30, 2009, Middle East Technical University, Ankara

Presentations in Congresses in Turkey:

- ✓ 4th National Veterinary Medicine Students Research Congress , May 9-11, 2002, Istanbul
- ✓ 18th National Electron Microscope Congress, August 26-29, 2007, Anadolu University, Eskisehir
- ✓ International Symposium on Biotechnology:Developments and Trends, September 27-30, 2009, Middle East Technical University, Ankara (abstract book page 105).

Joined Congresses in Foreign Countries:

- ✓ 10th Biomedical Science and Technology Symposium, Oct 10-12, 2003, METU Campus of Northern Cyprus

Presentations in Congresses in Foreign Countries:

- ✓ 11th Annual Seminar and Meeting " Ceramics, Cells and Tissues", October 2007, Faenza, Italy

Research experience:

- ✓ Experimental studies about cell culture and biomaterials, July 2004, Alberta University, Edmonton, Canada
- ✓ Experimental studies about cell culture, gene expression and biomaterials, June-August 2005, Alberta University, Edmonton, Canada
- ✓ Experimental studies about cell culture and bioceramics, March 2007, Selcuk University, Konya
- ✓ Experimental studies about cell culture, gene expression and biomaterials, July-August 2010, Alberta University, Edmonton, Canada

Publications:

- ✓ Kerman G, Korkusuz P, Hakkı SS, Puralı N, Koç N, Timuçin M, Korkusuz F. MC3T3-E1 hücre dizisinin uygulandığı biyoseramiklerin taramalı elektron miksroskobu ve konfokal mikroskop ile incelenmesi. Anadolu Universitesi Bilim ve Teknoloji dergisi, Vol. 10, Sayı:1, 239-247 (2009)

Award:

- ➢ 4th National Veterinary Medicine Students Research Congress, Best Poster Award, May 9-11 2002, Istanbul

Languages:

- ➢ **English :** Upper-intermediate, TOEFL (CBT 227)
  German: Elementary level